Copyright Warning & Restrictions

The copyright law of the United States (Title 17, United States Code) governs the making of photocopies or other reproductions of copyrighted material.

Under certain conditions specified in the law, libraries and archives are authorized to furnish a photocopy or other reproduction. One of these specified conditions is that the photocopy or reproduction is not to be "used for any purpose other than private study, scholarship, or research." If a, user makes a request for, or later uses, a photocopy or reproduction for purposes in excess of "fair use" that user may be liable for copyright infringement,

This institution reserves the right to refuse to accept a copying order if, in its judgment, fulfillment of the order would involve violation of copyright law.

Please Note: The author retains the copyright while the New Jersey Institute of Technology reserves the right to distribute this thesis or dissertation

Printing note: If you do not wish to print this page, then select "Pages from: first page # to: last page #" on the print dialog screen

ABSTRACT

DYNAMICAL SYSTEMS ASSOCIATED WITH PARTICLE FLOW MODELS: THEORY AND NUMERICAL METHODS

by
Roman V. Samulyak

A new class of integro - partial differential equation models is derived for the prediction of granular flow dynamics. These models are obtained using a novel limiting averaging method (inspired by techniques employed in the derivation of infinite-dimensional dynamical systems models) on the Newtonian equations of motion of a many-particle system incorporating widely used inelastic particle-particle force formulas. By using Taylor series expansions, these models can be approximated by a system of partial differential equations of the Navier-Stokes type. Solutions of the new models for granular flows down inclined planes and in vibrating beds are compared with known experimental and analytical results and good agreement is obtained.

Theorems on the existence and uniqueness of a solution to the granular flow dynamical system are proved in the Faedo-Galerkin method framework. A class of one-dimensional models describing the dynamics of thin granular layers and some related problems of fluid mechanics was studied from the Liouville-Lax integrability theory point of view. The integrability structures for these dynamical systems were constructed using Cartan's calculus of differential forms, Grassman algebras over jet-manifolds associated with the granular flow dynamical systems, the gradient-holonomic algorithm and generalized Hamiltonian methods. By proving the exact integrability of the systems, the quasi-periodicity of the solutions was explained as well as the observed regularity of the numerical solutions.

A numerical algorithm based on the idea of higher and lower modes separation in the theory of approximate inertial manifolds for dissipative evolutionary equations is developed in a finite-difference framework. The method is applied to the granular flow dynamical system. Numerical calculations show that this method has several advantages compared to standard finite-difference schemes.

A numerical solution to the granular flow in a hopper is obtained using the finite difference scheme in curvilinear coordinates. By making coefficients in the governing equations functionally dependent on the gradient of the velocity field, we were able to model the influence of the stationary friction phenomena in solids and reproduce in this way experimentally observable results.

Some analytical and numerical solutions to the dynamical system describing granular flows in vibrating beds are also presented. We found that even in the simplest case where we neglect the arching phenomena and surface waves, these solutions exhibit some of the typical features that have been observed in simulation and experimental studies of vibrating beds. The approximate analytical solutions to the governing system of equations were found to share several important features with actual granular flows. Using this approach we showed the existence of the typical dynamical structures of chaotic motion. By employing Melnikov theory the bifurcation parameter values were estimated analytically. The vortex solutions we obtained for the perturbed motion and the solutions corresponding to the vortex disintegration agree qualitatively with the dynamics obtained numerically.

DYNAMICAL SYSTEMS ASSOCIATED WITH PARTICLE FLOW MODELS: THEORY AND NUMERICAL METHODS

by
Roman V. Samulyak

A Dissertation
Submitted to the Faculty of
New Jersey Institute of Technology
in Partial Fulfillment of the Requirements for the Degree of
Doctor of Philosophy

Department of Mathematical Sciences

May 1999

APPROVAL PAGE

DYNAMICAL SYSTEMS ASSOCIATED WITH PARTICLE FLOW MODELS: THEORY AND NUMERICAL METHODS

Roman V. Samulyak

Denis Blackmore, Ph.D., Dissertation Advisor — Date
Professor, Department of Mathematical Sciences, NJIT

Amitabha Bose, Ph.D., Committee Member — Date
Assistant Professor, Department of Mathematical Sciences, NJIT

Demetrius Papageorgiou, Ph.D., Committee Member — Date
Associate Professor, Department of Mathematical Sciences, NJIT

Anthony Rosato, Ph.D., Committee Member — Date
Associate Professor, Department of Mechanical Engineering, NJIT

John Tavantzis, Ph.D., Committee Member — Date
Professor, Department of Mathematical Sciences, NJIT

BIOGRAPHICAL SKETCH

Author: Roman V. Samulyak

Degree: Doctor of Philosophy

Date: May 1999

Undergraduate and Graduate Education:

- Doctor of Philosophy in Applied Mathematics,
  New Jersey Institute of Technology, Newark, NJ, 1999
- Candidate of Sciences (Ph.D.) in Mathematical Physics,
  L'viv University, Ukraine, 1995
- Master of Science in Physics,
  L'viv University, Ukraine, 1992
- Bachelor of Science in Physics,
  L'viv University, Ukraine, 1989

Major: Applied Mathematics

Publications:

Blackmore, D., Rosato, A. and Samulyak, R., New mathematical models for granular flow dynamics, *J. Nonlinear Mathematical Physics*, **6** (1999), No. 3.

Blackmore, D., Prykarpatsky, Y. and Samulyak, R., The integrability of Lie-invariant geometric objects generated by ideals in the Grassmann algebra, *J. Nonlinear Mathematical Physics*, **5** (1998), 1-14.

Blackmore, D., Samulyak, R. and Dave, R., Approximate inertial manifold in finite differencies for granular flow dynamical system, *SIAM J. Numer. Anal.* (under review).

Papageorgiou, D., Tilley, B. and Samulyak, R., Potential flow instabilities in a thin fluid sheet, *SIAM J. Appl. Math.* (under review).

Blackmore, D., Leu, M.C. and Samulyak, R., Singularity theory approach to swept volumes, *International J. of Shape Modeling*, 1999 (under review).

Blackmore, D., Leu, M.C. and Samulyak, R., Trimming swept volumes, *Comp. Aided Design*, 1999 (in press)

Prykarpatsky, A., Samulyak, R. and Kopych, M., Adiabatic invariants of a generalized Henon-Heiles Hamiltonian system and the structure of chaotic motion, *Proc. of Ukr. Acad. of Sci.*, 1997, N2, 32-36.

Prykarpatsky, A.,Blackmore, D., Strampp, W., Sidorenko, Yu. and Samulyak, R., On Lagrangian and Hamiltonian formalisms for infinite dimensional dynamical systems with symmetries, CAMS Research Report: 96-22, New Jersey Institute of Technology, 1996. (also *Condensed Matter Phys.*, **6** (1995), 79-104.)

Prykarpatsky A. and Samulyak, R., Higgs model as an exactly integrable bi-Hamiltonian dynamical system of the classical field theory, *Proc. of Ukr. Acad. of Sci.* (1995), No 1, 34-37.

Prykarpatsky, A., Hentosh, O., Kopych, M. and Samulyak, R., The Neumann-Bogoliubov-Rosochatius oscillatory dynamical systems and their integrability via dual moment maps. Part I. *Nonlinear Mathematical Physics*, **2** (1995), 98-113.

Samulyak, R., Analysis of exact integrability of the classical nonlinear Higgs type dynamical system. In: *Differential equations and applications*, L'viv Technical University Press, 1995, No 277, 69-75.

Samulyak, R., Generalized Dicke type dynamical system as the inverse nonlinear Schrodinger equation, *Ukr. Math. J.*, **47** (1995), 149-151.

Samulyak, R., Hamiltonian analysis of exact solvability of the quantum 3-level superradiance Dicke model, *Ukr. Math. J.*, **44** (1992), 149-155.

Prykarpatsky, A., Ivankiv, L. and Samulyak, R., Nonequilibrium statistical mechanics of manyparticle systems in the restricted region with surface specialities and adsorbtion phenomena. Preprint of Inst. of Applied Problems of Mechanics and Mathematics of Ukr. Acad. Sci., N 1-92, 1992, 42p.

To my parents

ACKNOWLEDGMENT

I would like to express my most sincere gratitude and appreciation to Professor Denis Blackmore for his insight, guidance and invaluable support throughout this research. I have been greatly influenced by his organized and disciplined style of work. He really has made a big difference in my life and I will never forget it.

I am grateful to Professors Anthony Rosato and Demetrius Papageorgiou for their interest in my work, for their fruitful ideas and discussions. My special thanks also go to Professors John Tavantzis and Amit Bose. Their careful reading of the manuscript and suggestions helped me to clarify many parts of this work.

I thank also the Department of Mathematical Sciences, the Center of Applied Mathematics and Statistics, the Particle Technology Center and the Department of Mechanical Engineering at the New Jersey Institute of Technology for financial support during my three years of graduate study.

I would like to extend my gratitude to all the faculty, staff and my fellow graduate students in the Department of Mathematical Sciences for their help, encouragement and friendship.

TABLE OF CONTENTS

Chapter		Page
1	INTRODUCTION	1
2	NEW MATHEMATICAL MODEL FOR GRANULAR FLOW DYNAMICS	7
	2.1 Interparticle Forces	7
	2.2 Newtonian Equations of Motion	10
	2.3 Limiting Models	12
	2.4 A Simple Flow Model	17
	2.5 Exact Solutions to Some Simple Types of Granular Flows: Flows in Tubes	18
	2.6 Inclined Plane Flow Model	20
3	SOME ASPECTS OF THE THEORY OF DYNAMICAL SYSTEMS ASSOCIATED WITH PARTICLE FLOW MODELS	24
	3.1 Existence and Uniqueness of a Solution to the Granular Flow Problem	24
	3.2 Approximate Inertial Manifolds for Granular Flow Dynamical Systems	31
	3.2.1 Preliminaries: Approximate Inertial Manifolds	31
	3.2.2 AIM in Finite-Differences: the Modified Finite-Difference Scheme	35
	3.2.3 Application to a Granular Flow Dynamical System	39
	3.2.4 Numerical Example	43
4	GRANULAR FLOWS IN VIBRATING BEDS: THEORY AND NUMERICAL ANALYSIS	47

Chapter **Page**

4.1 Simple Vibrating Bed Model 47

4.2 Numerical Solutions 52

4.3 Analysis of Asymptotic Solutions 55

5 GRANULAR FLOWS IN HOPPERS: NUMERICAL SOLUTIONS 68

5.1 Numerical Methods for Hopper Problem 69

5.2 Numerical Solutions 73

6 ONE-DIMENSIONAL GRANULAR FLOW DYNAMICAL SYSTEMS AND SOME RELATED PROBLEMS OF FLUID MECHANICS 82

6.1 Integrability Structures for Burgers Equation 82

6.2 Dynamical Systems for the Description of Granular and Fluid Layers . 93

7 CONCLUSIONS 110

REFERENCES 115

LIST OF FIGURES

Figure		Page
2.1	Force functions: a) $y = \chi(x)$, b) $y = \eta(x)$, c) $y = \psi(x)$	9
2.2	Particle-particle forces: a) normal force, b) tangential force	9
2.3	Flow through a tube	18
2.4	Inclined plane flow	21
2.5	Velocity profiles for inclined plane flow	23
3.1	Flow in two-dimensional axisymmetric tube	25
3.2	Set of basis functions	36
3.3	Relative error of the finite-differences and the inertial form calculations along the line $x = 3$ at time $t = 1$, $h = 4$	45
3.4	Relative error of the finite-differences and the inertial form calculations along the line $y = 1$ at time $t = 1$, $h = 4$	46
3.5	Ratio of the errors of the inertial manifold calculation to those of the standard finite differences	46
4.1	Granular material in a vibrating container	49
4.2	Boundary conditions on the free surface	50
4.3	Motion of particles starting with four-vortex initial configuration (numerical solutions)	56
4.4	Motion of particles starting with random initial velocity distribution (numerical solutions)	57
4.5	Unperturbed trajectories of particles (asymptotic solutions)	61

Figure **Page**

4.6 Perturbed trajectories of particles: a) periodic trajectories between the invariant tori; b) mixing of particles 65

4.7 Possible positions of the perturbed stable and unstable manifolds 66

4.8 Amplitude of the Melnikov function 67

5.1 Types of industrial hoppers: a) conical or axisymmetric hopper; b) plane-flow wedge hopper; c) plane-flow chisel hopper; d) pyramid hopper. . . 69

5.2 Transformation to the "hopper coordinates" 71

5.3 Flow patterns in a core type hopper 75

5.4 Flow patterns in a mass type hopper 76

5.5 Numerical solution to the hopper flow problem; $\lambda = 0.5$, $\nu = 0.7$ (wide outlet) 78

5.6 Numerical solution to the hopper flow problem; $\lambda = 0.8$, $\nu = 1.0$ (narrow outlet) 79

5.7 Dependence of the coefficient of friction on the relative velocity between particles 80

5.8 Numerical solution to the hopper flow problem with variable friction coefficients 81

6.1 Phase portrait of the dynamical system $\frac{d}{dx}$ 103

6.2 Solutions $s = s(x)$ of the dynamical system $\frac{d}{dx}$ starting at different initial conditions 104

6.3 Small amplitude travelling wave solutions 105

CHAPTER 1

INTRODUCTION

The last two decades have witnessed an intensification of research in granular flow dynamics, in large measure spurred by a burgeoning array of engineering and industrial applications of particle technology. There are several features that make granular flow research attractive to engineers, mathematicians and scientists, among which are the following: A need still exists to formulate the underlying principles of particle interactions in a completely satisfactory manner; there are as yet few if any definitive mathematical models that can reliably predict a wide range of granular flows; particle flow phenomena such as arching, surface waves and convection are still not entirely understood from a mathematical or engineering perspective; there is a panoply of extremely complex nonlinear dynamical behaviors exhibited in granular flow regimes that has not yet been fully analyzed and has severely tested or exceeded the capabilities of current experimental and computer technologies for accurate characterization; and the techniques and devices for optimizing certain features of particle flows are for the most part only understood on an ad hoc basis. In this work we use some averaging and limiting ideas associated with infinite-dimensional dynamical systems theory to derive a new class of continuum mathematical models for granular flow that may be capable of predicting the dynamical characteristics of particle flows in a large variety of circumstances, and thereby help to make some progress in solving the many outstanding problems in this field. Our purpose is not to compete with the host of interesting models that try to incorporate as much of the physics of granular flows as possible, including (vibrational) energy equations. Rather, we aim to produce mathematical models that are relatively tractable and ignore just enough of the physics to still provide useful predictions of granular flow dynamics for a wide range of applications.

Although there have been several partial successes in recent years, the state-of-the-art in mathematical modelling of granular flow phenomena pales in comparison to that of fluid mechanics where there is a universally accepted model - the Navier-Stokes equations - whose reliability has been tested and confirmed for over a century, and is considered in many quarters to be capable of apprehending even what may be the most elusive of all physical processes - fluid turbulence. Approaches based on continuum mechanics (transport theory) and kinetic theory (statistical mechanics) have been those most often used for obtaining mathematical models for particle flows in the form of systems of partial differential equations. Notable examples derived using these methods which have enjoyed some success in predicting granular flow dynamics may be found in An & Pierce [5], Anderson & Jackson [6], Farrel, Lun & Savage [29], Gardiner & Schaeffer [37], Goldshtein & Shapiro [39], Jenike & Shield [45], Jenkins & Savage [47], Jenkins & Richman [46], Johnson, Nott & Jackson [48], Lun [59], Lun & Savage [58], Numan & Keller [70], Pasquarell [72], Pitman [74], Rajagopal [82], Richman [84], Tsimring & Aranson [106], Savage [92, 93], Savage & Jeffrey [94], Schaeffer [95], Schaeffer, Shearer & Pitman [96] and Shen & Ackermann [97] (see also Fan & Zhu [28] and Walton [107]). Several of these models have proven to be rather effective in characterizing certain granular flows, for example in chutes and hoppers with simple geometries, but they tend to be fairly complicated systems of nonlinear partial differential equations that are difficult to analyze and solve except by approximate numerical methods, and the information they provide has barely made a dent in the host of practical problems associated with industrial uses of particle technology. There have also been a number of simple, idealized models formulated by neglecting a variety of physical factors, but these tend to miss many of the features of granular flow of interest in applications. Much work still remains in finding a really effective balance between mathematical tractability and adherence to the underlying principles of physics in the models for a large class of

granular flow phenomena. It is hoped that the models introduced here will provide a useful step in the direction of achieving such a balance.

Granular flows have also been extensively studied using methods inspired by molecular dynamics research. The basic idea of the molecular dynamics approach is to use realistic models for interparticle forces, developed from both theory and empirical investigations, in a Newtonian dynamics context with a large number of particles (hundreds or thousands) to determine the evolution of a particle flow configuration. Analytical means are of little use in solving the very high dimensional dynamical systems encountered in such an approach, but some very sophisticated simulations, employing a variety of numerical solution techniques, have been devised for studying granular flows, such as those of Goldhirsch et al. [38], Lan & Rosato [53, 52], McNamara & Luding [66], Pöeschel & Herrmann [75], Rosato et al. [87], Swinney et al. [100] and Walton [107]. Alternative approaches based on cellular automata models and kinetic models of random walks in discrete lattices have also proven to be quite useful; see, for example, Baxter & Behringer [10] and Caram & Hong [21]. These and other simulations have proven to be so remarkably accurate in manifesting most of the complex aspects of particle flow behavior, that one is inescapably drawn to the conclusion that the formulation of a more concise and tractable mathematical representation of such simulations should greatly enhance our ability to analyze particle flow phenomena.

It was this idea of finding more succinct ways of mathematically characterizing granular flow simulations for extremely large numbers of particles that served as the inspiration for the new models derived here by computing limiting forms of the relevant Newtonian dynamical systems. To be more precise, we obtain systems of nonlinear partial differential equations - infinite-dimensional dynamical systems - for velocity fields of granular flows by using an averaging method together with the

computation of a limit as the number of particles tends to infinity, followed by a Taylor series approximation. The approach employed is akin to the methods used to obtain limiting partial differential equations for systems of ordinary differential equations (as the size of systems tend toward infinity) in the theory of infinite-dimensional dynamical systems; for example, as when the Korteweg-de Vries equation is obtained as the "limit" of an infinite string of coupled nonlinear oscillators (cf. Tabor [101] and Temam [102]). Our method leads to an infinite class of mathematical models of widely varying levels of complexity, depending on the form of the particle-particle force laws chosen and the order of the Taylor series expansions employed. Several of these models appear to enjoy certain advantages over existing models in terms of simplicity and ease of analysis, and they have the potential for providing a better developed mathematical understanding of granular flow phenomena.

We develop numerous theoretical aspects of the granular flow dynamical systems. By using the Faedo-Galerkin method framework we prove theorems on the existence and uniqueness of a solution to the boundary value problem for the granular flow dynamical system. Building on the idea of higher and lower modes separation in the theory of approximate inertial manifolds, we develop a numerical algorithm in the finite-difference framework for the inertial form calculation. The method developed in this thesis is applicable to any dissipative evolutionary equation possessing an approximate inertial manifold and we use it in numerical studies of the granular flow dynamical system. Numerical calculations show advantages of the method over the standard finite-difference schemes.

We investigate a series of one-dimensional dymanical systems associated with granular flow models. These equations can be used for the description of the dynamics of thin granular layers as well as for related problems in fluid mechanics. We prove the exact integrability by Liouville-Lax of some of these limiting dynamical

systems. By using Cartan's calculus of differential forms, Grassman algebras over jet-manifolds associated with the granular flow dynamical systems, the gradient-holonomic algorithm and generalized Hamiltonian methods we were able to construct the integrability structures for the one-dimensional models. The Liouville-Lax integrability that implies integrability of equations in the classical Liouville sense on every finite-dimensional invariant submanifold makes it possible to explain the regularity and quasi-periodicity of some classes of solutions obtained numerically.

Along with analysis of the mathematical structure of granular flow dynamical systems we also attempted to find numerical solutions for some problems having important applications, in particular, the hopper and vibrating bed problems. Studies of granular flows and processes in conveying particulate materials and, in particular, hopper flows, have been stimulated by industrial needs. In designing plants which involve the handling and processing of particulate solid materials, several problems are encountered which have no counterpart in fluid handling processes; unless this is recognized and appropriate steps are taken, serious and costly problems can be met in operating the plant. Among the most important industrial problems for hoppers is to ensure that when material is required it will discharge, under gravity, at the required rate and that flow will be uninterupted as long as there is material in the hopper. Other problems consist in theoretical prediction of the flooting phenomena that may take place under some conditions in core type hoppers and in the estimation of the size-segregation phenomena of a multicomponent mix of particles. These and several other problems are still not entirely understood from a mathematical or engineering perspective.

In this work we develop methods for solving the hopper problem numerically and compare our results with experimental data. By making coefficients in the governing equations functionally dependent on the gradient of the velocity field, we

were able to model the influence of the stationary friction phenomena in solids and reproduce in this way experimentally observable results. The solutions for different functional dependence of the dynamical system parameters corresponding to the interparticle and particle-wall friction were obtained for physically realistic boundary conditions.

We also present some analytical and numerical solutions to the dynamical system describing granular flows in vibrating beds. We found that even in the simplest case where we neglect the arching phenomena and surface waves, these solutions exhibit some of the typical features that have been observed in simulation and experimental studies of vibrating beds. In an effort to study the dynamics analytically, we employed asymptotic expansions and made a few simplifying assumptions. The approximate solutions were found to share several important features with actual granular flows. Using this approach, we showed the existence of the typical dynamical structures of chaotic motion; by employing Melnikov theory, we were able to estimate analytically the bifurcation parameter values. The vortex solutions we obtained for the perturbed motion and the solutions corresponding to vortex disintegration agree qualitatively with the dynamics obtained numerically. We believe that this and similar simplified analytical approaches might be useful for the investigation of phenomena related to the creation and destruction of various types of structures in granular flow and for the study of chaotic transport, and could lead to a better understanding of granular flow dynamics.

CHAPTER 2

NEW MATHEMATICAL MODEL FOR GRANULAR FLOW DYNAMICS

2.1 Interparticle Forces

In this section we shall describe the particle-particle force models that are the foundation upon which we construct our derivation of the governing equations of motion for the granular flows under consideration. We assume that the flow system is comprised of a large number N of identical inelastic spherical particles distributed throughout some region in $\mathbf{R}^3$ at points $\mathbf{x}^{(i)}$, $1 \leq i \leq N$. The common radius of all the particles is a very small positive number that we denote by r, and the point $\mathbf{x}^{(i)}$ corresponding to the ith particle is located at the center of the particle for all $1 \leq i \leq N$.

We may select any particle, say the ith one, and suppose that the jth particle at $\mathbf{x}^{(j)}$ is near $\mathbf{x}^{(i)}$. For convenience, we define

$$\mathbf{r}_i^j := \mathbf{x}^{(j)} - \mathbf{x}^{(i)} \tag{2.1}$$

and $\mathbf{v}_i^j$ to be the velocity of the jth particle relative to the ith particle; namely,

$$\mathbf{v}_i^j := \mathbf{v}(\mathbf{x}^{(j)}) - \mathbf{v}(\mathbf{x}^{(i)}). \tag{2.2}$$

Taking our cue from Hertz-Mindlin theory as supported by numerous experimental observations and granular flow simulations (see [28, 45, 87, 92] and [107]), we shall assume that the model for the force $\mathbf{P}_i^j$ exerted on the ith particle by the jth particle is described as follows: $\mathbf{P}_i^j$ is the sum of a (inelastic) *normal force* $\mathcal{N}_i^j$ and a *tangential force* $\mathcal{T}_i^j$ due to friction

$$\mathbf{P}_i^j = \mathcal{N}_i^j + \mathcal{T}_i^j, \tag{2.3}$$

where

$$\mathcal{N}_i^j := \left[-\chi(\left\|\mathbf{r}_i^j\right\|^2)\left\|\mathbf{r}_i^j\right\|^\alpha + \eta(\left\|\mathbf{r}_i^j\right\|^2)\left\langle \mathbf{v}_i^j, \mathbf{r}_i^j\right\rangle \left\|\mathbf{r}_i^j\right\|^\beta\right] \hat{\mathbf{r}}_i^j \tag{2.4}$$

and

$$\mathcal{T}_i^j := \psi(\left\|\mathbf{r}_i^j\right\|^2) \left\|\mathbf{r}_i^j\right\|^\gamma \left\|\vartheta(\mathbf{v}_i^j)\right\|^\delta \widehat{\vartheta(\mathbf{v}_i^j)}. \tag{2.5}$$

Here α, β, γ and δ are positive exponents chosen according to the particular properties of the material particles; among the most often used values are $\alpha = 1$ or $3/2$ (Hertzian), $\beta = 1$, $\gamma = 0$, $1/3$, $2/3$ or $3/2$ and $\delta = 1$ or 2. The functions χ, ψ and η are smooth ($= C^\infty$) on $[0, \infty)$ and have the following properties:

$$\chi(\tau), \psi(\tau), \eta(\tau) \geq 0 \quad \text{for all} \quad \tau \geq 0; \tag{2.6}$$

$$\chi'(\tau), \psi'(\tau), \eta'(\tau) \leq 0 \quad \text{for all} \quad \tau \geq 0 \quad (' = d/d\tau); \tag{2.7}$$

$$\chi(\tau) = \psi(\tau) = \eta(\tau) = 0 \quad \text{when} \quad \tau > 4r^2; \tag{2.8}$$

$$\chi'(\tau) = \psi'(\tau) = \eta'(\tau) = 0 \quad \text{for} \quad 0 \leq \tau \leq q^2 < 4r^2; \tag{2.9}$$

$$\eta(0) < \chi(0); \tag{2.10}$$

and

$$\eta(\tau) \leq \chi(\tau) \quad \text{for all} \quad \tau \geq 0. \tag{2.11}$$

Graphs of these functions are shown in Figure 2.1. As we are going to ignore the rotational motion of the particles in our treatment, we shall assume that the tangential force is very small compared to the normal force and, more specifically, that $\psi(\tau) << \eta(\tau)$ for all τ such that $\psi(\tau) > 0$.

The role of the function η is to represent an energy loss due to inelasticity in the restoring mode when the particles are separating after a collision. A caret over a vector $\mathbf{u}$ indicates the unit vector in the direction of $\mathbf{u}$; i.e., $\hat{\mathbf{u}}$:=$\mathbf{u}/\left\|\mathbf{u}\right\|$. The vector $\vartheta(\mathbf{v}_i^j)$ is the component of the relative velocity at the point of contact of a pair of particles obtained by projecting $\mathbf{v}_i^j$ onto the tangent plane of the ith particle at the point of contact. This vector can be written in the form

$$\vartheta(\mathbf{v}_i^j) := \mathbf{v}_i^j - \left\langle \mathbf{v}_i^j, \hat{\mathbf{r}}_i^j \right\rangle \hat{\mathbf{r}}_i^j. \tag{2.12}$$

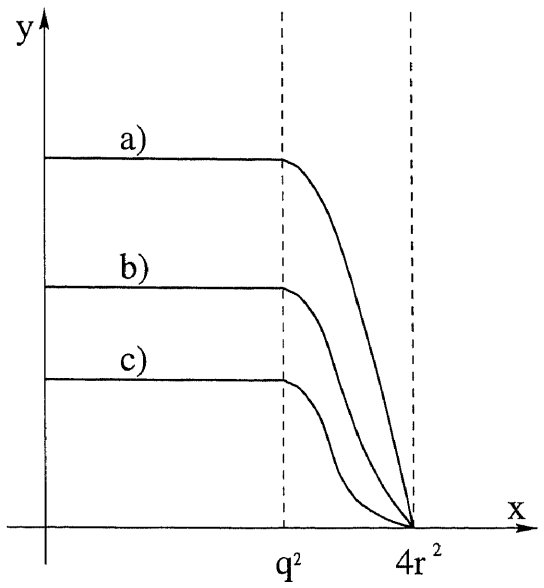

Figure 2.1 Force functions: a) $y = \chi(x)$, b) $y = \eta(x)$, c) $y = \psi(x)$

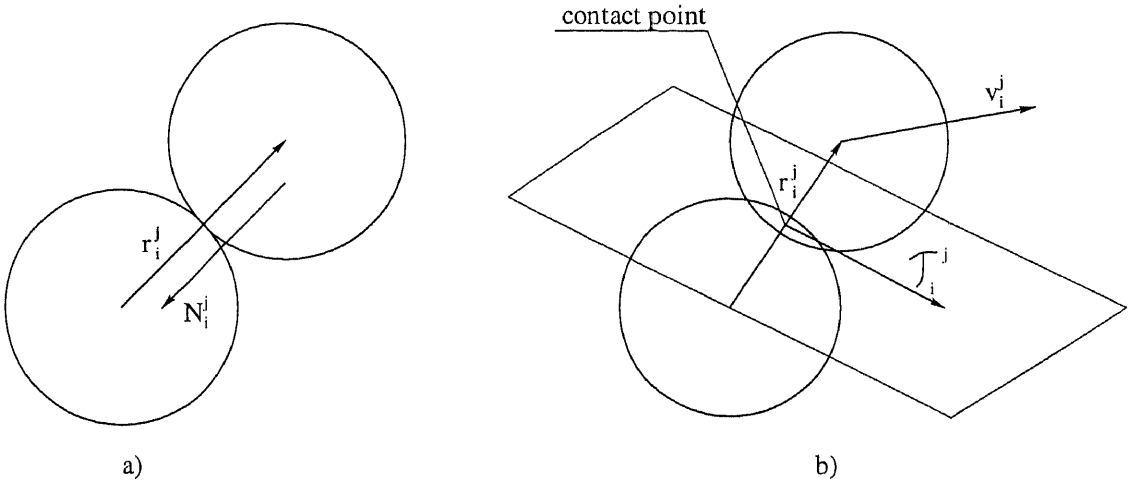

Figure 2.2 Particle-particle forces: a) normal force, b) tangential force

The normal and tangential interparticle forces are depicted in Figure 2.2.

Summing over all particles in the granular flow system, we find that the total force exerted by all the particles on the ith particle is

$$\mathbf{P}_i := \sum_{j=1, j\neq i}^{N} \mathbf{P}_i^j = \sum_{j=1, j\neq i}^{N} \left(\mathcal{N}_i^j + \mathcal{T}_i^j\right). \tag{2.13}$$

Note that our assumed particle-particle force models account for the geometry of the particles only with regard to the region where the force vanishes (its *support)* and the manner in which the tangential frictional component of force is defined. We observe that (2.13) can also be obtained from a specific force density field surrounding the ith particle with the force supplied by each grain equal to this specific density multiplied by the volume $\frac{4}{3}\pi r^3$. We shall return to this point in the sequel when we compute limiting forms of the particle dynamical system.

2.2 Newtonian Equations of Motion

The motion of the particles in the granular flow field may be described by a system of $3N$ second-order, ordinary differential equations expressing Newton's second law of motion; viz.

$$m\ddot{\mathbf{x}}^{(i)} = \mathbf{F}_i := \mathbf{P}_i + \mathbf{T}_i + \mathbf{E}_i + \mathbf{B}_i \quad (1 \leq i \leq N), \tag{2.14}$$

where $\dot{} = d/dt$, m is the mass of each of the N identical particles, $\mathbf{P}_i$ is the force exerted on the ith particle by all particles in direct contact with it as described in the preceding section, $\mathbf{T}_i$ is the *transmitted force* on the ith particle exerted by connected arrays of particles in contact with one another that touch a particle in direct contact with the ith particle, $\mathbf{E}_i$ is the *external* or *body force* on the ith particle which is usually just the gravitational force (but may sometimes also include electromagnetic and other forces) and $\mathbf{B}_i$ is the *boundary force* exerted on the ith particle by fixed or motile boundaries in direct contact with it that delimit the region in space in which

the particles can move. Observe that the variables on which each of the components of force depend can be described as follows:

$$\mathbf{P}_i = \mathbf{P}_i\left(\mathbf{x}^{(1)}, ..., \mathbf{x}^{(N)}, \dot{\mathbf{x}}^{(1)}, ...\dot{\mathbf{x}}^{(N)}\right)$$

$$\mathbf{T}_i = \mathbf{T}_i\left(\mathbf{x}^{(1)}, ..., \mathbf{x}^{(N)}, \dot{\mathbf{x}}^{(1)}, ...\dot{\mathbf{x}}^{(N)}\right)$$

$$\frac{\mathbf{E}_i}{m} \text{ is usually constant}$$

$$\mathbf{B}_i = \mathbf{B}_i\left(\mathbf{x}^{(i)}, \dot{\mathbf{x}}^{(i)}, t\right),$$

where the dependence on t in $\mathbf{B}_i$ occurs when the material boundary of the flow region moves with time such as in the case of particles moving in a vibrating container.

We can write the Newtonian equations of motion in a more concise form by introducing the following vector notation: Define the vector $\mathbf{X}$ in $\mathbf{R}^{3N}$ to be

$$\mathbf{X} := \left(\mathbf{x}^{(1)}, \mathbf{x}^{(2)}, ..., \mathbf{x}^{(N)}\right).$$

Then (2.14) can be rewritten in vector form as

$$\ddot{\mathbf{X}} = \mathbf{\Phi}(\mathbf{X}, \dot{\mathbf{X}}, t) := \mathbf{\Phi}_p(\mathbf{X}, \dot{\mathbf{X}}) + \mathbf{\Phi}_T(\mathbf{X}, \dot{\mathbf{X}}, t) + \mathbf{\Phi}_e + \mathbf{\Phi}_b(\mathbf{X}, \dot{\mathbf{X}}, t), \tag{2.15}$$

where

$$\mathbf{\Phi}_p := m^{-1}\left(\mathbf{P}_1(\mathbf{X}, \dot{\mathbf{X}}), ..., \mathbf{P}_N(\mathbf{X}, \dot{\mathbf{X}})\right)$$

is the *interparticle force per unit mass,*

$$\mathbf{\Phi}_T := m^{-1}(\mathbf{T}_1(\mathbf{X}, \dot{\mathbf{X}}, t), \ldots, \mathbf{T}_N(\mathbf{X}, \dot{\mathbf{X}}, t))$$

is the *transmitted force per unit mass,*

$$\mathbf{\Phi}_e := m^{-1}\left(\mathbf{E}_1, ..., \mathbf{E}_N\right)$$

is the *external force per unit mass* and

$$\mathbf{\Phi}_b := m^{-1}\left(\mathbf{B}_1(\mathbf{x}^{(1)}, \dot{\mathbf{x}}^{(1)}, t), ..., \mathbf{B}_N(\mathbf{x}^{(N)}, \dot{\mathbf{x}}^{(N)}, t)\right)$$

is the *boundary force per unit mass.* In theory, if initial values of $\mathbf{X}$ and $\dot{\mathbf{X}}$ are specified, then (2.15) uniquely determines the ensuing motion of all the particles, at least for small values of $|t|$ (see [101] and [102]). However, for extremely large values of N the work required to integrate (2.15) - analytically, when in the rare cases that this is possible, or numerically otherwise - tends to be prohibitive. Thus it is desirable to find an infinite-dimensional limit in some sense for (2.15) as $N \to \infty$, presumably in the form of a partial differential equation, that may prove to be more amenable to analysis. This is precisely what we shall do in the next section.

2.3 Limiting Models

We shall demonstrate how new models for granular flow phenomena can be obtained by applying a certain type of dynamical limit procedure to the Newtonian equations (2.15). The reader will no doubt notice at least a vague similarity between our method and the continuum limit used in the Fermi-Ulam-Pasta model to obtain the Korteweg-de Vries equation (cf. [101]). To begin with, we restrict our attention to points in the interior of the granular flow region that are not directly affected by interaction with the boundary. Consequently, for the time being we ignore the boundary force contribution in (2.14) or (2.15); the boundary effects shall be considered in the sequel when we study specific boundary-value problems.

Referring to (2.14), we assume that the body forces are exclusively gravitational and that the Cartesian coordinate system has been chosen so that the gravitational force acting on each particle has the form

$$\dot{\mathbf{x}}^{(i)} = \mathbf{v}\left(\mathbf{x}^{(i)}, t\right) \tag{2.16}$$

where g is the acceleration of gravity and $\hat{\mathbf{e}}$ is a unit vector in the opposite direction to the gravitational field. Now we select a point in the interior of the granular flow

field corresponding to the ith particle (at time t) which is moving along a trajectory determined by the vector field

$$\dot{\mathbf{x}}^{(i)} = \mathbf{v}\left(\mathbf{x}^{(i)}, t\right) \tag{2.17}$$

and the location of this particle at time $t = 0$.

The interparticle forces on the ith particle at the point $\mathbf{x}^{(i)} = \mathbf{x}$ are given by (2.13). Since we are going to take a limit as the number of grains goes to infinity, we need to average or distribute these forces in a way that insures the existence of such a limit and is conducive to its computation. This can be done by smearing the particles into a continuum and considering the interparticle force field to be obtained from a specific force density field. To be more precise, we assume that each particle is surrounded by a specific force density field of the same form $c\mathbf{P}_*$. Whence, the force on the ith particle can be written

$$\mathbf{P}_i := c\sum_{j\neq i} \mathbf{P}_*(\mathbf{x}^{(j)}; \mathbf{v}_i^j)\Delta V_j, \tag{2.18}$$

where ΔV_j is the volume increment occupied by the jth particle and $c > 0$ is a multiplicative factor with units $volume^{-1}$ (associated with the geometry of the particles). This can be rewritten in the form

$$\mathbf{P}_i = (N-1)^{-1} c c_0 \sum_{j\neq i} \mathbf{P}_*(\mathbf{x}^{(j)}; \mathbf{v}_i^j), \tag{2.19}$$

where c_0 is a positive constant equal to the volume of the (compact) support of $\mathbf{P}_i$ and we have assumed that all the particles occupy volume increments of the same size. In (2.19) we plainly see the averaging aspect of this approach. Taking the limit as $N \to \infty$ in (2.19) [or equivalently as $\Delta V_j \to 0$ in (2.18)] using standard results from integration theory, we obtain

$$\lim_{N\to\infty} \mathbf{P}_i = c\int_{\mathbf{R}^3} \mathbf{P}_* dy_1 dy_2 dy_3 = c\int_{\mathbf{R}^3} \mathbf{P}_* d\mathbf{y}, \tag{2.20}$$

where it follows from (2.3), (2.4), (2.5) and (2.12) that

$$\begin{aligned}\mathbf{P}_* \ :&= \mathbf{P}_*(\mathbf{y};\mathbf{v}(\mathbf{x}),\mathbf{v}(\mathbf{x}+\mathbf{y})) = \\ &= \left[-\chi(\|\mathbf{y}\|^2)\,\|\mathbf{y}\|^{\alpha-1} + \eta(\|\mathbf{y}\|^2)\,\langle \mathbf{v}(\mathbf{x}+\mathbf{y})-\mathbf{v}(\mathbf{x}),\mathbf{y}\rangle\,\|\mathbf{y}\|^{\beta-1}\right]\mathbf{y} + \\ &+\psi(\|\mathbf{y}\|^2)\,\|\mathbf{y}\|^{\gamma}\left\|\mathbf{v}(\mathbf{x}+\mathbf{y})-\mathbf{v}(\mathbf{x})-\langle \mathbf{v}(\mathbf{x}+\mathbf{y})-\mathbf{v}(\mathbf{x}),\mathbf{y}\rangle\,\frac{\mathbf{y}}{\|\mathbf{y}\|^2}\right\|^{\delta-1}\times \\ &\left[\mathbf{v}(\mathbf{x}+\mathbf{y})-\mathbf{v}(\mathbf{x})-\langle \mathbf{v}(\mathbf{x}+\mathbf{y})-\mathbf{v}(\mathbf{x}),\mathbf{y}\rangle\,\frac{\mathbf{y}}{\|\mathbf{y}\|^2}\right],\end{aligned}$$

where $\mathbf{y} = (y_1, y_2, y_3)$ represents the position vector measured from the reference point $\mathbf{x}$ that has been introduced to simplify the notation for $\mathbf{r}_i^j$. As for the transmitted force in the Newtonian equation (2.14), we make the standard assumption that in the continuum limit it can be represented by a gradient field, $\operatorname{grad} p$, where the function $p = p(\mathbf{x}, t)$ is naturally called the *pressure*. The particle at $\mathbf{x}^{(i)}$ is represented by a *density field*, $\rho = \rho(\mathbf{x}, t)$, with compact support. Hence the external force is

$$\left(\int_{W_i} \rho g \, dV\right)\hat{\mathbf{e}},$$

where W_i is a spherical (control) region centered at $\mathbf{x}^{(i)}$ with (Lebesgue) measure ΔV_i, and this converges to $\rho g\hat{\mathbf{e}}$ as $N \to \infty$ ($\Leftrightarrow \Delta V_i \to 0$). In the same spirit, the right-hand side of (2.14) is replaced by

$$\frac{d}{dt}\int_{W_i} \rho\mathbf{v}\, dV,$$

which upon applying the usual continuum limit converges to the density times the total (material) derivative of the velocity:

$$\rho\frac{D\mathbf{v}}{Dt} := \rho\left(\frac{\partial \mathbf{v}}{\partial t} + \sum_{k=1}^{3}\frac{\partial \mathbf{v}}{\partial x_k}v_k\right).$$

Upon combining all of the above computations, we obtain the following system of nonlinear integro-partial differential equations for the momentum balance of the particle flow in the interior of the region under consideration:

$$\frac{D\mathbf{v}}{Dt} = \frac{\partial \mathbf{v}}{\partial t} + v_k\frac{\partial \mathbf{v}}{\partial x_k} = -g\hat{\mathbf{e}} + \frac{1}{\rho}\operatorname{grad} p + \kappa\int_{\mathbf{R}^3}\mathbf{P}_*(\mathbf{y};\mathbf{v}(\mathbf{x}),\mathbf{v}(\mathbf{x}+\mathbf{y}))d\mathbf{y}, \qquad (2.21)$$

where $\kappa := c/\rho$ and we have employed the Einstein summation convention. If ρ is constant and grad p is known a priori, then (2.21) together with appropriate initial and boundary data suffices to determine the velocity field. When the granular flow is compressible and grad p is known a priori, we have to add the continuity equation

$$\frac{\partial \rho}{\partial t} + \operatorname{div}(\rho \mathbf{v}) = 0 \tag{2.22}$$

to (2.21), and then by imposing additional auxiliary data the velocity field and density may be determined. Of course, in general, both p and ρ are unknown variables, in which case (2.21) and (2.22) are insufficient to determine p, ρ and $\mathbf{v}$. One more equation must be added, and this may be accomplished by appending an energy equation to (2.21) and (2.22). The easiest way to do this is to obtain an equation of state of the granular flow medium that provides a relationship between the pressure and the density. If we make the same assumption as above (in particular, that the particles are uniformly and isotropically distributed locally), then by applying the same type of limit as $N \to \infty$ to the equations representing the kinetic energy of the Newtonian system (2.14), we obtain the equation of state of an ideal gas; namely

$$p = A\,\rho^{\omega},$$

where $A > 0$ and $\omega > 1$ are constants that are obtained from the properties of the granular flow medium. The same result can be derived by applying the standard thermodynamic limit of statistical mechanics in conjunction with the virial theorem.

For certain purposes, including comparison with other continuum models for particle flows, it is useful to replace (2.21) with an approximate partial differential equation. Although, it should be pointed out that, mathematically speaking, (2.21) enjoys certain inherent advantages over such partial differential equation models. In particular, solutions of the system with (2.21) should exhibit considerably more regularity than the pure differential equation models.

In order to approximate (2.21) by a system of mth order partial differential equations, we may use the following Taylor series expansion of order m :

$$\mathbf{v}(\mathbf{x}+\mathbf{y})-\mathbf{v}(\mathbf{x}) \simeq \sum_{k=1}^{m} \frac{1}{k!} \frac{\partial^k \mathbf{v}}{\partial \mathbf{x}^k}(\mathbf{x})\mathbf{y}^k. \tag{2.23}$$

The positive integer m is at our disposal, and it is plausible to assume that the larger we choose m, the more accurate the approximation. Substituting (2.23) in (2.21), we obtain the system of mth order, nonlinear partial differential equations as an approximate model for the momentum balance of the granular flow field given by

$$\frac{\partial \mathbf{v}}{\partial t} + v_k \frac{\partial \mathbf{v}}{\partial x_k} = -g\hat{\mathbf{e}} + \frac{1}{\rho}\operatorname{grad} p + \mathbf{\Gamma}\left(\mathbf{v}, \frac{\partial \mathbf{v}}{\partial \mathbf{x}}, ..., \frac{\partial^m \mathbf{v}}{\partial \mathbf{x}^m}\right), \tag{2.24}$$

where $\mathbf{\Gamma}$, a function that does not depend explicitly on $\mathbf{x}$, is defined by

$$\begin{aligned}\mathbf{\Gamma} \ : \ = \kappa \Bigg\{ & -\int_{\mathbf{R}^3} \chi(\|\mathbf{y}\|^2)\, \|\mathbf{y}\|^{\alpha-1}\, \mathbf{y} d\mathbf{y} + \sum_{k=1}^{m} \frac{1}{k!} \int_{\mathbf{R}^3} \left\langle \frac{\partial^k \mathbf{v}}{\partial \mathbf{x}^k}\mathbf{y}^k, \mathbf{y} \right\rangle \|\mathbf{y}\|^{\beta-1}\, \eta(\|\mathbf{y}\|^2)\mathbf{y} d\mathbf{y} \\ & + \sum_{k=1}^{m} \frac{1}{k!} \int_{\mathbf{R}^3} \psi(\|\mathbf{y}\|^2)\, \|\mathbf{y}\|^{\gamma} \left\| \sum_{k=1}^{m} \frac{1}{k!} \left[\frac{\partial^k \mathbf{v}}{\partial \mathbf{x}^k}\mathbf{y}^k - \left\langle \frac{\partial^k \mathbf{v}}{\partial \mathbf{x}^k}\mathbf{y}^k, \mathbf{y} \right\rangle \frac{\mathbf{y}}{\|\mathbf{y}\|^2} \right] \right\|^{\delta-1} \times \\ & \left[\frac{\partial^k \mathbf{v}}{\partial \mathbf{x}^k}\mathbf{y}^k - \left\langle \frac{\partial^k \mathbf{v}}{\partial \mathbf{x}^k}\mathbf{y}^k, \mathbf{y} \right\rangle \frac{\mathbf{y}}{\|\mathbf{y}\|^2} \right] d\mathbf{y} \Bigg\}.\end{aligned}$$

Hence we have infinitely many possible partial differential equation models for granular flow corresponding to the choices of the functions χ, η and ψ, of parameters α, β, γ and δ, and the order m of the Taylor series approximation. This leads to a very natural question: What order of Taylor series approximation in (2.24) should be used for a given application? As we shall show in the sequel, $m = 2$ works rather well for tube, inclined plane and vibrating bed flows. However, it will probably be necessary to consider several choices in other applications and determine an acceptable order of approximation on a case-by-case basis, where an educated guess is made based upon known properties of the flow.

2.4 A Simple Flow Model

Depending on the choice of parameters and the order, the model (2.24) can range from relatively simple to quite complicated. In this section we make a choice of parameters and order that leads to a rather simple yet ostensibly realistic model for the velocity field of a granular flow. Specifically, we choose $\alpha = \beta = 1$, $\gamma = 0, \delta = 1$ and $m = 2$. Then (2.24) takes the form

$$\begin{aligned}\frac{\partial \mathbf{v}}{\partial t} + v_k \frac{\partial \mathbf{v}}{\partial x_k} &= -g\hat{\mathbf{e}} + \frac{1}{\rho}\operatorname{grad} p + \kappa \int_{\mathbf{R}^3} \left\{ -\chi(\|\mathbf{y}\|^2)\mathbf{y} + \sum_{k=1}^{2} \frac{1}{k!} \left[\psi(\|\mathbf{y}\|^2) \frac{\partial^k \mathbf{v}}{\partial \mathbf{x}^k} \mathbf{y}^k + \right.\right. \\ &\qquad \left.\left. \left\langle \frac{\partial^k \mathbf{v}}{\partial \mathbf{x}^k} \mathbf{y}^k, \mathbf{y} \right\rangle \left(\eta(\|\mathbf{y}\|^2) - \psi(\|\mathbf{y}\|^2) \|\mathbf{y}\|^{-2} \right) \mathbf{y} \right] \right\} d\mathbf{y},\end{aligned}$$

which upon integration using spherical coordinates simplifies to

$$\frac{\partial \mathbf{v}}{\partial t} + v_k \frac{\partial \mathbf{v}}{\partial x_k} = -g\hat{\mathbf{e}} + \frac{1}{\rho}\operatorname{grad} p + \nu \Delta \mathbf{v} + \lambda \operatorname{grad}(\operatorname{div} \mathbf{v}), \tag{2.25}$$

where

$$\nu := \frac{2\pi\kappa}{15} \int_0^\infty \left[\eta(\rho^2)\rho^2 - 4\psi(\rho^2) \right] \rho^4 d\rho$$

and

$$\lambda := \frac{4\pi\kappa}{15} \int_0^\infty \left[\eta(\rho^2)\rho^2 - \psi(\rho^2) \right] \rho^4 d\rho \tag{2.26}$$

depend only on the particle-particle force functions described in Section 2.1 and may be assumed to be constants in many applications.

Observe that (2.25) is essentially just the momentum part of the Navier-Stokes equations (cf. [73, 101] and [102]). There are at least two interesting inferences that may be drawn from this result: Firstly, it provides a partial confirmation of the validity of our integro-partial differential equation model as a predictive tool for granular flow. Secondly, it lends support to the contention that the Navier-Stokes equations are a good model for granular flow behavior obtained from simulation of the Newtonian equations of motion.

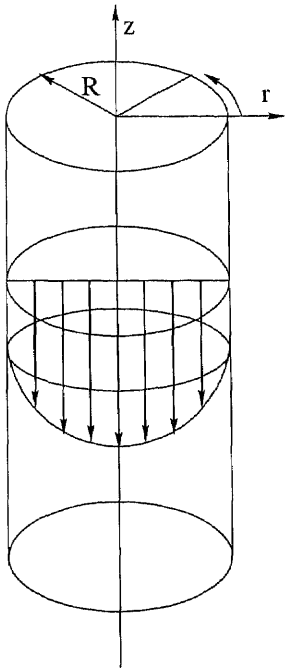

Figure 2.3 Flow through a tube

2.5 Exact Solutions to Some Simple Types of Granular Flows: Flows in Tubes

In this section we obtain an exact solution of the approximate model (2.25) subject to appropriate boundary conditions, for the case of fully developed (steady-state) granular flow, under the action of gravity, through a vertical circular cylindrical pipe illustrated in Figure 2.3. We assume that the density and pressure are constant, hence it suffices to solve (2.25) subject to some boundary conditions.

Under the circumstances, it is convenient to recast (2.25) in terms of standard cylindrical coordinates (r, θ, z) with corresponding velocity components (u, v, w), where u is the radial, v the azimuthal and w is the vertical(axial) component of the flow velocity. The system assumes the following form with respect to cylindrical coordinates:

$$\frac{\partial u}{\partial t} + u\frac{\partial u}{\partial r} + \frac{v}{r}\frac{\partial u}{\partial \theta} + w\frac{\partial u}{\partial z} - \frac{v^2}{r} = \nu\left[\frac{1}{r}\frac{\partial}{\partial r}\left(r\frac{\partial u}{\partial r}\right) + \frac{1}{r^2}\frac{\partial^2 u}{\partial \theta^2} + \frac{\partial^2 u}{\partial z^2}\right] +$$

$$\lambda \frac{\partial}{\partial r}\left[\frac{1}{r}\frac{\partial (ru)}{\partial r} + \frac{1}{r}\frac{\partial v}{\partial \theta} + \frac{\partial w}{\partial z}\right]$$

$$\begin{aligned} \frac{\partial v}{\partial t} + u\frac{\partial v}{\partial r} + \frac{v}{r}\frac{\partial v}{\partial \theta} + w\frac{\partial v}{\partial z} + \frac{uv}{r} &= \nu\left[\frac{1}{r}\frac{\partial}{\partial r}\left(r\frac{\partial v}{\partial r}\right) + \frac{1}{r^2}\frac{\partial^2 v}{\partial \theta^2} + \frac{\partial^2 v}{\partial z^2}\right] + \\ &\quad \frac{\lambda}{r}\frac{\partial}{\partial \theta}\left[\frac{1}{r}\frac{\partial (ru)}{\partial r} + \frac{1}{r}\frac{\partial v}{\partial \theta} + \frac{\partial w}{\partial z}\right] \end{aligned} \tag{2.27}$$

$$\begin{aligned} \frac{\partial w}{\partial t} + u\frac{\partial w}{\partial r} + \frac{v}{r}\frac{\partial w}{\partial \theta} + w\frac{\partial w}{\partial z} &= -g + \nu\left[\frac{1}{r}\frac{\partial}{\partial r}\left(r\frac{\partial w}{\partial r}\right) + \frac{1}{r^2}\frac{\partial^2 w}{\partial \theta^2} + \frac{\partial^2 w}{\partial z^2}\right] + \\ &\quad \lambda\frac{\partial}{\partial z}\left[\frac{1}{r}\frac{\partial (ru)}{\partial r} + \frac{1}{r}\frac{\partial v}{\partial \theta} + \frac{\partial w}{\partial z}\right], \end{aligned}$$

where g is the acceleration of gravity. We assume that the pipe has radius $R > 0$ and that its length is so great that the domain of the granular flow can be represented in idealized form as

$$\Omega := \{(r, \theta, z) : 0 \leq r < R\}.$$

Now we deal with the task of appending appropriate auxiliary data to (2.27) on Ω. As we are seeking a steady-state solution, we assume that the velocity is independent of the time t. There remains the question of realistic auxiliary data on the boundary $\partial\Omega$. Of course, $u \leq 0$ on $\partial\Omega$ is required by the geometry of the pipe (assuming it is rigid and impenetrable). Over time, one may reasonably expect the radial and azimuthal fluctuations in velocity along the inside surface of the pipe to cease, so we shall assume that both u and v vanish on $\partial\Omega$. As for the axial velocity along $\partial\Omega$: the motion of a particle in contact with $\partial\Omega$ is that of free fall with a resisting force due to friction. This suggests that there is a constant limiting (or terminal) velocity along the wall of the pipe (that is achieved in the long-term flow configuration), so it is reasonable to assume that w is a negative constant along $\partial\Omega$. In summary, we take the auxiliary data for (2.27) in Ω to be

$$\frac{\partial u}{\partial t} = \frac{\partial v}{\partial t} = \frac{\partial w}{\partial t} \equiv 0 \quad \text{in } \Omega$$

(2.28)

$$u = v = 0 \quad \text{and} \quad w = -w_0 \quad \text{on} \quad \partial\Omega,$$

where w_0 is a positive constant.

In view of the boundary conditions, it makes sense to seek a solution of (2.27)-(2.28) with $u = v = 0$ and $w = \varphi(r)$. Then the first two equations of (2.27) are trivially satisfied and the third equation yields

$$\frac{\nu}{r}\frac{d}{dr}\left(r\frac{d\varphi}{dr}\right) = g. \tag{2.29}$$

Integrating (2.29), we obtain

$$\varphi = \frac{g}{4\nu}r^2 + c_1 \log r + c_2,$$

where c_1 and c_2 are constants of integration. The solution should be regular at $r = 0$, so we must set $c_1 = 0$. Then (2.28) leads to the following solution:

$$u = v = 0 \quad \text{and} \quad w = \frac{g}{4\nu}\left(r^2 - R^2\right) - w_0. \tag{2.30}$$

It is easy to check that (2.30) satisfies (2.27)-(2.28).

2.6 Inclined Plane Flow Model

The fully developed flow of particles down a two-dimensional inclined plane will be studied in this section using the governing equations (2.25).As inclined plane flow has been extensively investigated (see, for example [6] and [39]), we shall have an opportunity to compare the predictions based upon (2.25) with the results obtained by other researchers, thereby further testing the effectiveness of our approach.

Figure 2.4 depicts the flow geometry for a plane inclined at an angle of θ to the horizontal.

It is convenient to use a Cartesian coordinate system with x measured down along the surface of the inclined plane and $y-$axis normal to the plane and pointing into

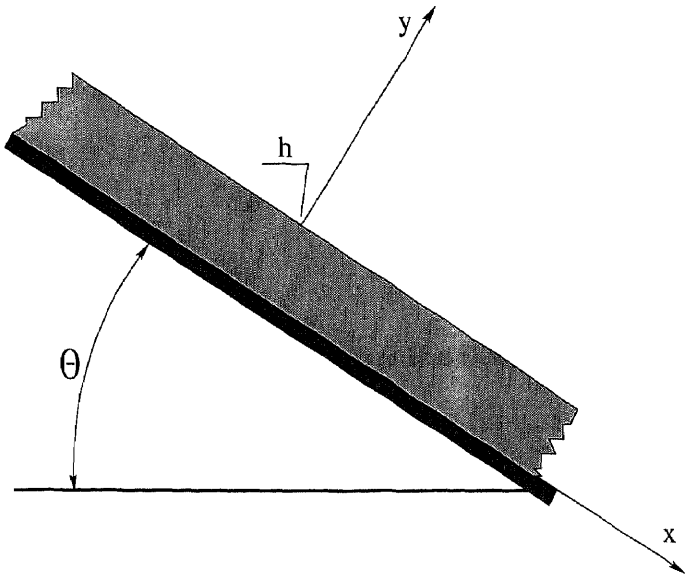

Figure 2.4 Inclined plane flow

the flowing layer of granular material. Here u represents the component of the flow velocity along the $x-$axis and h the depth of the flowing layer. Of course, the figure embodies the usual assumption that the granular flow is essentially two-dimensional.

A clockwise rotation of θ of the coordinate system and a balancing of the gravitational and reaction forces normal to the inclined plane yields the following pair of equations for the granular flow:

$$\frac{\partial u}{\partial t} + u\frac{\partial u}{\partial x} + v\frac{\partial u}{\partial y} = g\,\sin\theta + \nu\left(\frac{\partial^2 u}{\partial x^2} + \frac{\partial^2 u}{\partial y^2}\right) + \lambda\left(\frac{\partial^2 u}{\partial x^2} + \frac{\partial^2 v}{\partial x \partial y}\right) \tag{2.31}$$

$$\frac{\partial v}{\partial t} + u\frac{\partial v}{\partial x} + v\frac{\partial v}{\partial y} = \nu\left(\frac{\partial^2 v}{\partial x^2} + \frac{\partial^2 v}{\partial y^2}\right) + \lambda\left(\frac{\partial^2 u}{\partial x \partial y} + \frac{\partial^2 v}{\partial y^2}\right), \tag{2.32}$$

where v is the $y-$component of the velocity of the granular flow. We assumed in (2.31)-(2.32) that the y-component of the gravity force is balanced by the stationary pressure distribution in the $y-$direction: $\frac{1}{\rho}\frac{\partial p}{\partial y} - g\,cos\,\theta = 0$, and that the pressure is constant along the x-axis. Since the flow is taken to be fully developed (steady-state), it is reasonable to assume that both u and v are independent of the time t. It is also sensible to presuppose that the $y-$component of the velocity vanishes identically and

that u is a function of y only. With these assumptions (2.32) reduces to the trivial equation $0 = 0$ and we are left only with the simple ordinary differential equation

$$\frac{d^2u}{dy^2} = -\frac{g}{\nu}\sin\theta \tag{2.33}$$

representing (2.32).

Appropriate auxiliary data for (2.33) are the free-boundary condition along the free surface representing the interface between the flowing particles and the air that defines the depth of the flowing layer h as the smallest number satisfying

$$\frac{du}{dy}(h) = 0 \quad (h > 0), \tag{2.34}$$

and a slip condition along the inclined plane granular material interface

$$\frac{du}{dy}(0) = ku_0, \tag{2.35}$$

where u_0 is a limiting velocity along the surface of the plane. The component u_0 may be the result of a partial balance between the frictional properties of the plane and the particles and the gravitational component of the force in the $x-$direction or a combination of gravitational and frictional effects and some constant mass flow rate supplied to the system. Here k is some nonnegative constant connected with the nature of the shearing stress in the flowing layer adjacent to the plane that is related to the frictional characteristics of the plane and particles and the dynamical state of the system.

Integrating (2.33) twice using (2.35), we obtain the solution

$$u = u(y) = -\left(\frac{g\,\sin\theta}{2\nu}\right)y^2 + u_0\,(ky + 1)\,. \tag{2.36}$$

Whence we determine the depth of the flowing layer by substitution of (2.34) in (2.36); namely,

$$h = \frac{k\nu u_0}{g\,\sin\theta}, \tag{2.37}$$

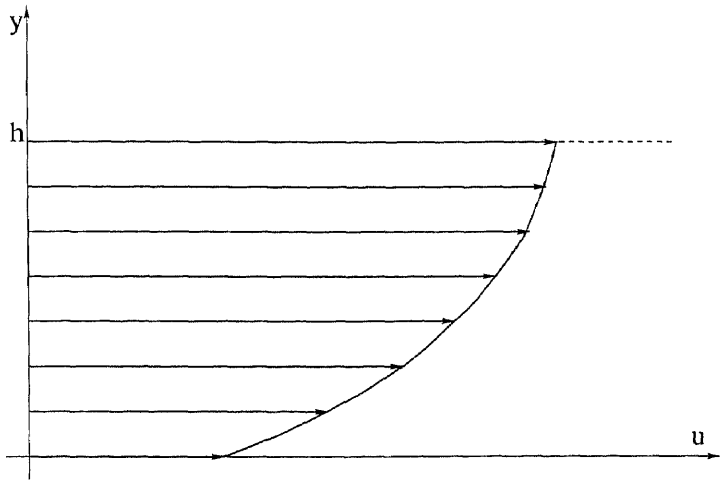

Figure 2.5 Velocity profiles for inclined plane flow

for $\theta > 0$. A typical velocity profile is shown in Figure 2.5.

The extremely simple nature of the solution (2.36) obtained from the governing equation (2.26) notwithstanding, it compares rather well with observations from experimental studies and the predictions from more complicated flow models (cf. [6] and [48]). For example, the form of the velocity profiles illustrated in Figure 5 is qualitatively similar to those measured in experiments and derived from more comprehensive constitutive equations and unlike some fairly popular models, (2.37) shows that our approach predicts a decrease in the depth of the flowing layer with increasing inclination angle of the plane.

CHAPTER 3

SOME ASPECTS OF THE THEORY OF DYNAMICAL SYSTEMS ASSOCIATED WITH PARTICLE FLOW MODELS

3.1 Existence and Uniqueness of a Solution to the Granular Flow Problem

In this chapter we shall prove theorems of existence and uniqueness of a solution to the dynamical system (2.25) subject to some prescribed boundary conditions. Let us consider a two-dimensional steady-state granular flow in a symmetric infinite tube with curvilinear walls (see Fig. 3.1). This flow generalizes granular flows in tubes and hoppers. Let Ω be a bounded open set in $\mathbf{R}^2$ with boundary $\partial\Omega$. We shall denote by $\bar{\Omega}$ the closure $\Omega \bigcup \partial\Omega$. Let $\partial\Omega = \partial\Omega_1 \bigcup \partial\Omega_2 \bigcup \partial\Omega_3 \bigcup \partial\Omega_4$, where $\partial\Omega_1$ and $\partial\Omega_2$ are horizontal intersections of the tube.

The equation governing the steady-state granular flow in the tube is

$$(\mathbf{v} \cdot \nabla)\mathbf{v} = \mathbf{G} - \nabla p + \nu\Delta\mathbf{v} + \lambda\nabla(\nabla\mathbf{v}) \quad \text{in } \Omega, \tag{3.1}$$

and the boundary conditions are

$$\begin{aligned} u|_{\partial\Omega_1} &= u|_{\partial\Omega_2} = 0, \\ \left.\frac{\partial v}{\partial y}\right|_{\partial\Omega_1} &= \left.\frac{\partial v}{\partial y}\right|_{\partial\Omega_2} = 0, \end{aligned} \tag{3.2}$$

where $u(x, y)$ and $v(x, y)$ are the horizontal and vertical components of the velocity field, respectively. The second expression in (3.2) means that boundaries $\partial\Omega_1$ and $\partial\Omega_2$ are sufficiently far from the domain of spatially nonuniform flow, as is shown in the Fig. 3.1. We use the same boundary conditions for the side walls as in the previous chapter:

$$\begin{aligned} u_n|_{\partial\Omega_3} &= u_n|_{\partial\Omega_4} = 0, \\ \left.\left(\frac{\partial u_\tau}{\partial n} - k u_\tau\right)\right|_{\partial\Omega_3} &= \left.\left(\frac{\partial u_\tau}{\partial n} - k u_\tau\right)\right|_{\partial\Omega_4} = 0, \end{aligned} \tag{3.3}$$

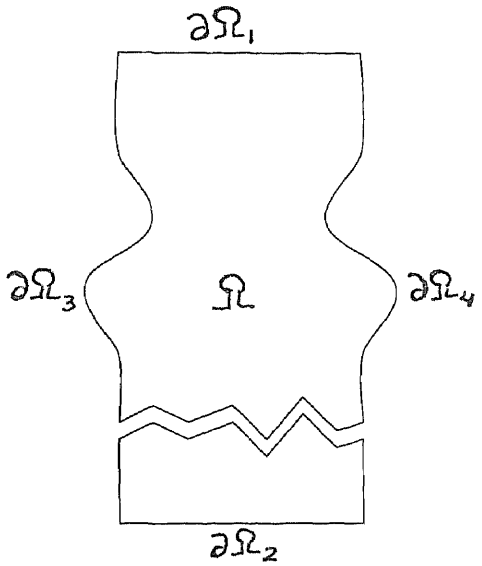

Figure 3.1 Flow in two-dimensional axisymmetric tube

where u_n and u_τ denote the component of the velocity field normal to the wall and the tangential component of the velocity field, respectively. The axial symmetry of the problem implies the following additional boundary conditions:

$$u_\tau|_{\partial\Omega_3} = u_\tau|_{\partial\Omega_4}\,. \tag{3.4}$$

Some functional spaces

Let Ω be an open set in $\mathbf{R}^n$. We denote by $L^p(\Omega)$, $1 < p < \infty$, the space of real functions defined on Ω which are p-th power absolutely integrable (or essentially bounded real functions) for the Lebesgue measure $dx = dx_1 \ldots dx_n$. This is a Banach space with the norm

$$\|\mathbf{u}\|_{L^p(\Omega)} = \left(\int_\Omega |\mathbf{u}(x)|^p\, dx\right)^{1/p}. \tag{3.5}$$

For $p = 2$, $L^2(\Omega)$ is a Hilbert space with the scalar product

$$(\mathbf{u}, \mathbf{v}) = \int_\Omega \mathbf{u}(x)\mathbf{v}(x)\, dx. \tag{3.6}$$

The Sobolev space $W^{m,p}(\Omega)$ is the space of functions in $L^p(\Omega)$ with derivatives of order less than or equal to m in $L^p(\Omega)$ (m an integer, $1 \leq p \leq +\infty$). This is a

Banach space with the norm

$$\|\mathbf{u}\|_{W^{m,p}(\Omega)} = \left(\sum_{[j]\leq m} \|D^j \mathbf{u}\|^p_{L^p(\Omega)} \right)^{1/p}. \tag{3.7}$$

When $p = 2$, $W^{m,p}(\Omega) = H^m(\Omega)$ is a Hilbert space with the scalar product

$$((\mathbf{u}, \mathbf{v}))_{H^m(\Omega)} = \sum_{[j]\leq m} (D^j \mathbf{u}, D^j \mathbf{v}). \tag{3.8}$$

We shall denote by $\tilde{H}^1(\bar{\Omega})$ the space

$$\tilde{H}^1(\bar{\Omega}) = \{\mathbf{u} \,|\mathbf{u} \in H^1(\bar{\Omega}),\ (\nabla \cdot \mathbf{u}) \in L^2(\bar{\Omega})\}, \tag{3.9}$$

and by $\tilde{H}^1_0(\bar{\Omega})$ the following space:

$$\tilde{H}^1_0(\bar{\Omega}) = \{\mathbf{u} \,|\mathbf{u} \in \tilde{H}^1(\bar{\Omega}),\ \ \mathbf{u} \text{ satisfies (3.2)-(3.4)}\} \tag{3.10}$$

The spaces $H^1(\bar{\Omega})$ and $\tilde{H}^1_0(\bar{\Omega})$ are two basic spaces in the study of the granular flow dynamical system. Our consideration will be similar to that presented in [61].

Variational formulation of the problem

Let Ω be a bounded open set in $\mathbf{R}^2$ with boundary $\partial\Omega$ as described above. We are looking for a vector function $\mathbf{v} = (u(x, y), v(x, y))$ representing the velocity field of the system of particles and a vector function $\mathbf{f}$ representing the gravity forces and the internal pressure gradient as follows

$$\mathbf{f} = \mathbf{G} - \operatorname{grad} p,$$

which are defined on Ω and satisfy the equation (3.1) and the boundary conditions (3.2)-(3.4). Therefore, $\mathbf{v} \in \tilde{H}^1_0$. By taking the scalar product of (3.1) with a function $\mathbf{u} \in \tilde{H}^1_0$ we obtain

$$\nu((\mathbf{v}, \mathbf{u})) + b(\mathbf{v}, \mathbf{v}, \mathbf{u}) + \lambda(\nabla \mathbf{v}, \nabla \mathbf{u}) = (\mathbf{f}, \mathbf{u}), \tag{3.11}$$

where $((.,.)) \equiv ((.,.))_{H^1(\Omega)}$ and b is the trilinear form

$$b(\mathbf{u},\mathbf{v},\mathbf{w}) = \sum_{i,j=1}^{n} \int_{\Omega} u_i (D_i v_j) w_j \, dx. \tag{3.12}$$

We shall associate with (3.1)-(3.4) the following variational problem: to find $\mathbf{v} \in \tilde{H}_0^1$ such that (3.11) to be satisfied for $\forall \mathbf{u} \in \tilde{H}_0^1$. We shall need the following theorem of de Rham [55]:

Proposition 3.1. *Let Ω be an open set in $\mathbf{R}^n$ and $\mathbf{f} = (f_1, \ldots, f_n)$, $f_i \in \mathcal{D}^1(\Omega)$, $i = 1, \ldots, n$. Here we denoted by $\mathcal{D}^1(\Omega)$ the space of C^1 functions with compact support contained in Ω (or $\bar{\Omega}$). Then necessary and sufficient conditions that*

$$\mathbf{f} = grad\, p$$

for some p in $\mathcal{D}^1(\Omega)$, is that

$$\langle \mathbf{f}, \mathbf{v} \rangle = 0$$

for $\forall \mathbf{v} \in \mathcal{V} \equiv \{\mathbf{u} \,|\, \mathbf{u} \in \mathcal{D}(\Omega),\ div\, \mathbf{u} = 0\}$.

The following theorem is closely connected with Proposition 3.1.

Proposition 3.2. *Let Ω be a bounded Lipschitz open set in $\mathbf{R}^n$.*

i) If a distribution p has all its first-order derivatives $D_i p$, $1 \le i \le n$, in $L^2(\Omega)$, then $p \in L^2(\Omega)$ and

$$\|p\|_{L^2(\Omega)/\mathbf{R}} \le c(\Omega) \|grad\, p\|_{L^2(\Omega)},$$

where $c(\Omega)$ is a constant depending only on Ω.

ii) If a distribution has all first derivatives $D_i p$, $1 \le i \le n$, in $H^{-1}(\Omega)$, then $p \in L^2(\Omega)$ and

$$\|p\|_{L^2(\Omega)/\mathbf{R}} \le c(\Omega) \|grad\, p\|_{H^{-1}(\Omega)},$$

where H^{-1} denotes the dual space to H^1.

In both cases, if Ω is any open set in $\mathbf{R}^n$, $p \in L^2_{loc}(\Omega)$, where L^2_{loc} represents the space of locally square integrable functions.

Now, we can prove the

Theorem 3.1 (Equivalence of formulations).

i) If $\mathbf{v} \in \tilde{H}^1_0$ satisfies (3.1)-(3.4), then (3.11) is satisfied for $\forall \mathbf{u} \in \tilde{H}^1_0(\Omega)$;

ii) If $\mathbf{v} \in \tilde{H}^1_0$ satisfies (3.11) for any $\mathbf{u} \in \tilde{H}^1_0(\Omega)$, then there is an internal pressure distribution p such that (3.1) is satisfied (in the distribution sense), and (3.2)-(3.4) are satisfied since $\mathbf{v} \in \tilde{H}^1_0(\Omega)$.

Proof. The proof of i) consists of a direct calculation. If $\mathbf{v}$ and p are smooth functions satisfying (3.1)-(3.4), then by taking the scalar product with any $u \in \tilde{H}^1_0(\Omega)$ we can show that $\mathbf{v}$ satisfies (3.11) for $\forall \mathbf{u} \in \tilde{H}^1_0$. Conversely, if $\mathbf{v} \in \tilde{H}^1_0$ satisfies (3.11), then

$$\langle -\nu \Delta \mathbf{v} + \sum_i v_i D_i \mathbf{v} - \lambda \nabla(\nabla \mathbf{v}) - \mathbf{f}, \mathbf{u} \rangle = 0 \tag{3.13}$$

for $\forall u \in \tilde{H}^1_0(\Omega)$, $\Delta \mathbf{v} \in H^{-1}(\Omega)$, $\mathbf{f} \in L^2(\Omega)$, and $D_i \mathbf{v}$, v_i and $v_i D_i \mathbf{v} \in L^2$. Now, according to Propositions 3.1 and 3.2, there exists a distribution $p \in L^1_{loc}(\Omega)$ such that (3.1) is satisfied in the distribution sense; thus (3.2)-(3.4) are satisfied respectively in the distribution and trace theorem senses. □

Theorem 3.2. (Existence of a solution) *Under the above assumptions, the problem (3.11) has at least one solution $\mathbf{v} \in \tilde{H}^1_0(\Omega)$ and there exists a distribution $p \in L^1_{loc}(\Omega)$ such that (3.1)-(3.4) are satisfied.*

Proof. We have only to prove the existence of $\mathbf{v}$. The existence of p and the interpretation of (3.1)-(3.4) have already been shown. The idea of the proof is to construct Galerkin's approximations for a solution to (3.11) and then pass to the limit.

We shall use the following properties of the form $b(\mathbf{u}, \mathbf{v}, \mathbf{w})$ that follow directly from the same properties of the form b formulated in [103] for a slightly different functional space.

Proposition 3.3. *The form $b(\mathbf{u}, \mathbf{v}, \mathbf{w})$ is defined and trilinear continuous on $\tilde{H}^1(\Omega) \times \tilde{H}^1(\Omega) \times (\tilde{H}^1(\Omega) \bigcap L^2(\Omega))$, for Ω bounded or unbounded. If Ω is bounded then b is trilinear continuous on $\tilde{H}^1(\Omega) \times \tilde{H}^1(\Omega) \times \tilde{H}^1(\Omega)$. In addition, on this space*

$$b(\mathbf{u}, \mathbf{v}, \mathbf{v}) = 0, \tag{3.14}$$

$$b(\mathbf{u}, \mathbf{v}, \mathbf{w}) = -b(\mathbf{u}, \mathbf{w}, \mathbf{v}), \tag{3.15}$$

$$\|b(\mathbf{u}, \mathbf{v}, \mathbf{w})\| \leq c\|\mathbf{u}\|\|\mathbf{v}\|\|\mathbf{w}\|, \tag{3.16}$$

where c is a constant.

Let w_j, $j = 1, 2, \ldots$ be a basis in $\tilde{H}_0^1(\Omega)$. For each fixed integer $m \geq 1$ an approximate solution to (3.11) is defined by

$$\mathbf{v}_m = \sum_{i=1}^{m} \xi_i^m \mathbf{w}_i, \quad \xi_i^m \in \mathbf{R}^1, \tag{3.17}$$

$$\nu((\mathbf{v}_m, \mathbf{w}_k)) + b(\mathbf{v}_m, \mathbf{v}_m, \mathbf{w}_k) + \lambda(\nabla \mathbf{v}_m, \nabla \mathbf{w}_k) = (\mathbf{f}, \mathbf{w}), \quad k = 1, \ldots, m. \tag{3.18}$$

The equations (3.17)-(3.18) are a system of nonlinear equations for $\xi_1^m, \ldots, \xi_m^m$. The existence of a solution to this system is a consequence of the following result [103].

Proposition 3.4. *Let X be a finite-dimensional Hilbert space with a scalar product $[.,.]$ and a norm $[.]$ and let P be a continuous mapping from X into itself such that*

$$[P(\xi), \xi] > 0 \quad \textit{for } [\xi] = k > 0.$$

Then there exists $\xi \in X$, $[\xi] \leq k$ such that

$$P(\xi) = 0.$$

Let X be a space spanned by $w_1, \ldots, w_n$; the scalar product on X is the scalar product induced by H^1, and $P = P_m$ is defined by the expression

$$[P_m(\mathbf{v}), \mathbf{u}] = \nu((\mathbf{v}, \mathbf{u})) + b(\mathbf{v}, \mathbf{v}, \mathbf{u}) + \lambda(\nabla\, \mathbf{v}, \nabla\, \mathbf{u}) - (\mathbf{f}, \mathbf{u}), \quad \mathbf{u}, \mathbf{v} \in X. \tag{3.19}$$

The mapping P_m is obviously continuous. Then

$$[P_m(\mathbf{v}), \mathbf{v}] = \nu\|\mathbf{v}\|^2 + b(\mathbf{v}, \mathbf{v}, \mathbf{v}) + \lambda\|\nabla u\|^2 - (\mathbf{f}, \mathbf{v}) =$$

$$= \text{ by (3.14)} \quad \nu\|\mathbf{v}\|^2 + \lambda\|\nabla \mathbf{v}\|^2 - (\mathbf{f}, \mathbf{v}) \geq$$

$$\geq \nu\|\mathbf{v}\|^2 + \lambda\|\nabla \mathbf{v}\|^2 - \|\mathbf{f}\|\|\mathbf{v}\| > 0$$

for $\|\mathbf{v}\|$ sufficiently large. The hypotheses of Proposition 3.4 are satisfied that implies the existence of a solution to (3.17)-(3.18).

Passage to the limit

Now we multiply (3.18) by ξ_k^m and sum up these expressions for $k = 1, \ldots, m$; this gives

$$\nu\|\mathbf{v}_m\|^2 + b(\mathbf{v}_m, \mathbf{v}^m, \mathbf{v}_m) + \lambda\|\nabla \mathbf{v}_m\|^2 = \langle \mathbf{f}, \mathbf{v}_m \rangle, \tag{3.20}$$

or because of (3.14)

$$\nu\|\mathbf{v}_m\|^2 + \lambda\|\nabla \mathbf{v}_m\|^2 = \langle \mathbf{f}, \mathbf{v}_m \rangle \leq \|\mathbf{f}\|\|\mathbf{v}_m\|,$$

$$\nu\|\mathbf{v}_m\|^2 + \frac{\lambda}{\|\mathbf{v}_m\|}\|\nabla \mathbf{v}_m\|^2 \leq \|\mathbf{f}\|. \tag{3.21}$$

The inequality (3.21) implies that $\{\mathbf{v}_m\}$ has an upper bound. Since the sequence $\{\mathbf{v}_m\}$ is bounded in $\tilde{H}_0^1$, there exists some $\mathbf{v}$ in $\tilde{H}_0^1$ and a subsequence $\{\mathbf{v}_{m'}\}$ such that

$$\mathbf{v}_{m'} \to \mathbf{v} \quad \text{in the norm of } L^2(\Omega)$$

as $m' \to \infty$. Then we can pass to the limit in (3.18) for the subsequence as $m' \to \infty$ and find that

$$\nu((\mathbf{v}, \mathbf{u})) + b(\mathbf{v}, \mathbf{v}, \mathbf{u}) + \lambda(\nabla \mathbf{v}, \nabla \mathbf{u}) = (\mathbf{f}, \mathbf{u}) \tag{3.22}$$

for any $\mathbf{u} = w_1, \ldots, w_n, \ldots$. Equation (3.22) also holds for any $\mathbf{u}$ which is a linear combination of $w_1, \ldots, w_n, \ldots$. Since these combinations are dense in $\tilde{H}_0^1$, a continuity argument finally shows that (3.22) holds for each $\mathbf{u} \in \tilde{H}_0^1$ and that $\mathbf{v}$ is a solution of (3.11).

Uniqueness of a solution

Let $\mathbf{v}_1$ and $\mathbf{v}_2$ be two different solutions and $\mathbf{v} = \mathbf{v}_1 - \mathbf{v}_2$. Then we subtract the equations (3.11) corresponding to $\mathbf{v}_1$ and $\mathbf{v}_2$ and obtain

$$\nu((\mathbf{v}, \mathbf{u})) + \lambda(\nabla \mathbf{v}, \nabla \mathbf{u}) + b(\mathbf{v}_1, \mathbf{v}, \mathbf{u}) + b(\mathbf{v}, \mathbf{v}_1, \mathbf{u}) = (\mathbf{f}, \mathbf{u}) \tag{3.23}$$

Taking $\mathbf{u} = \mathbf{v}$ and using the properties of the trilinear form (3.14)-(3.16) we obtain

$$\nu\|\mathbf{v}\|^2 + \lambda\|\mathbf{v}\| = -b(\mathbf{v}, \mathbf{v}_1, \mathbf{v}),$$

$$\nu\|\mathbf{v}\|^2 + \lambda\|\mathbf{v}\| \leq c\|\mathbf{v}\|^2\|\mathbf{v}_1\|,$$

$$(\nu - c\|\mathbf{v}_1\|)\|\mathbf{v}\|^2 + \lambda\|\nabla \mathbf{v}\| \leq 0. \tag{3.24}$$

Since $\mathbf{v}_1$ is bounded (as was shown in the previous theorem), the relations (3.24) fail when

$$(c\|\mathbf{v}_1\| - \nu) \leq \lambda \frac{\|\nabla \mathbf{v}\|}{\|\mathbf{v}\|^2},$$

which must be true for some values of the parameters if $\mathbf{v} \neq 0$. We conclude that $\mathbf{v} = 0$, and thus the solution is unique.

3.2 Approximate Inertial Manifolds for Granular Flow Dynamical Systems

3.2.1 Preliminaries: Approximate Inertial Manifolds

The concept of the approximate inertial manifold (AIM) introduced in [32, 33, 34] is a link between the rigorous mathematical theory of inertial manifolds [102, 8] and

the applied theory of dynamical systems. The AIM is a finite-dimensional smooth submanifold of the phase space of a dissipative dynamical system such that all the orbits enter (and remain in) a thin neighborhood of this manifold after some finite (transient) time. The definition of an AIM allows us to reduce an infinite-dimensional dynamical system to a finite-dimensional one called the inertial form, to establish localization theorems for global attractors, and to develop new approaches to numerical investigations of the long-time dynamics. These numerical methods, called nonlinear Galerkin methods [61, 44], use the main idea of the AIM theory, namely that the "higher" order modes in an expansion of a solution can be expressed in terms of the "lower" order ones by making use of the nonlinearity of a dissipative dynamical system. The nonlinear Galerkin methods have been implemented widely, in conjunction with spectral techniques, for different types of dynamical systems and have demonstrated an essential improvement in accuracy over traditional schemes. An alternative approach in nonlinear Galerkin methods was suggested in [60], where an approximate inertial form in finite differences was constructed using some specific set of basis functions. The aim of this study is to generalize these ideas, to develop a numerical scheme for two-dimensional inertial form calculation, and to apply this method to a granular flow dynamical system. The main advantage of the method over spectral nonlinear Galerkin schemes is its flexibility in terms of the variety of boundary conditions it can accomodate.

Definition. Let a nonlinear dynamical system be given as a semigrioup of continuous operators $\{S(t)\}_{t\geq 0}$ in a Hilbert space H. An inertial manifold for this semigroup is a Lipshitz finite-dimensional manifold $\mathcal{M}$ in H such that

$$S(t)\mathcal{M} \subset \mathcal{M}, \quad t \geq 0,$$

and for every $u_0 \in H$, $S(t)u_0$ converges to $\mathcal{M}$ at an exponential rate, i.e.,

$$dist\,(S(t)u_0, \mathcal{M}) \leq c_1\, exp(-c_2 t),$$

where c_1, c_2 depend on $\|u_0\|$.

When an inertial manifold exists, the restriction of $S(t)$ to $\mathcal{M}$ defines a finite-dimensional semigroup of operators $\{\Sigma(t)\}_{t\geq 0}$,

$$\Sigma(t) = S(t)|_{\mathcal{M}},$$

$$\Sigma(t) : \mathcal{M} \to \mathcal{M},$$

which fully reproduces the dynamics of the initial dynamical system (or the semigroup of operators). This system is called an *inertial system.*

Let a dissipative evolution partial differential equation (PDE) be given in the functional form

$$\frac{du}{dt} + Au + F(u) = 0, \quad u \in H \tag{3.25}$$

where H is a Hilbert space of solutions, Au is the leading order linear term corresponding to dissipation and $F(u)$ is the nonlinear part of equation. We assume that the operator A has eigenvalues with the following property:

$$Aw_j = -\lambda_j w, \quad j = 0, 1, \ldots$$

$$0 \leq \lambda_0 \leq \lambda_1 \leq \ldots, \quad \lambda_j \to \infty \text{ as } j \to \infty,$$

and a complete set of eigenfunctions.

For a fixed integer m we denote by P_m the orthogonal projector onto the space spanned by $w_0, \ldots, w_m$. Then $Q_m = I - P_m$ is the projector onto the complement space. The equation (3.25) can be written as

$$\begin{aligned} &\frac{dp_m}{dt} + Ap_m + P_m F(p_m + q_m) = 0, \\ &\frac{dq_m}{dt} + Aq_m + Q_m F(p_m + q_m) = 0, \end{aligned} \tag{3.26}$$

where $p_m = P_m u$, $q_m = Q_m u$, and $u = p_m + q_m$.

The main idea of an approximate inertial manifold (AIM) comes from the following observation [33, 102, 8]: after a certain time, depending only on the initial data u_0 and on the equation, the size of $q_m(t)$ for some dissipative dynamical systems becomes and remains small in some sense, say

$$|q_m(t)| \leq \delta,$$

where δ is proportional to an appropriate power of λ_0/λ_{m+1}. Then the approximate inertial manifold is the graph of the function $\Phi : P_m H \to Q_m H$

$$q_m = \Phi(p_m), \tag{3.27}$$

and the dynamics of (3.25) can be expressed in terms of the finite-dimensional dynamical system

$$\frac{dp_m}{dt} + Ap_m + P_m F(p_m + \Phi(p_m)) = 0, \tag{3.28}$$

called the inertial form of (3.25). Notice that the inertial form reduces to the usual Galerkin approximation of the initial PDE if we assume $\Phi(p_m) = 0$.

A common approach in finding approximate inertial manifolds is based on the assumption $\frac{dq_m}{dt} = 0$. It consists in finding a fixed point of the mapping (which in certain cases is a contraction)

$$q_m = -A^{-1}Q_m F(p_m + q_m). \tag{3.29}$$

Taking the first and second iterates yields explicit functions

$$\Phi_1(p_m) = -A^{-1}Q_m F(p_m),$$

$$\Phi_2(p_m) = -A^{-1}Q_m F(p_m + \Phi_1(p_m)), \tag{3.30}$$

respectively. These two approximations were used in [32, 105, 44] for practical calculations. A slightly different approach motivated by an implicit Euler integration step was introduced by Foias *et al.* [34] and tested numerically in [35].

In the present section we apply the concept of separating modes in the theory of AIM to two-dimensional finite-differences. Our derivation uses the ideas similar to those applied by Margolin and Jones [60] to the one-dimensional Burgers equation.

3.2.2 AIM in Finite-Differences: the Modified Finite-Difference Scheme

In order to use the fact that higher order modes in the expansion of a solution to some dissipative dynamical systems can approximately be expressed in terms of the lower order ones, we need to introduce an appropriate set of basis functions for finite-differences. This set is not so natural as the set of eigenfunctions for the spectral method in AIM-theory where the lower modes correspond to the first N eigenfunctions and the higher ones are eigenfunctions $w_{N+1}, \ldots, w_{N+k}, \ldots$. The standard higher order finite-difference method employes an increase in the number of cells by, say, 4 times, but all the new cells are equal and cannot be subdivided into the "main" and "second" modes. We can avoid this difficulty by introducing the following set of basis functions for higher order finite-differences (see Fig. 3.2):

$$|f_{i,j}(x,y)>=\begin{cases} 1, & (x,y)\in\Omega_{i,j}\equiv(x_j-\frac{\Delta x}{2},x_j+\frac{\Delta x}{2})\times(y_i-\frac{\Delta y}{2},y_i+\frac{\Delta y}{2}),\\ 0, & (x,y)\notin\Omega_{i,j},\end{cases}$$

$$|h_{i,j}(x,y)>=\begin{cases} 1, & (x,y)\in(x_j-\frac{\Delta x}{2},x_j+\frac{\Delta x}{2})\times(y_i,y_i+\frac{\Delta y}{2}),\\ -1, & (x,y)\in(x_j-\frac{\Delta x}{2},x_j+\frac{\Delta x}{2})\times(y_i-\frac{\Delta y}{2},y_i),\\ 0, & (x,y)\notin\Omega_{i,j},\end{cases} \tag{3.31}$$

$$|g_{i,j}(x,y)>=\begin{cases} 1, & (x,y)\in(x_j,x_j+\frac{\Delta x}{2})\times(y_i-\frac{\Delta y}{2},y_i+\frac{\Delta y}{2}),\\ -1, & (x,y)\in(x_j-\frac{\Delta x}{2},x_j)\times(y_i-\frac{\Delta y}{2},y_i+\frac{\Delta y}{2}),\\ 0, & (x,y)\notin\Omega_{i,j}.\end{cases}$$

We use the notation $|\ldots>$ for basis functions to distinguish them from coefficients in our equations.

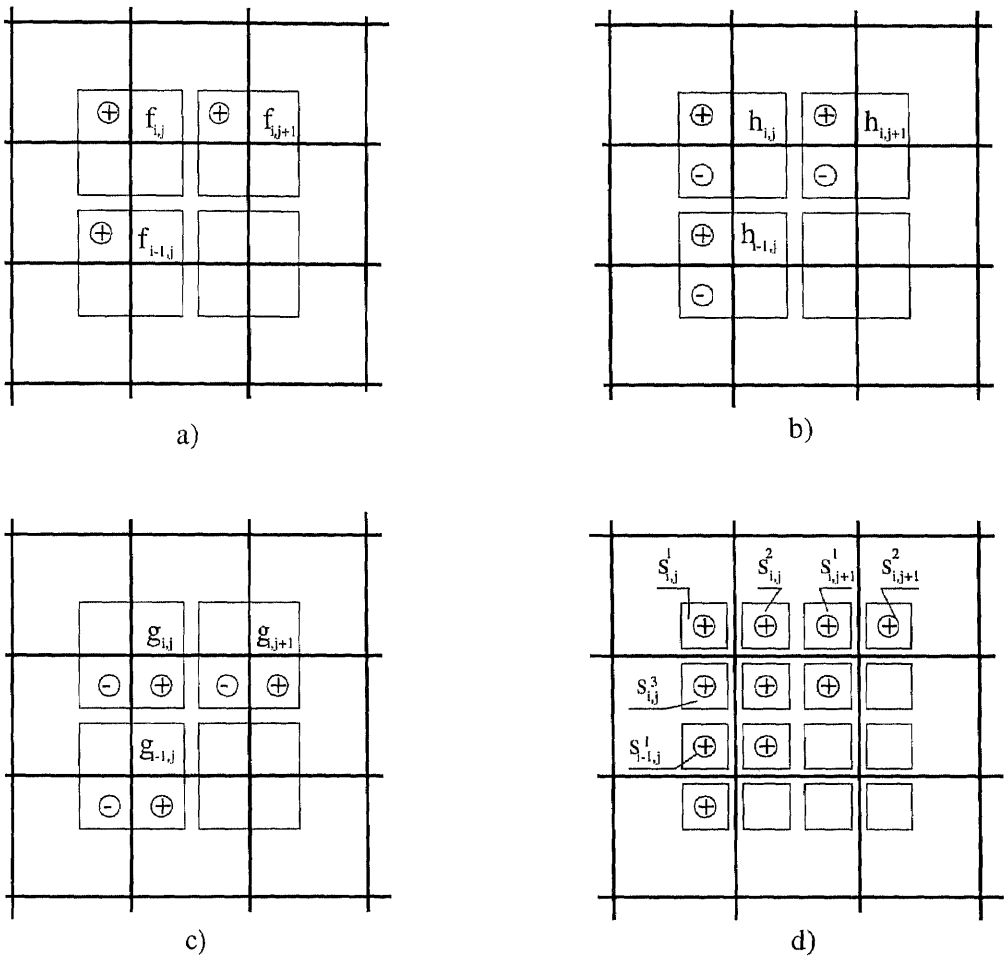

Figure 3.2 Set of basis functions

The functions $|f_{i,j}(x,y)>$ corresponding to the standard finite-difference scheme represent average values of some function within the cell. In that sense the functions $|h_{i,j}(x,y)>$ and $|g_{i,j}(x,y)>$ represent values of the partial derivatives ($\partial/\partial x$ and $\partial/\partial y$) within the cell and can be treated as the higher order modes. We shall prove that the following representation of a function $u(x,y)$ in this basis,

$$u(x,y)=\sum_{i,j=1}^{N}(a_{i,j}|f_{i,j}(x,y)>+b_{i,j}|g_{i,j}(x,y)>+c_{i,j}|h_{i,j}(x,y)>), \tag{3.32}$$

has the same order of accuracy as its representation in the standard higher order finite-difference basis with $4N^2$ cells:

$$u(x,y)=\sum_{i,j=1}^{N}(\alpha_{i,j}|S^1_{i,j}(x,y)>+\beta_{i,j}|S^2_{i,j}(x,y)>+\gamma_{i,j}|S^3_{i,j}(x,y)>)+\delta_{i,j}|S^4_{i,j}(x,y)>. \tag{3.33}$$

Here $|S^k_{i,j}(x,y)>$, $k=1,\ldots,4$ are the following functions (see Fig. 3.2):

$$\begin{aligned}
|S^1_{i,j}(x,y)> &= \begin{cases} 1, & (x,y)\in(x_j-\frac{\Delta x}{2},x_j)\times(y_i,y_i+\frac{\Delta y}{2}),\\ 0, & (x,y)\notin(x_j-\frac{\Delta x}{2},x_j)\times(y_i,y_i+\frac{\Delta y}{2}),\end{cases}\\
|S^2_{i,j}(x,y)> &= \begin{cases} 1, & (x,y)\in(x_j,x_j+\frac{\Delta x}{2})\times(y_i,y_i+\frac{\Delta y}{2}),\\ 0, & (x,y)\notin(x_j,x_j+\frac{\Delta x}{2})\times(y_i,y_i+\frac{\Delta y}{2}),\end{cases}\\
|S^3_{i,j}(x,y)> &= \begin{cases} 1, & (x,y)\in(x_j-\frac{\Delta x}{2},x_j)\times(y_i-\frac{\Delta y}{2},y_i),\\ 0, & (x,y)\notin(x_j-\frac{\Delta x}{2},x_j)\times(y_i-\frac{\Delta y}{2},y_i),\end{cases}\\
|S^4_{i,j}(x,y)> &= \begin{cases} 1, & (x,y)\in(x_j,x_j+\frac{\Delta x}{2})\times(y_i-\frac{\Delta y}{2},y_i),\\ 0, & (x,y)\notin(x_j,x_j+\frac{\Delta x}{2})\times(y_i-\frac{\Delta y}{2},y_i).\end{cases}
\end{aligned} \tag{3.34}$$

We define the inner product in the space of basis functions by

$$<f_{i,j}(x,y)|g_{m,n}(x,y)>=\int_D|f_{i,j}(x,y)>\,|g_{m,n}(x,y)>\,dxdy. \tag{3.35}$$

The basis elements are orthogonal with respect to this inner product:

$$\begin{aligned}
&<f_{i,j}|f_{m,n}>=<h_{i,j}|h_{m,n}>=<g_{i,j}|g_{m,n}>=\Delta x\Delta y\delta_{im}\delta_{jn},\\
&<f_{i,j}|h_{m,n}>=<f_{i,j}|g_{m,n}>=<g_{i,j}|h_{m,n}>=0
\end{aligned} \tag{3.36}$$

for the first set of functions, where δ is the Kronecker delta, and

$$< S^k_{i,j} | S^p_{m,n} >= \frac{1}{4}\Delta x \Delta y \delta_{im}\delta_{jn}\delta_{kp} \tag{3.37}$$

for the second one. We shall also need values of the inner product between elements of different bases:

$$\begin{aligned}
< f_{i,j} | S^k_{m,n} > &= \frac{1}{4}\Delta x \Delta y \delta_{im}\delta_{jn}, \quad k = 1,2,3,4, \\
< h_{i,j} | S^k_{m,n} > &= \begin{cases} \frac{1}{4}\Delta x \Delta y \delta_{im}\delta_{jn}, & k = 1,2, \\ -\frac{1}{4}\Delta x \Delta y \delta_{im}\delta_{jn}, & k = 3,4, \end{cases} \\
< g_{i,j} | S^k_{m,n} > &= \begin{cases} \frac{1}{4}\Delta x \Delta y \delta_{im}\delta_{jn}, & k = 2,4, \\ -\frac{1}{4}\Delta x \Delta y \delta_{im}\delta_{jn}, & k = 1,3. \end{cases}
\end{aligned} \tag{3.38}$$

By taking the inner product of (3.32) and (3.33) with different basis elements, we can show that the coefficients of the expansion of $u(x,y)$ in the two sets of basis elements satisfy the following relations:

$$\begin{aligned}
a_{i,j} &= \frac{1}{4}(\alpha_{i,j} + \beta_{i,j} + \gamma_{i,j} + \delta_{i,j}), \\
b_{i,j} &= \frac{1}{4}(-\alpha_{i,j} + \beta_{i,j} - \gamma_{i,j} + \delta_{i,j}), \\
c_{i,j} &= \frac{1}{4}(\alpha_{i,j} + \beta_{i,j} - \gamma_{i,j} - \delta_{i,j}),
\end{aligned} \tag{3.39}$$

$$\begin{aligned}
\alpha_{i,j} &= \frac{1}{4}(a_{i,j} - b_{i,j} + c_{i,j}), \\
\beta_{i,j} &= \frac{1}{4}(a_{i,j} + b_{i,j} + c_{i,j}), \\
\gamma_{i,j} &= \frac{1}{4}(a_{i,j} - b_{i,j} - c_{i,j}). \\
\delta_{i,j} &= \frac{1}{4}(a_{i,j} + b_{i,j} - c_{i,j}).
\end{aligned} \tag{3.40}$$

Using (3.33), (3.34) and the explicit finite-difference formulas for derivatives, we can write an arbitrary dynamical system in the higher order basis $|S^k_{i,j}(x,y)>$. For example, the partial derivative $\partial^2 u(x,y)/\partial x^2$ can be expressed as

$$\frac{\partial^2 u}{\partial x^2} = \frac{4}{\Delta x^2}\sum_{i,j=1}^{N}\Big[(\beta_{i,j} - 2\alpha_{i,j} + \beta_{i,j-1})|S^1_{i,j}> + (\alpha_{i,j+1} - 2\beta_{i,j} + \alpha_{i,j})|S^2_{i,j}> +$$

$$+(\delta_{i,j} - 2\gamma_{i,j} + \delta_{i,j-1})|S^3_{i,j}> +(\gamma_{i,j+1} - 2\delta_{i,j} + \gamma_{i,j})|S^3_{i,j}>\Big] .$$

Then rewriting this system in terms of $|f_{i,j}>$, $|g_{i,j}>$ and $|h_{i,j}>$ we shall be able to construct a finite-difference analog of the AIM (3.30) and to describe the dynamics of our system in terms of only the coefficients $a_{i,j}$.

3.2.3 Application to a Granular Flow Dynamical System

We shall implement the finite-difference construction of the AIM for the two-dimensional granular flow dynamical system (2.25).

As we mentioned in Chapter 1, the approximate model for granular flow dynamics differs from the Navier-Stokes equations for incompressible fluid by only the last term that is proportional to λ. Thus the velocity field is not divergence-free and this is responsible for local changes in pressure due to small changes in the density of the flow. We did not study in detail in this manuscript the problem of existence of an aproximate inertial manifols for the granular flow dynamical system; rather, we studied the AIM existence problem for one form of our model equations. Many efforts have been made to prove the existence of an exact inertial manifolds for the Navier-Stokes equations, but no one succeded in this, due to some tricky technical difficulties. The only exact result was formulated recently by Kwak [50] for the Navier-Stokes equations restricted to a sphere, but it was later shown that his proof is incorrect. Therefore the problem still remains an open question despite "empirical evidence". These difficulties finally lead to the development of the approximate inertial manifold theory. The existence of an approximate inertial manifold for the Navier-Stokes equations has been widely studied in the literature [105]. Because of the same type of dissipativity and nonlinearity in (2.25) and in the Navier-Stokes equation, it can be shown that an AIM exists for the granular flow dynamical system. A proof of this fact requires only minor changes to the

proof presented in [105]. The AIM construction for the Navier-Stokes equation was implemented numerically in [44] using spectral technique. We shall study an inertial form of (2.25) using techniques other then spectral methods.

Let us consider a two-dimensional flow in a bounded domain with some prescribed boundary conditions. Let the horizontal and vertical components of the velocity field have the following representation in the $|S^k_{i,j}(x,y)>$-basis:

$$u(x,y,t)=\sum_{i,j=1}^{N}(\alpha_{i,j}(t)|S^1_{i,j}>+\beta_{i,j}(t)|S^2_{i,j}>+\gamma_{i,j}(t)|S^3_{i,j}> \quad +\delta_{i,j}(t)|S^4_{i,j}>,$$

$$v(x,y,t)=\sum_{i,j=1}^{N}(\bar{\alpha}_{i,j}(t)|S^1_{i,j}>+\bar{\beta}_{i,j}(t)|S^2_{i,j}>+\bar{\gamma}_{i,j}(t)|S^3_{i,j}>)+\bar{\delta}_{i,j}(t)|S^4_{i,j}> \quad . \tag{3.41}$$

Then the dynamical system (2.25) can be represented in terms of the functions $|S^k_{i,j}(x,y)>$ as

$$\begin{aligned}
\sum_{i,j}|S^1_{i,j}> \quad & \left[\frac{\partial\alpha_{i,j}}{\partial t}+\alpha\left(\alpha_{i,j}\frac{\beta_{i,j}-\beta_{i,j-1}}{\Delta x}+\bar{\alpha}_{i,j}\frac{\gamma_{i+1,j}-\gamma_{i,j}}{\Delta y}\right)-G^1_{i,j}-\right.\\
& -\frac{4(\nu+\lambda)}{\Delta x^2}(\beta_{i,j}-2\alpha_{i,j}+\beta_{i,j-1})+\frac{4\nu}{\Delta y^2}(\gamma_{i+1,j}-2\alpha_{i,j}+\gamma_{i,j})+\\
& \left.+\frac{\lambda}{\Delta x\Delta y}(\bar{\delta}_{i+1,j}+\bar{\delta}_{i,j-1}-\bar{\delta}_{i+1,j}-\bar{\delta}_{i,j})\right]+\\
+|S^2_{i,j}> \quad & \left[\frac{\partial\beta_{i,j}}{\partial t}+\alpha\left(\beta_{i,j}\frac{\alpha_{i,j+1}-\alpha_{i,j}}{\Delta x}+\bar{\beta}_{i,j}\frac{\delta_{i+1,j}-\delta_{i,j}}{\Delta y}\right)-G^2_1-\right.\\
& -\frac{4(\nu+\lambda)}{\Delta x^2}(\alpha_{i,j+1}-2\beta_{i,j}+\alpha_{i,j})+\frac{4\nu}{\Delta y^2}(\delta_{i+1,j}-2\beta_{i,j}+\delta_{i,j})+\\
& \left.+\frac{\lambda}{\Delta x\Delta y}(\bar{\gamma}_{i+1,j+1}+\bar{\gamma}_{i,j}-\bar{\gamma}_{i+1,j}-\bar{\gamma}_{i,j+1})\right]+ \qquad (3.42)\\
+|S^3_{i,j}> \quad & \left[\frac{\partial\gamma_{i,j}}{\partial t}+\alpha\left(\gamma_{i,j}\frac{\delta_{i,j}-\delta_{i,j-1}}{\Delta x}+\bar{\gamma}_{i,j}\frac{\alpha_{i,j}-\alpha_{i-1,j}}{\Delta y}\right)-G^3_1-\right.\\
& -\frac{4(\nu+\lambda)}{\Delta x^2}(\delta_{i,j}-2\gamma_{i,j}+\delta_{i,j-1})+\frac{4\nu}{\Delta y^2}(\alpha_{i,j}-2\gamma_{i,j}+\alpha_{i-1,j})+\\
& \left.+\frac{\lambda}{\Delta x\Delta y}(\bar{\beta}_{i,j}+\bar{\beta}_{i-1,j-1}-\bar{\beta}_{i,j-1}-\bar{\beta}_{i-1,j})\right]+\\
+|S^4_{i,j}> \quad & \left[\frac{\partial\delta_{i,j}}{\partial t}+\alpha\left(\delta_{i,j}\frac{\gamma_{i,j+1}-\gamma_{i,j}}{\Delta x}+\bar{\delta}_{i,j}\frac{\beta_{i,j}-\beta_{i-1,j}}{\Delta y}\right)-G^4_1-\right.\\
& \left.-\frac{4(\nu+\lambda)}{\Delta x^2}(\gamma_{i,j+1}-2\delta_{i,j}+\gamma_{i,j})+\frac{4\nu}{\Delta y^2}(\beta_{i,j}-2\delta_{i,j}+\beta_{i-1,j})+\right.
\end{aligned}$$

$$+\frac{\lambda}{\Delta x\Delta y}(\bar{\alpha}_{i,j+1}+\bar{\alpha}_{i-1,j}-\bar{\alpha}_{i,j}-\bar{\alpha}_{i-1,j+1})\Big],$$

plus a similar equation with overlined coefficients for the second component of (2.25). Here we included in the function G both the external forces and the gradient of pressure and the coefficients of its expansion in our set of basis functions are G^i, $i=1,\ldots,4$. Using relations (3.39)-(3.40) for coefficients of the two different basis sets, we can derive from (3.42) the system of equations for the evolution of $a_{i,j}(t)$, $b_{i,j}(t)$, $c_{i,j}(t)$ and $\bar{a}_{i,j}(t)$, $\bar{b}_{i,j}(t)$, $\bar{c}_{i,j}(t)$. As with the AIM construction in the spectral case, we neglect the time derivatives for $b_{i,j}$, $c_{i,j}$ and $\bar{b}_{i,j}$, $\bar{c}_{i,j}$. We also neglect in these last equations nonlinear terms proportional to the product of these coefficients that are obviously small compared with the other terms. Finally we obtain the following system of equations:

$$\begin{aligned}
\frac{d}{dt}a_{i,j} &= \frac{1}{4}(G_1^1+G_1^2+G_1^3+G_1^4)+\frac{2(\nu+\lambda)}{\Delta x^2}(a_{i,j+1}-2a_{i,j}+a_{i,j-1}-b_{i,j+1}+b_{i,j-1})+\\
&+\frac{2\nu}{\Delta y^2}(a_{i+1,j}-2a_{i,j}+a_{i-1,j}-c_{i+1,j}+c_{i-1,j})+\\
&+\frac{\lambda}{\Delta x\Delta y}(\bar{a}_{i+1,j+1}+\bar{a}_{i-1,j-1}-\bar{a}_{i-1,j+1}-\bar{a}_{i+1,j-1}-\\
&-\bar{b}_{i+1,j+1}+\bar{b}_{i-1,j-1}+\bar{b}_{i-1,j+1}-\bar{b}_{i+1,j-1}+2\bar{b}_{i+1,j}-2\bar{b}_{i-1,j}- \qquad (3.43)\\
&-\bar{c}_{i+1,j+1}+\bar{c}_{i-1,j-1}-\bar{c}_{i-1,j+1}+\bar{c}_{i+1,j-1}-2\bar{c}_{i,j+1}-2\bar{c}_{i,j-1})-\\
&-\frac{2\alpha}{\Delta x}[a_{i,j}(a_{i,j+1}-a_{i,j-1}-b_{i,j+1}-b_{i,j-1})+b_{i,j}(a_{i,j+1}+a_{i,j-1})]-\\
&-\frac{2\alpha}{\Delta y}[\bar{a}_{i,j}(a_{i+1,j}-a_{i-1,j}-c_{i+1,j}+c_{i,j}-c_{i-1,j})+\bar{c}_{i,j}(a_{i+1,j}-a_{i,j}+a_{i-1,j})],
\end{aligned}$$

$$\begin{aligned}
&\frac{8(\nu+\lambda)}{\Delta x^2}(6b_{i,j}+b_{i,j+1}+b_{i,j-1}-a_{i,j+1}+a_{i,j-1})-\frac{8\nu}{\Delta y^2}(b_{i+1,j}-2b_{i,j}+b_{i-1,j})-\\
-\;&\frac{\lambda}{\Delta x\Delta y}[-4\bar{c}_{i,j}+\bar{a}_{i+1,j+1}-\bar{a}_{i-1,j-1}-\bar{a}_{i-1,j+1}+\bar{a}_{i+1,j-1}+\\
+\;&2(\bar{a}_{i-1,j}-\bar{a}_{i+1,j})-\bar{b}_{i+1,j+1}-\bar{b}_{i-1,j-1}+\bar{b}_{i-1,j+1}+\bar{b}_{i+1,j-1}-\\
-\;&\bar{c}_{i+1,j+1}-\bar{c}_{i-1,j-1}-\bar{c}_{i-1,j+1}-\bar{c}_{i+1,j-1}+2(\bar{c}_{i,j+1}+\bar{c}_{i,j-1}+\bar{c}_{i+1,j}+\bar{c}_{i-1,j})]+\\
+\;&\frac{2\alpha}{\Delta x}[-2a_{i,j}^2+a_{i,j}(a_{i,j-1}+b_{i,j-1}-b_{i,j+1})-a_{i,j-1}b_{i,j}+a_{i,j+1}(a_{i,j}+b_{i,j})]+\\
+\;&\frac{2\alpha}{\Delta y}[\bar{a}_{i,j}(b_{i+1,j}-b_{i-1,j})+\bar{b}_{i,j}(a_{i+1,j}-a_{i-1,j})]+(G_1^1-G_1^2+G_1^3-G_1^4)=0, \qquad (3.44)
\end{aligned}$$

$$
\begin{aligned}
& \frac{8(\nu+\lambda)}{\Delta x^2}(c_{i,j+1}-2c_{i,j}+c_{i,j-1})-\frac{8\nu}{\Delta y^2}(6c_{i,j}+c_{i+1,j}+c_{i-1,j}-a_{i+1,j}+a_{i-1,j})+ \\
+ \; & \frac{\lambda}{\Delta x\Delta y}[-4\bar{b}_{i,j}+2(\bar{b}_{i+1,j}+\bar{b}_{i-1,j}-\bar{b}_{i,j+1}+\bar{b}_{i,j-1}+\bar{a}_{i,j+1}+\bar{a}_{i,j-1})+ \\
+ \; & \bar{a}_{i+1,j+1}-\bar{a}_{i-1,j-1}-\bar{a}_{i+1,j-1}+\bar{a}_{i-1,j+1}-\bar{b}_{i+1,j+1}-\bar{b}_{i-1,j-1}- \\
- \; & \bar{b}_{i+1,j-1}-\bar{b}_{i-1,j+1}-\bar{c}_{i+1,j+1}-\bar{c}_{i-1,j-1}+\bar{c}_{i+1,j-1}+\bar{c}_{i-1,j+1}]- \\
- \; & \frac{2\alpha}{\Delta x}[a_{i,j}(c_{i,j+1}-c_{i,j-1})+c_{i,j}(a_{i,j+1}-a_{i,j-1})]-\frac{2\alpha}{\Delta y}[\bar{a}_{i,j}(a_{i+1,j}-2a_{i,j}+ \\
+ \; & a_{i-1,j}-c_{i+1,j}+c_{i-1,j})+\bar{c}_{i,j}(a_{i+1,j}-a_{i-1,j})]+(G_1^1+G_1^2-G_1^3-G_1^4)=0.
\end{aligned}
$$

In order to construct an AIM, we need to solve the system (3.44) for $b_{i,j}$, $c_{i,j}$. Although it is possible to apply an iterative procedure and the boundary data to obtain a solvable system of linear equations for $b_{i,j}$ and $c_{i,j}$, this approach seems to be so complicated and numerically "expensive", that the entire method of solving an inertial form of (2.25) becomes very ineffective and nonintuitive from the computational point of view. A possible way to avoid these difficulties is to use the following simplifications. We can see from (3.39) that

$$
\begin{aligned}
b_{i,j} &\sim \frac{\beta_{i,j}-\alpha_{i,j}}{4}+\frac{\delta_{i,j}-\gamma_{i,j}}{4}\sim\frac{\partial u(x_{i,j},y_{i,j})}{\partial x}\frac{\Delta x}{4}, \\
c_{i,j} &\sim \frac{\alpha_{i,j}-\gamma_{i,j}}{4}+\frac{\beta_{i,j}-\delta_{i,j}}{4}\sim\frac{\partial u(x_{i,j},y_{i,j})}{\partial y}\frac{\Delta y}{4},
\end{aligned}
\tag{3.45}
$$

where derivatives are approximated with the step sizes $\Delta x/2$ and $\Delta y/2$, respectively. On the other hand

$$
\begin{aligned}
\frac{\partial u(x_{i,j},y_{i,j})}{\partial x} &\sim \frac{a_{i,j+1}-a_{i,j-1}}{2\Delta x}, \\
\frac{\partial u(x_{i,j},y_{i,j})}{\partial y} &\sim \frac{a_{i+1,j}-a_{i-1,j}}{2\Delta y},
\end{aligned}
\tag{3.46}
$$

where the step sizes for the derivative approximation are $2\Delta x$ and $2\Delta y$. Therefore

$$
\begin{aligned}
b_{i,j} &\sim \frac{1}{8}(a_{i,j+1}-a_{i,j-1}), \\
c_{i,j} &\sim \frac{1}{8}(a_{i+1,j}-a_{i-1,j}).
\end{aligned}
\tag{3.47}
$$

Obviously (3.47) does not have any relation to the separation of modes property of a dissipative dynamical system. Substitution of (3.47) into (3.43) would reduce the degree of accuracy to that of a simple low order finite-difference scheme. But we can apply (3.47) without a big loss of accuracy to the boundary as well as in the nonlinear terms of (3.44) and for the coefficients $b_{i,j\pm1}$, $b_{i\pm1,j}$, $c_{i,j\pm1}$, $c_{i\pm1,j}$ shifted from the main point (i,j) (they are multiplied by constants much smaller then $b_{i,j}$ and $c_{i,j}$). Notice that these algebraic equations can be solved easely on a computer by using analytical tools of MATHEMATICA. For example, the equation for $c_{i,j}$ is

$$\begin{aligned}
c_{i,j} &= -2\alpha\Delta x\Delta y a_{i,j}(-a_{i-1,j-1}+a_{i-1,j+1}+a_{i+1,j-1}-a_{i+1,j+1})+8\Delta x^2\Delta y^2(G_1^1+\\
&+ G_1^2-G_1^3-G_1^4)+8(\lambda+\nu)\Delta y^2(-a_{i-1,j-1}-a_{i-1,j+1}+a_{i+1,j-1}+a_{i+1,j+1})+\\
&+ 8\nu\Delta x^2(-8a_{i-1,j}+a_{i-2,j}+8a_{i+1,j}-a_{i+2,j})+2\alpha\Delta x^2\Delta y\bar{a}_{i,j}(14a_{i,j}+\\
&+ 28(a_{i-1,j}-a_{i+1,j})+a_{i-2,j}+a_{i+2,j})+\lambda\Delta x\Delta y(2\bar{a}_{i,j}+8\bar{a}_{i,j-1}-\bar{a}_{i,j-2}+8\bar{a}_{i,j+1}-\\
&- \bar{a}_{i,j+2})+\alpha\Delta x^2\Delta y\bar{a}_{i-1,j}(-2a_{i-1,j}+a_{i+1,j})+\lambda\Delta x\Delta y(10\bar{a}_{i-1,j+1}-\\
&- \bar{a}_{i-1,j+2}+\bar{a}_{i-2,j-1}-\bar{a}_{i-2,j+1})-2\alpha\Delta x^2\Delta y\bar{a}_{i+1,j}(a_{i-1,j}-a_{i+1,j})+ \qquad (3.48)\\
&+ \lambda\Delta x\Delta y(10\bar{a}_{i+1,j-1}+\bar{a}_{i+1,j-2}+\bar{a}_{i+1,j+1}-\bar{a}_{i+1,j+2}+\bar{a}_{i+2,j-1}-\bar{a}_{i+2,j-1})/\\
&\alpha\Delta x\Delta y^2(16a_{i,j-1}-a_{i,j+1})-8(\nu+\lambda)\Delta y^2-24\nu\Delta x^2.
\end{aligned}$$

Finally, the AIM is constituted from (3.48) with similar equation for $b_{i,j}$ for $i,j=3,\ldots,N-2$, and from similar expressions obtained with backward and forward versions of (3.46) for i or $j=2$ or $N-1$, and (3.47) for boundary values.

3.2.4 Numerical Example

We shall test our method for the inertial form calculations on the following example. Let us consider a granular flow in an infinite tube $\Omega=\{(x,y)\,|\,x\in(-\infty,+\infty),\ y\in[0,2]\}$ and let the velocity field be given explicitly as

$$u(x,y,t) = (2y-y^2)\,(2+sin(2\pi t)),$$

$$v(x,y,t) = 0.2\,sin(4\pi x/3)\,(2y-y^2). \tag{3.49}$$

Then (3.49) satisfies the governing equation (2.25) if the function G comprising the external forces and the gradient of pressure has the following form:

$$\begin{aligned} G_1(x,y,t) &= 2\pi(2y-y^2)\,cos(2\pi t) - 0.533\lambda\pi(1-y)\,cos(4\pi x/3) + \\ &+ [0.4\alpha\,sin(4\pi x/3)(y^3-3y^2+2y) + 2\nu](2+sin(2\pi t)), \\ G_2(x,y,t) &= 0.267\pi(2y-y^2)^2(2+sin(2\pi t))\,cos(4\pi x/3) + \\ &+ 0.08\alpha\,sin^2(4\pi x/3)(y^3-3y^2+2y) + \\ &+ [0.356\nu\pi^2(2y-y^2) + 0.4\nu + 0.4\lambda]\,sin(4\pi x/3). \end{aligned} \tag{3.50}$$

The advantage of an a priori chosen analytical solution is that it provides an exact criteria for testing the accuracy of different numerical schemes.

We consider a finite domain in the tube $\bar{\Omega} = \{(x,y)\,|\,x \in [0,6],\, y \in [0,2]\}$. Then the exact solution (3.49) determines the boundary conditions

$$\begin{aligned} u(0,y,t) &= u(6,y,t) = (2y-y^2)\,(2+sin(2\pi t)), \\ v(0,y,t) &= v(6,y,t) = 0, \\ u(x,0,t) &= v(x,0,t) = u(x,2,t) = v(x,2,y) = 0, \end{aligned} \tag{3.51}$$

and the initial condition

$$\begin{aligned} u(x,y,0) &= 2(2y-y^2), \\ v(x,y,0) &= 0.2\,sin(4\pi x/3)\,(2y-y^2). \end{aligned} \tag{3.52}$$

We applied the standard finite-difference method with different values of the step size $h = \Delta x = \Delta y$ for solving the system (2.25), (3.51)-(3.52), the inertial form calculation method with the same step sizes and the double precision finite-difference scheme. The relative errors of the numerical solutions with respect to the analytical one are shown in Fig. 3.3-3.4. We observe that the error of the inertial form calculation is close to the error of the double precision finite-difference scheme for the

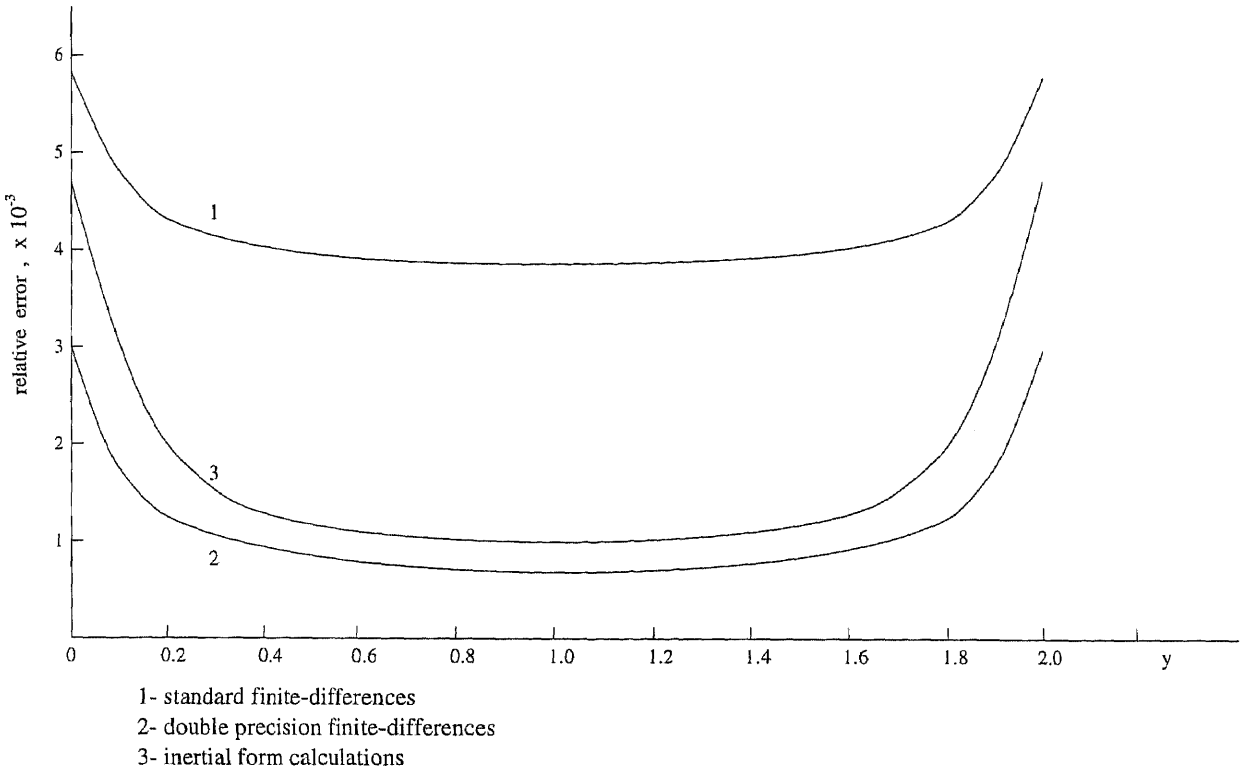

Figure 3.3 Relative error of the finite-differences and the inertial form calculations along the line $x = 3$ at time $t = 1$, $h = 4$

interior part of the domain of interest. Since the inertial manifold near the boundaries was approximated by using the expressions (3.47), the error of the inertial form calculation in the boundary layer coincides with the error of the standard finite-differences. The efficiency of the method depends on the number of cells or on the step size h. In particular, we calculated the ratio of the errors of the two methods, that is the average error of the inertial form calculations divided by the error of the standard finite-differences. The result is shown in Fig. 3.5.

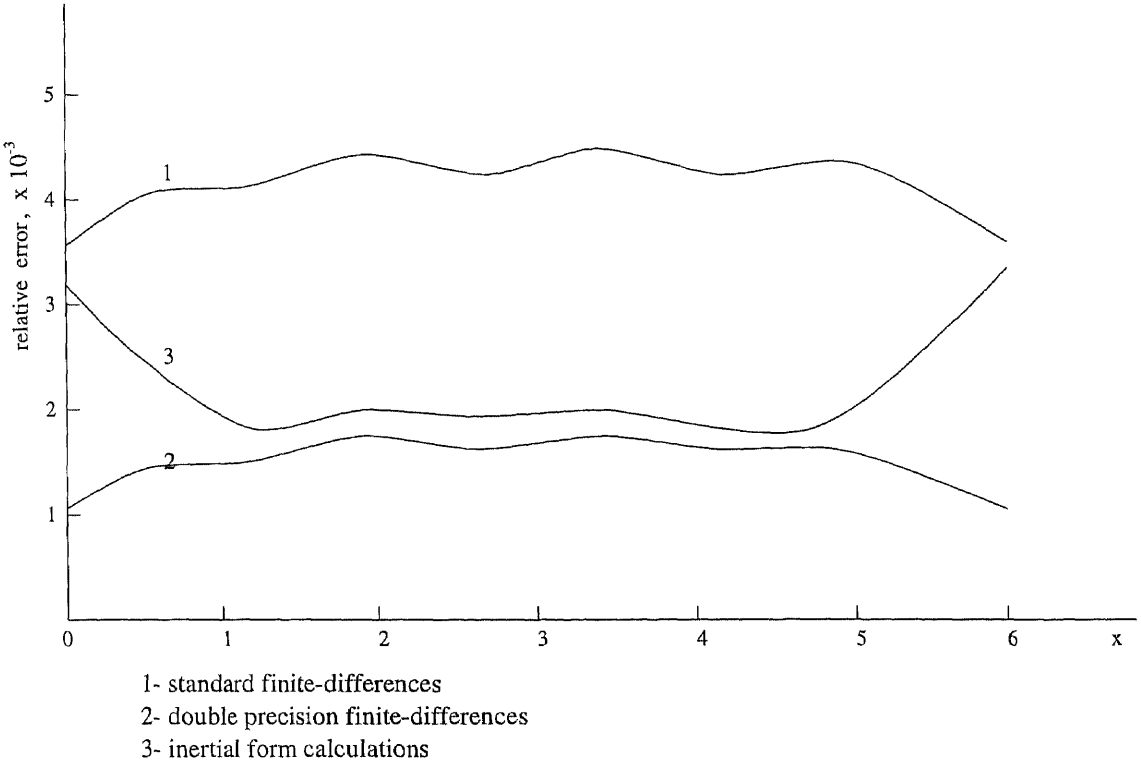

Figure 3.4 Relative error of the finite-differences and the inertial form calculations along the line $y = 1$ at time $t = 1$, $h = 4$

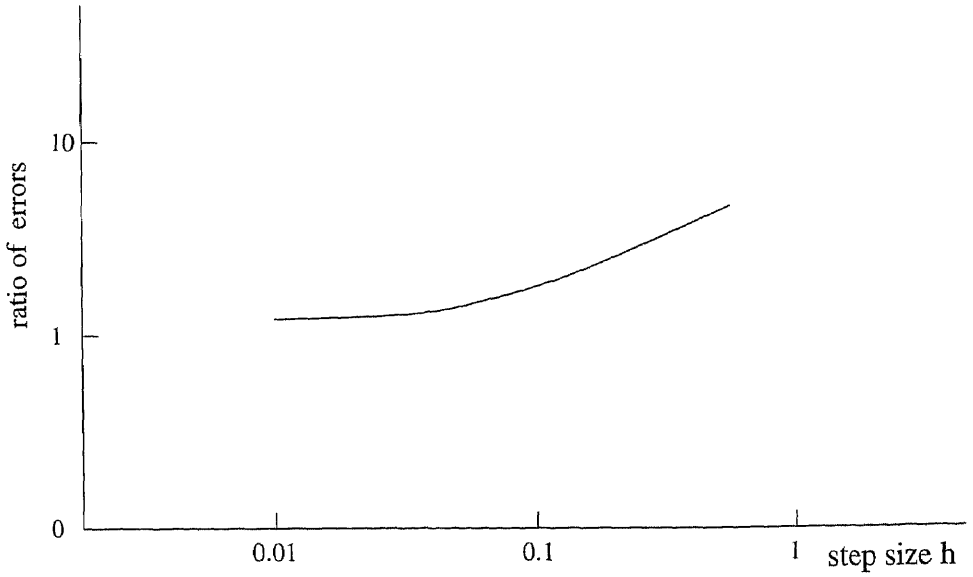

Figure 3.5 Ratio of the errors of the inertial manifold calculation to those of the standard finite differences

CHAPTER 4

GRANULAR FLOWS IN VIBRATING BEDS: THEORY AND NUMERICAL ANALYSIS

This chapter is organized as follows. Starting with well known interparticle and particle-boundary forces we derive in Section 4.1 the boundary conditions corresponding to the vibrating motion of a container of particles. Then, in Section 4.2, we solve our model numerically assuming the volume of granular material to be constant and neglecting such phenomena as arching and surface waves. We construct particular analytic solutions to the system of equations under some simplifying conditions in Section 4.3. We obtain in a natural way a system of ordinary differential equations for the particle trajectories in the form of an harmonic perturbation of an integrable Hamiltonian system. We study numerical solutions to this system for different regimes of forced perturbations. We also apply Melnikov theory to analyze the qualitative behavior of the perturbed dynamical system as well as the values of bifurcation parameters.

4.1 Simple Vibrating Bed Model

The granular flow of particles in a two-dimensional vibrating bed will be studied in this chapter using the governing equations (2.25). We shall see that one of the most challenging parts of formulating this problem mathematically is the assignment of realistic auxiliary data (initial and boundary conditions) to our model equations.

We consider the motion of a very large number of particles in a rectangular container in the plane with fixed vertical side walls and a horizontal bottom that is oscillating periodically in the vertical (y) direction. The only body force is a gravitational force in the negative (y) direction and the interstitial and surrounding medium is air which we assume has no effect on the granular flow.

At $t = 0$ the particles are contained in the following region:

$$K_0 := \{(x, y) \in \mathbf{R}^2 : |x| < \sigma,\ y > 0\}, \tag{4.1}$$

where $\sigma > 0$ is half of the width of the container. We employ here the idealization of infinite height so that we do not have to concern ourselves with the possibility of particles exiting the container from its top. The bottom of the container, which is free to move up and down along the fixed side walls $x = \pm\sigma$, is subject to a vertical oscillation of the form $a\,sin(\omega t)$, so that the particles are confined to the region

$$K_t := \{(x, y) \in \mathbf{R}^2 : |x| < \sigma,\ y > a\,sin(\omega t)\}, \tag{4.2}$$

for each $t \geq 0$.

We assume that the particles initially fill the region

$$\Omega_0 := \{(x, y) \in \mathbf{R}^2 : |x| < \sigma,\ 0 \leq y \leq h\}, \tag{4.3}$$

where $h > 0$ is the height of the particle continuum at time $t = 0$. The particle continuum at time $t \geq 0$ will be denoted by Ω_t. Naturally we must have $\Omega_t \subset K_t$ for all $t \geq 0$. It is expected that some portions of $\partial\Omega_t$ will not coincide with ∂K_t at the bottom of the container and will have a nonzero curvature on its top (reflecting such phenomena as arching and surface waves). These notions are illustrated in Fig. 4.1.

Our derivation of auxiliary conditions for the vibrating bed flow starts with initial conditions. We assume that prior to the initiation of motion due to the oscillation of the bottom of the container, the particles in Ω_0 have settled under the force of gravity so that they initially move like parts of a rigid body. Hence we set $v_1 = 0$ and $v_2 = a\,\omega$ at $t = 0$.

In order to assign boundary condition on ∂K_t for the vibrating granular flow under consideration, we must take into account the boundary forces discussed in [11]. If the particle is on a smooth part of ∂K_t for $t > 0$, this boundary exerts a normal

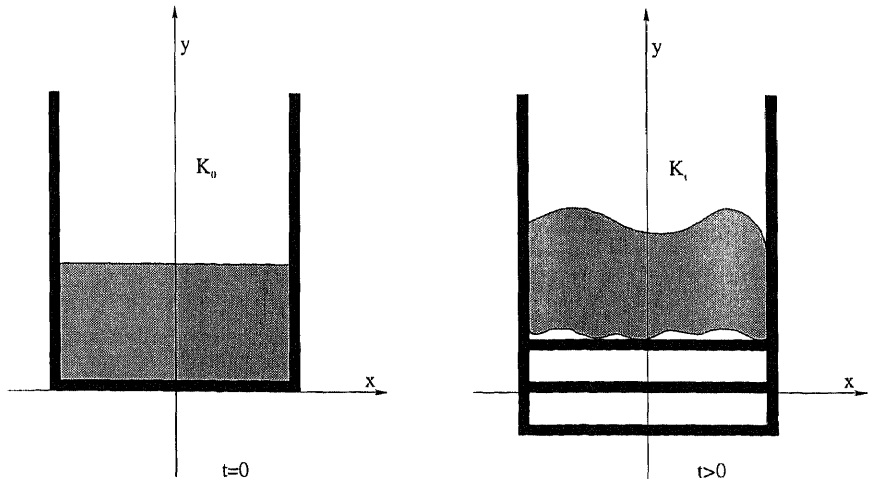

Figure 4.1 Granular material in a vibrating container

force on the particle and an additional tangential force if there is friction between the particle and container boundary. In the instant of contact, both particle and wall move together in the normal direction to the wall. Consequently, on K_t we have

$$v_n = w_n, \tag{4.4}$$

where v_n and w_n are, respectively, the velocity component of the particle and the wall in the direction normal to the wall at the particle position. As for the tangential direction, we observe that

$$\frac{\partial v_T}{\partial n} = -kv_T, \tag{4.5}$$

where v_T denotes the relative tangential component of velocity between the particle and ∂K_t, $\partial/\partial n$ is the partial derivative in the inner normal direction, and $k > 0$ is a constant that is a measure of the boundary friction that we shall call the *wall friction coefficient*. Note that $k = 0$ if ∂K_t is frictionless.

It remains to formulate boundary conditions on the free-boundary components – those portion of $\partial\Omega_t$ that are disjoint from ∂K_t. Here we reason as follows: At time $t > 0$ let a particle be at a point x on a smooth arc C contained in a component of the free-boundary. Then if we take a sufficiently small open disk neighborhood U

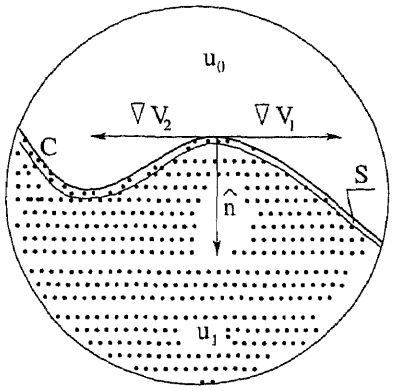

Figure 4.2 Boundary conditions on the free surface

of x, C separates U into a component U_i contained in the particle continuum and a component U_0 in the surrounding medium (air). As the influence of the surrounding medium is neglible by assumption, the boundary force B supplied along C by U_0 is zero. Hence if S is a very thin strip in the closure of U_i whose interface with the air is $C \bigcap U$, there should be no shearing along curves in S parallel to C during a small time interval inclusive of t. It is therefore reasonable to conclude that if S is sufficiently thin, then it moves like a rigid body in the granular flow during a small interval of time. Consequently, we infer that a physically realistic boundary condition for a free-boundary point is that the shear stress is zero and so the normal derivative of the velocity vanishes:

$$\frac{\partial \mathbf{v}}{\partial n} = \nabla \mathbf{v} \cdot \hat{n} = (< \nabla v_1, \hat{n} >, < \nabla v_2, \hat{n} >) = 0, \tag{4.6}$$

where $\hat{n}$ is a unit normal to the free-boundary directed into the particle continuum. This free-boundary condition is consistent with simulation and experimental results [52, 90, 75] and can also be obtained as an approximation of the conditions obtained from more comprehensive kinetic theory approaches [58]. It is interesting to compare this with the constant pressure condition characterizing free surfaces in fluid flows. The configuration at the heart of this derivation is depicted in Fig. 4.2.

The following approach is also helpful in understanding the nature of the free-boundary. Select either of the velocity components, say, v_1, for concreteness, and suppose that Φ is a smooth, real-valued function that is a solution of the partial differential equation

$$< \nabla v_1, \nabla \Phi >= 0 \tag{4.7}$$

in some open neighborhood of a free-boundary component. Then the free-boundary component must be of the form

$$\Phi(x, y) = c, \tag{4.8}$$

where c is a real constant, and Φ is an integral of the ordinary differential equation

$$\frac{\partial v_1}{\partial y} dx - \frac{\partial v_1}{\partial x} dy = 0. \tag{4.9}$$

Then $\nabla\Phi$ is normal to the free-boundary wherever it is nonvanishing and we can obtain the free-boundary component by solving (4.9) subject to the auxiliary condition $< \nabla v_2, \nabla\Phi >= 0$ (which fixes the appropriate constant in (4.8)). We can also obtain this component (under the usual regularity assumption) by integrating (4.9) starting with an initial condition at an endpoint of a component of the solid boundary. Note that the free-boundary component may have a singularity (possibly corresponding to the crest of a surface wave) at a point at which $\nabla\Phi = 0$.

We assume that at $t = 0$ the pressure is constant along the $x-$axis, the gravity force is balanced by the stationary pressure distribution along the $y-$axis and that the flow is driven by the boundary forces exerted by the vibrating walls at $t > 0$. In summary then, we take the following as the governing equations plus the initial and boundary conditions for the granular flow in the planar vibrating bed:

$$\begin{aligned}
\frac{\partial v_1}{\partial t} + v_1 \frac{\partial v_1}{\partial x} + v_2 \frac{\partial v_1}{\partial y} &= \nu \left(\frac{\partial^2 v_1}{\partial x^2} + \frac{\partial^2 v_1}{\partial y^2} \right) + \lambda \left(\frac{\partial^2 v_1}{\partial x^2} + \frac{\partial^2 v_2}{\partial x \partial y} \right) \\
\frac{\partial v_2}{\partial t} + v_1 \frac{\partial v_2}{\partial x} + v_2 \frac{\partial v_2}{\partial y} &= \nu \left(\frac{\partial^2 v_2}{\partial x^2} + \frac{\partial^2 v_2}{\partial y^2} \right) + \lambda \left(\frac{\partial^2 v_1}{\partial x \partial y} + \frac{\partial^2 v_2}{\partial y^2} \right)
\end{aligned} \tag{4.10}$$

in $\Sigma := \{(x,t) : x \in \Omega_t, t > 0\}$;

$$v_1(x,y,0) = v_1^0(x,y), \qquad v_2(x,y,0) = v_2^0(x,y) \quad at \quad t = 0 \tag{4.11}$$

for all $x \in \Omega_0 = \{x \in \mathbf{R}^2 : |x| < \sigma, 0 < y < h\}$, where the functions $v_1^0(x,y)$ and $v_2^0(x,y)$ determine the initial velocity distribution;

$$\frac{\partial v_1}{\partial y} = -kv_1, \quad v_2 = a\omega\, cos(\omega t) \tag{4.12}$$

for all particles on the bottom, $\{(x,y) : |x| < \sigma, y = a\, sin(\omega t)\}$, of the bed when $t > 0$;

$$v_1 = 0, \quad \frac{\partial v_2}{\partial x} = -kv_2 \tag{4.13}$$

for all particles on the left wall, $\{(x,y) : x = -\sigma,\ y > a\, sin(\omega t)\}$, of the container when $t > 0$;

$$v_1 = 0, \quad \frac{\partial v_2}{\partial x} = -kv_2 \tag{4.14}$$

for all particles on the right wall, $\{(x,y) : x = \sigma,\ y > a\, sin(\omega t)\}$, of the container when $t > 0$; and

$$\frac{\partial \mathbf{v}}{\partial n} = 0 \tag{4.15}$$

for all particles on the free-boundary, consisting of all points in $\partial\Omega_t \backslash \partial K_t$, when $t > 0$.

4.2 Numerical Solutions

We shall consider in this section some numerical solutions to the model (4.10) subject to the initial and the boundary conditions (4.11)-(4.14). To simplify our analysis, we shall ignore the effects of surface waves and free-boundary components at the bottom of the container.

In order to avoid difficulties with vibrating bed boundary conditions like

$v_2(x, a\,sin(\omega t)) = a\omega\,cos(\omega t)$ at the bottom, we shall write our equations in the vibrating system of coordinates:

$$\begin{aligned} x &= x^* \\ y &= y^* + a\,sin(\omega t) \\ t &= t^* \end{aligned} \tag{4.16}$$

The operators of partial differentiation in this frame are

$$\frac{\partial}{\partial x} = \frac{\partial}{\partial x^*}, \quad \frac{\partial}{\partial y} = \frac{\partial}{\partial y^*}, \quad \frac{\partial}{\partial t} = \frac{\partial}{\partial t^*} - a\omega\,cos(\omega t^*)\frac{\partial}{\partial y^*}. \tag{4.17}$$

We have to include also into the system (4.10) the inertial force term proportional to $a\omega^2 sin(\omega t)$ and directed along the $y-$axis. The governing system of equations in the "starred" system takes the following form (we have dropped the index '*')

$$\begin{aligned} v_{1,t} &= \nu(v_{1,xx} + v_{1,yy}) + a\omega\,cos(\omega t)v_{1,y} - \alpha(v_1 v_{1,x} + v_2 v_{1,y}) + \lambda(v_{1,xx} + v_{2,xy}), \\ v_{2,t} &= -a\omega^2 sin(\omega t) + \nu(v_{2,xx} + v_{2,yy}) + a\omega\,cos(\omega t)v_{2,y} - \alpha(v_1 v_{2,x} + v_2 v_{2,y}) \\ &+ \lambda(v_{1,xy} + v_{2,yy}), \end{aligned} \tag{4.18}$$

where $0 \le x \le 2$, $0 \le y \le 2$, and the boundary conditions can be written as

$$\begin{aligned} v_1(0, y, t) = 0, \qquad & v_1(2, y, t) = 0, \\ v_2(x, 0, t) = 0, \qquad & v_2(x, 2, t) = 0, \\ \frac{\partial v_1}{\partial y}(x, 0, t) + k v_1(x, 0, t) = 0, \quad & \frac{\partial v_1}{\partial y}(x, 2, t) = 0, \\ \frac{\partial v_2}{\partial x}(0, y, t) + k v_2(0, y, t) = 0, \quad & \frac{\partial v_2}{\partial x}(2, y, t) + k v_2(2, y, t) = 0. \end{aligned} \tag{4.19}$$

We use an explicit finite difference scheme for solving the system (4.18)-(4.19) with the spatial step $\Delta x = \Delta y = 0.001$ and the time step $\Delta t = 10^{-5}$. Estimates show that such a small time step is needed to satisfy the stability condition for the explicit finite-difference scheme.

We investigated the system (4.18)-(4.19) using both multi-vortex and random initial conditions. For certain ranges of the parameters (corresponding to the particle-particle forces) the motion of the system starting with a multi-vortex configuration changes rapidly into a pair of vortices that persists for a long time (relative to the period of the forced oscillations). The centers of this "stable" vortex pair oscillate with small amplitude synchronically with the forced oscillations. In some cases this vortex pair evolved into a single vortex after a very large time period. Increase of the constant ν results in a corresponding increase of the particle-particle friction and leads to damping of the vorticity (see Fig. 4.3).

When the motion starts from a random initial velocity distribution we also observed the "stable" vortex type of motion and bifurcation between different types of relatively stable patterns (Fig. 4.4). Some of the values used for the control parameters were

$$\omega = 2, \quad a = 1, \quad \nu = 0.3, \quad \lambda = 1.0$$

in the case of the vortex type of motion, and

$$\omega = 3, \quad a = 1, \quad \nu = 1.0 \quad \lambda = 0.5$$

in the case of a mixing motion. These types of particle dynamics are in agreement with experimental observations and computer simulation results [52, 75]. We note also that Hayakawa and Hong [41] obtained similar results from numerical solutions of their models but they assumed no-slip boundary conditions at the walls which are not physically realistic for vibrating bed granular flows.

Similar types of the flow behavior were obtained by Bourzutschky and Miller [20] for their Navier-Stokes models. By using negative slip boundary conditions in numerical experiments corresponding to granular flows with a high mobility boundary layer, they obtained (experimentally observable) vortex type solutions.

Unlike us, they did not obtain convective flow behavior coinciding with experimentally observed results for possible values of the wall friction coefficient. A possible explanation for this discrepancy between their findings and ours may be the fact that we included the gravity force directly in our model and they did not.

As mentioned above, we have suppressed the free-boundary conditions that occur in an actual vibrating bed in our numerical experiments. This has been done to simplify the numerical solution of the problem, since incorporation of the free-boundaries significantly complicates the problem and for us is still in the developmental stage. Preliminary results indicate that the addition of free-boundaries will still result in the appearance of "stable" convective vortices. Apparently, the frictional effects of the walls is the primary mechanism in the generation of convective rolls. For now then, our analysis of the vortices must be considered to be of a local rather than a global nature.

4.3 Analysis of Asymptotic Solutions

In this section we shall find particular analytic approximate solutions to the system (4.18)-(4.19) using asymptotic methods. These solutions approximate roughly the relatively stable patterns obtained numerically and depicted in Fig. 4.3 and 4.4 as well as the breakdown and diffusion of these patterns. We shall consider the system of equations (4.18) in the form

$$\mathbf{v}_t + (\mathbf{v}\nabla)\mathbf{v} = -a\omega^2 sin(\omega t)\hat{e}_2 + a\omega\, cos(\omega t)\mathbf{v}_y + \nu\nabla^2\mathbf{v} + \lambda\nabla(\nabla\mathbf{v}), \qquad (4.20)$$

where $\hat{e}_2$ is a unit vector along the $y-$axis and ϕ_0 is the initial phase of the external vibrations. Based on our experience with numerical solutions to the problem, namely on the existence of relatively stable two-vortex patterns oscillating with small amplitude and with the frequency of the forced vibrations, it is natural to assume that the solution to the problem can be expanded as the sum of a time

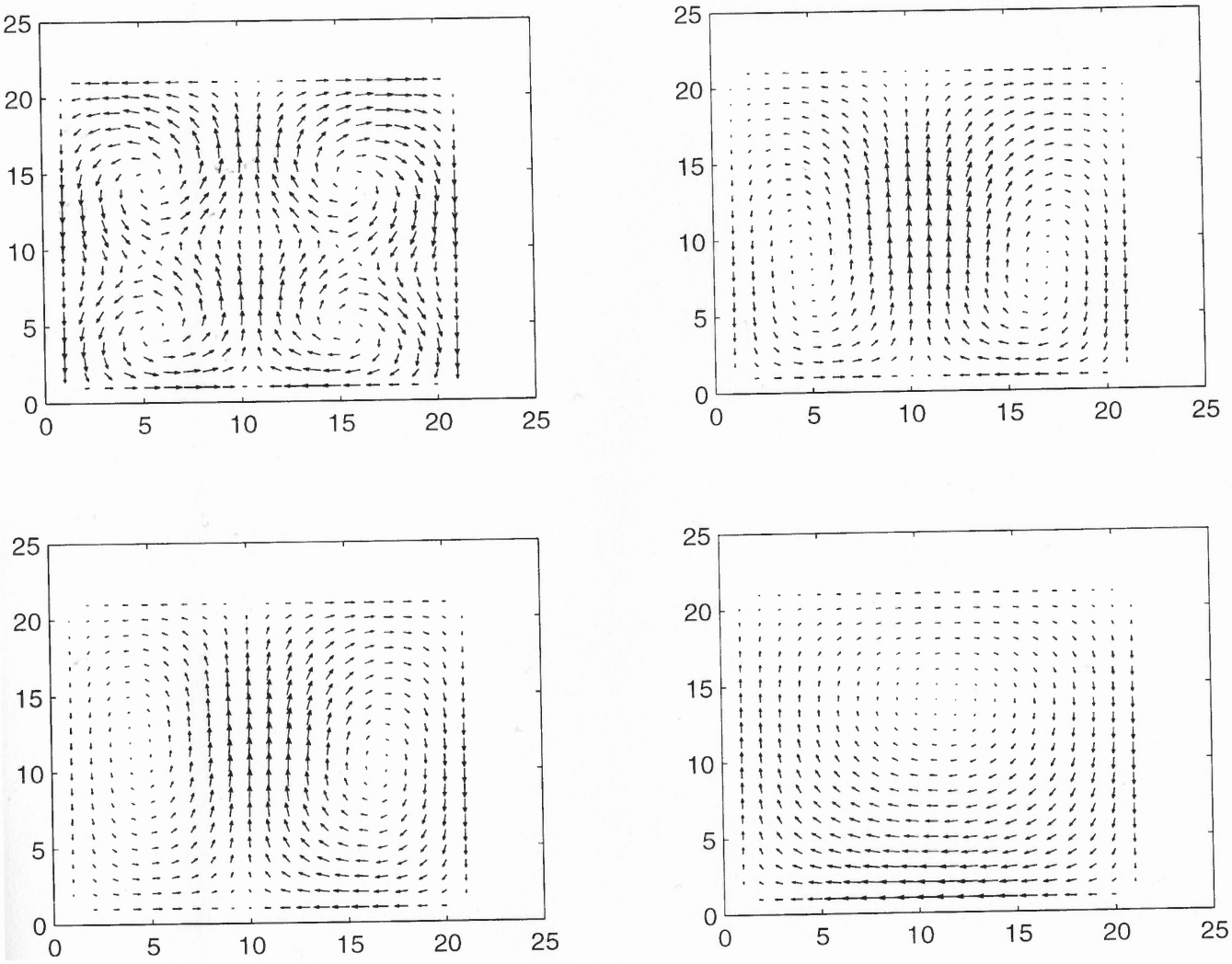

Figure 4.3 Motion of particles starting with four-vortex initial configuration (numerical solutions)

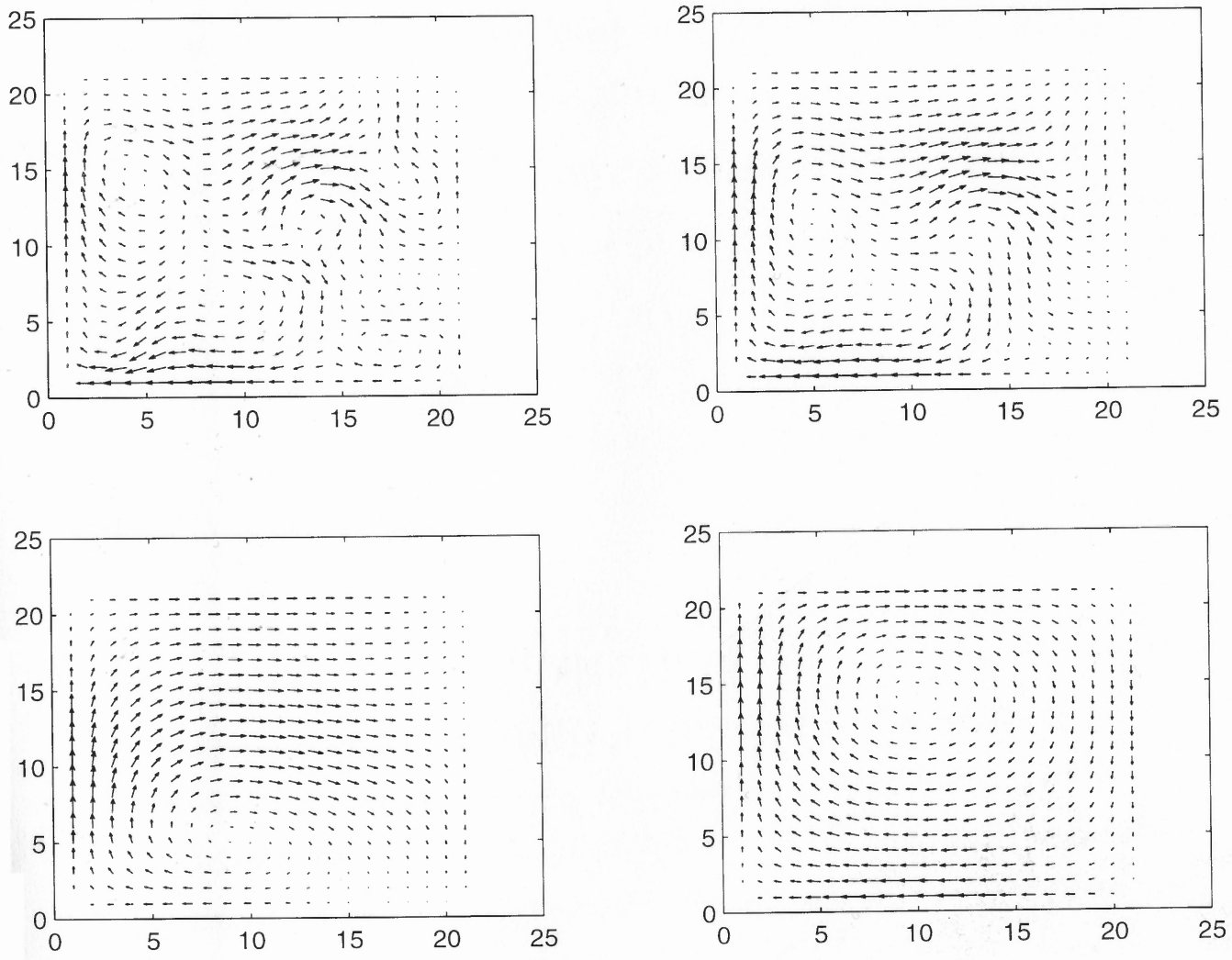

Figure 4.4 Motion of particles starting with random initial velocity distribution (numerical solutions)

independent solution $\mathbf{v}^s$ and one oscillating with the frequency ω and amplitude function $\mathbf{v}^c$:

$$\mathbf{v}(x,y,t) = \mathbf{v}^s(x,y) + a\mathbf{v}^{(1)}\,cos(\omega t) + a\mathbf{v}^{(2)}\,sin(\omega t) + O(a^2), \tag{4.21}$$

where we assume a to be small. Substituting (4.21) into the equation (4.20) and collecting the zero order terms with respect to a we obtain

$$(\mathbf{v}^s\nabla)\mathbf{v}^s = \nu\nabla^2\mathbf{v}^s + \lambda\nabla(\nabla\mathbf{v}^s). \tag{4.22}$$

The linear terms in a constitute the following equations

$$\begin{aligned} &-\omega\mathbf{v}^{(1)} + [(\mathbf{v}^{(2)}\nabla\mathbf{v}^s + (\mathbf{v}^s\nabla)\mathbf{v}^{(2)}] = \\ &= -\omega^2\hat{e}_2 + \nu\nabla^2\mathbf{v}^{(2)} + \lambda\nabla(\nabla\mathbf{v}^{(2)}), \\ &\omega\mathbf{v}^{(2)} + [(\mathbf{v}^{(1)}\nabla)\mathbf{v}^s + (\mathbf{v}^s\nabla)\mathbf{v}^{(1)}] = \\ &= \omega\mathbf{v}^s_y + \nu\nabla^2\mathbf{v}^{(1)} + \lambda\nabla(\nabla\mathbf{v}^{(1)}). \end{aligned} \tag{4.23}$$

We shall use the identities

$$(\mathbf{v}\nabla)\mathbf{v} = \frac{1}{2}\nabla(\mathbf{v},\mathbf{v}) - \mathbf{v}\times(\nabla\times\mathbf{v}), \tag{4.24}$$

$$\nabla\times(\nabla\times\mathbf{v}) = \nabla(\nabla\mathbf{v}) - \nabla^2\mathbf{v}, \tag{4.25}$$

and assume that terms depending on the divergence of $\mathbf{v}$ are small and can be neglected for vortex-type solutions. This assumption follows from the analysis of our numerical solutions, but we shall show later that the analytical solution corresponding to a stable vortex pair does satisfy the condition $div\,\mathbf{v}^s = 0$. Therefore the stable solution $\mathbf{v}^s$ satisfies the equation

$$\nabla\times(\mathbf{v}^s\times(\nabla\times\mathbf{v}^s)) = \nu\nabla\times(\nabla\times(\nabla\times\mathbf{v}^s)). \tag{4.26}$$

Equation (4.26) is used in hydrodynamics for the description of flows near obstacles [51]. Therefore, it is convenient to introduce a stream function $\Psi(x,y)$ with the following property: each vector $\mathbf{v}^s$ is tangent to the curve $\Psi = const$. Namely, let

$$\mathbf{v}^s(x,y) = \nabla\times\Psi(x,y)\hat{e}_3, \tag{4.27}$$

where $\hat{e}_3$ is the unit vector along the z-direction. In terms of the stream function, the velocity field of the system of particles can be expressed as

$$\mathbf{v}^s(x,y) = \left(\frac{\partial \Psi}{\partial y}, -\frac{\partial \Psi}{\partial x}\right). \tag{4.28}$$

Using the stream function representation we can rewrite (4.26) as follows

$$\left[\frac{\partial}{\partial x}\left(\frac{\partial \Psi}{\partial y}\nabla^2\Psi\right) + \frac{\partial}{\partial y}\left(\frac{\partial \Psi}{\partial x}\nabla^2\Psi\right)\right] = \nu\Delta^2\Psi. \tag{4.29}$$

Now we are interested in finding particular analytical solutions to the system (4.28), (4.29), (4.24) corresponding to both the stable vortex type of patterns and to the diffusion of these vortices. First we shall consider the case where the friction forces between particles are small and describe the behavior of the oscillating vortex pair.

The simplest vortex type solution satisfying (4.29) is

$$\Psi = log\frac{(x-x_0)^2+(y-y_0)^2}{(x+x_0)^2+(y-y_0)^2} + kx, \tag{4.30}$$

where $(x_0,\ y_0)$ is the location of the vortex center. A stream function of this type was derived first by Lamb [51]. According to (4.28) the stream function (4.30) determines an exact integrable Hamiltonian system

$$\begin{aligned} v_1^s &\equiv \frac{dx}{dt} = \frac{\partial \Psi}{\partial y} \\ v_2^s &\equiv \frac{dy}{dt} = -\frac{\partial \Psi}{\partial x}, \end{aligned}$$

which in explicit form is

$$\begin{aligned} \frac{dx}{dt} &= (y-y_0)\left(\frac{1}{(x+x_0)^2+(y-y_0)^2} - \frac{1}{(x-x_0)^2+(y-y_0)^2}\right), \\ \frac{dy}{dt} &= \frac{x-x_0}{(x-x_0)^2+(y-y_0)^2} - \frac{x+x_0}{(x+x_0)^2+(y-y_0)^2} - k. \end{aligned} \tag{4.31}$$

The Hamiltanian function (4.30) is unbounded from the below in one vortex center point (x_0, y_0) and from the above in the other point $(-x_0, y_0)$. Therefore we

need to exclude these points from the phase space. The trajectories of particles in the phase space of the system (4.31) are depicted in Fig. 4.5. There are two hyperbolic fixed points p_1 and p_2 at $x = 0, \quad y = \pm\sqrt{2x_0/k - x_0^2}$ for $y_0 = 0$. The eigenvalues of the linear problem

$$\lambda = \pm \left(\frac{k}{x_0}\right)^2 \sqrt{2\frac{x_0}{k} - x_0}$$

are real for the parameter values $x_0 = 1$, $k = 0.5$ that were used in numerical calculations. The hyperbolic fixed points are connected by the heteroclinic separatrices s_0, s_1, s_2. These limiting streamlines serve as the invariant stable and unstable manifolds for the fixed points; in particular, s_1 and s_2 comprise the stable manifolds and s_0 is a portion of the unstable manifold for p_1, and s_0 is a portion of the stable manifold and s_1 and s_2 comprise the unstable one for the point p_2.

Substituting the explicit expressions (4.31) in (4.23) we can find a system of equations determining the functions $\mathbf{v}^{(1)}(x, y)$, $\mathbf{v}^{(2)}(x, y)$. This system can be solved numerically subject to the vibrating bed boundary conditions. But we are interested here in an analytical study of the behavior of a local solution. We can find the following simple particular solution for $\mathbf{v}^{(1)}$, $\mathbf{v}^{(2)}$ satisfying the system of equations (4.23) (but not boundary conditions):

$$v_1^{(1)} = 0, \quad v_2^{(1)} = \omega, \quad \mathbf{v}^{(2)} = 0. \tag{4.32}$$

Thus the system of equations for the perturbed trajectories of particles takes the following form:

$$\begin{aligned} \frac{dx}{dt} &= (y - y_0)\left(\frac{1}{(x + x_0)^2 + (y - y_0)^2} - \frac{1}{(x - x_0)^2 + (y - y_0)^2}\right), \\ \frac{dy}{dt} &= \frac{x - x_0}{(x - x_0)^2 + (y - y_0)^2} - \frac{x + x_0}{(x + x_0)^2 + (y - y_0)^2} - k + a\omega\, cos(\omega t). \end{aligned} \tag{4.33}$$

We shall determine the motion of the vortex centers by passing to the limit as

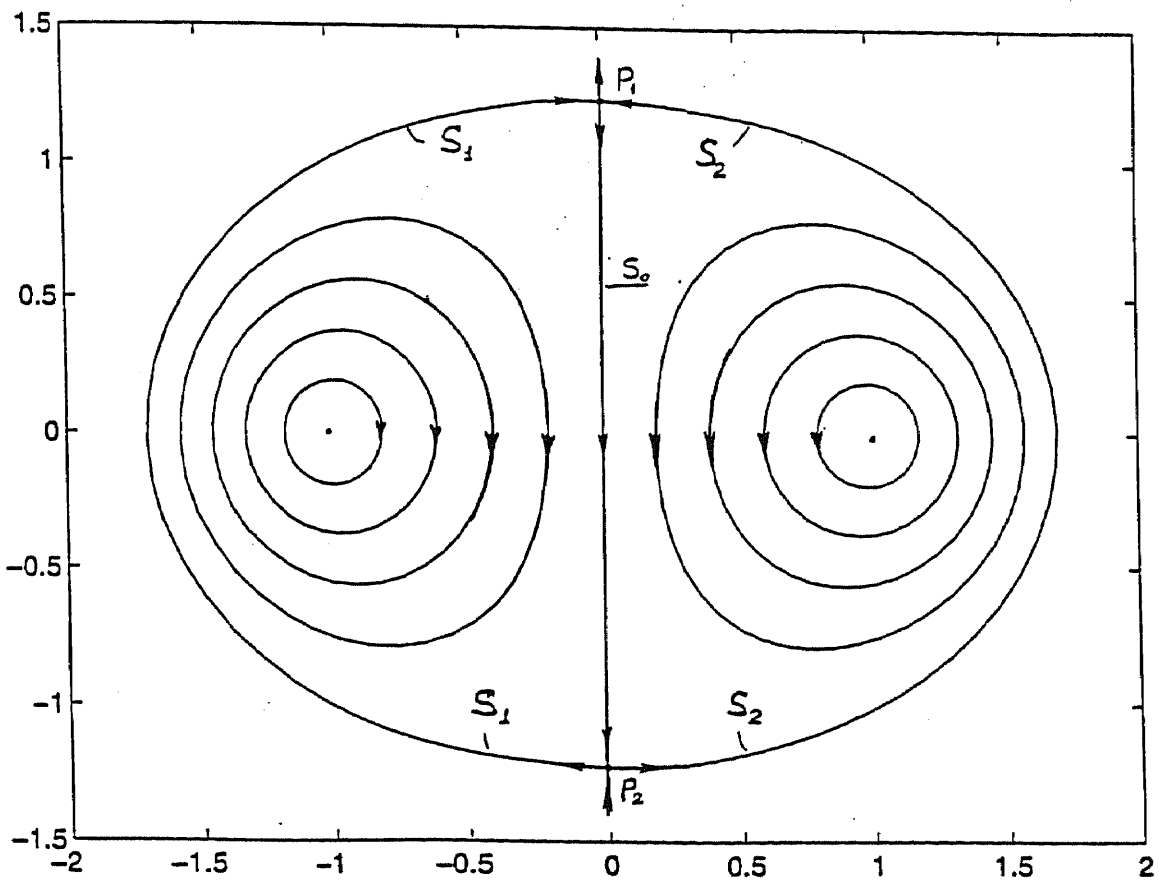

Figure 4.5 Unperturbed trajectories of particles (asymptotic solutions)

$x \to x_0$. In order to avoid singularities in the system (4.33) we shall use the local polar coordinates near the center:

$$x = x_0 + r\cos\theta,$$

$$y = y_0 + r\sin\theta.$$

Substituting these expression into the system (4.33) we obtain

$$\begin{aligned} \cos\theta\, r_t - r\sin\theta\,\theta_t + x_{0,t} &= \frac{r\sin\theta}{(r\cos\theta + 2x_0)^2 + r^2\sin^2\theta} - \frac{r\sin\theta}{r^2}, \\ \sin\theta\, r_t + r\cos\theta\,\theta_t + y_{0,t} &= \frac{r\cos\theta}{r^2} - \frac{r\cos\theta + 2x_0}{(r\cos\theta + 2x_0)^2 + r^2\sin^2\theta} - k + a\omega\cos(\omega t). \end{aligned} \tag{4.34}$$

Multiplying the first equation in (4.34) by $\cos\theta$, the second one by $\sin\theta$ and adding them together we obtain

$$r_t + \cos\theta\, x_{0,t} + \sin\theta\, y_{0,t} = \frac{r\sin\theta\cos\theta}{(r\cos\theta + 2x_0)^2 + r^2\sin^2\theta} -$$

$$-\frac{(r\cos\theta + 2x_0)\sin\theta}{(r\cos\theta + 2x_0)^2 + r^2\sin^2\theta} - k\sin\theta + a\omega\cos(\omega t)\sin\theta.$$

Passing to the limit as $r \to 0$ and comparing the terms near $\cos\theta$ and $\sin\theta$ respectively we obtain the following equations for the motion of the vortex center:

$$\begin{aligned} \frac{dx_0}{dt} &= 0, \quad x_0(0) = 1, \\ \frac{dy_0}{dt} &= \frac{1}{2x_0} + a\omega\cos(\omega t) - k, \quad y_0(0) = 0. \end{aligned} \tag{4.35}$$

The solution to (4.35) is

$$x_0 = 1, \quad y_0 = a\sin(\omega t).$$

We constructed the solutions by using the numerical value of the parameter $k = \frac{1}{2}$ corresponding to the pure oscillatory motion. At different values of this parameter the oscillating motion combines with slow displacement either towards the top or the bottom of the container as observed for our numerical solutions. But the additional

translational motion of the centers of vortices does not affect typical features of the perturbed motion of particles and we shall not consider these cases.

Substituting the solutions for the vortex centers motion into (4.33) we obtain the system of equation for the perturbed motion:

$$\begin{aligned}
\frac{dx}{dt} &= \frac{y - a\,sin(\omega t)}{(x \pm 1)^2 + (y - a\,sin(\omega t))^2} - \frac{y - a\,sin(\omega t)}{(x \mp 1)^2 + (y - a\,sin(\omega t))^2}, \\
\frac{dy}{dt} &= \frac{x \mp 1}{(x \mp 1)^2 + (y - a\,sin(\omega t))^2} - \frac{x \pm 1}{(x \pm 1)^2 + (y - a\,sin(\omega t))^2} - \\
&- k + a\omega cos(\omega t).
\end{aligned} \tag{4.36}$$

For the analytical estimation of bifurcation values of the parameters we shall consider the case of small a. Expanding the right hand side in a Taylor series and taking into consideration only the zero and first order terms we obtain

$$\begin{aligned}
\frac{dx}{dt} &= y\left(\frac{1}{P_+} - \frac{1}{P_-}\right) - a\,sin(\omega t)\left[\frac{1}{P_+} - \frac{1}{P_-} + 2y^2\left(\frac{1}{P_-^2} - \frac{1}{P_+^2}\right)\right] \\
\frac{dy}{dt} &= \frac{x \mp 1}{P_-} - \frac{x \pm 1}{P_+} + a\left[\omega\,cos(\omega t) - 2y\,sin(\omega t)\left(\frac{x \pm 1}{P_+^2 -} - \frac{x \mp 1}{P_-^2}\right)\right],
\end{aligned} \tag{4.37}$$

where $P_\pm = (x \pm 1)^2 + y^2$.

The dynamical system (4.35) has the form of a periodically perturbed integrable Hamiltonian system:

$$\begin{aligned}
\frac{dx}{dt} &= f_1(x, y) + a\,g_1(x, y, t, a, \omega) \\
\frac{dy}{dt} &= f_2(x, y) + a\,g_2(x, y, t, a, \omega),
\end{aligned} \tag{4.38}$$

where $a \ll 1$ and ω are parameters and the functions g_1 and g_2 are time-periodic. This makes it possible to estimate values of the bifurcation parameters by applying the Melnikov technique [40, 67].

We shall consider first the numerical solutions to the system (4.36). It was mentioned above that the phase portrait of these equations at $a = 0$ consists of

a pair of vortices as is shown in Fig. 4.5. The periodic trajectories of particles are associated with invariant tori of the integrable dynamical system (4.31). This picture changes in an essential way when $a \neq 0$. For small a the invariant tori still exist in a slightly deformed form for a wide range of parameters a and ω in accordance with the KAM theory [7, 40, 110]. The trajectories of particles are still periodic and constrained to lie between these tori (see Fig. 4.6a). The picture is qualitively the same for some range of parameters a and ω when a is close to 1 that corresponds to the real model and to the numerical solution depicted in Fig. 4.3. But an increase in the amplitude a of the oscillations leads to new qualitative behavior of the particle trajectories. The motion of the particles is chaotic with intensive mixing (fig. 4.6b). This type of particle dynamics corresponds roughly to the numerical solution to the partial differential system of equations (4.18)-(4.19) depicted in Fig. 4.4.

In the case of small a we can estimate bifurcation values of the parameters analytically by employing Melnikov's method. The Melnikov technique allows us to predict the behavior of the perturbed stable and unstable manifolds $W^s_{+,\varepsilon}$ and $W^u_{-,\varepsilon}$ and consists of a measurement of the distance between $W^s_{+,\varepsilon}$ and $W^u_{-,\varepsilon}$. Here we denoted by ε the perturbation rate. The first order term in the Taylor series expansion of this distance is given by

$$d(t_0, \varepsilon) = \varepsilon \frac{M(t_0)}{\|\mathbf{f}(\mathbf{q}(-t_0))\|} + O(\varepsilon^2), \tag{4.39}$$

where $\mathbf{q}(t)$ is the particle trajectory of the unperturbed phase space lying on the heteroclinic separatrix s, t_0 defines a particular point of the heteroclinic orbit in a particular Poincaré section, and

$$\|\mathbf{f}(\mathbf{q}(-t_0))\| = [(f_1(\mathbf{q}(-t_0)))^2 + (f_1(\mathbf{q}(-t_0)))^2]^{1/2}. \tag{4.40}$$

The Melnikov function is defined to be

$$M(t_0) = \int_{-\infty}^{+\infty} [f_1(\mathbf{q}(t)) g_2(\mathbf{q}(t), t + t_0) - f_2(\mathbf{q}(t)) g_1(\mathbf{q}(t), t + t_0)] dt. \tag{4.41}$$

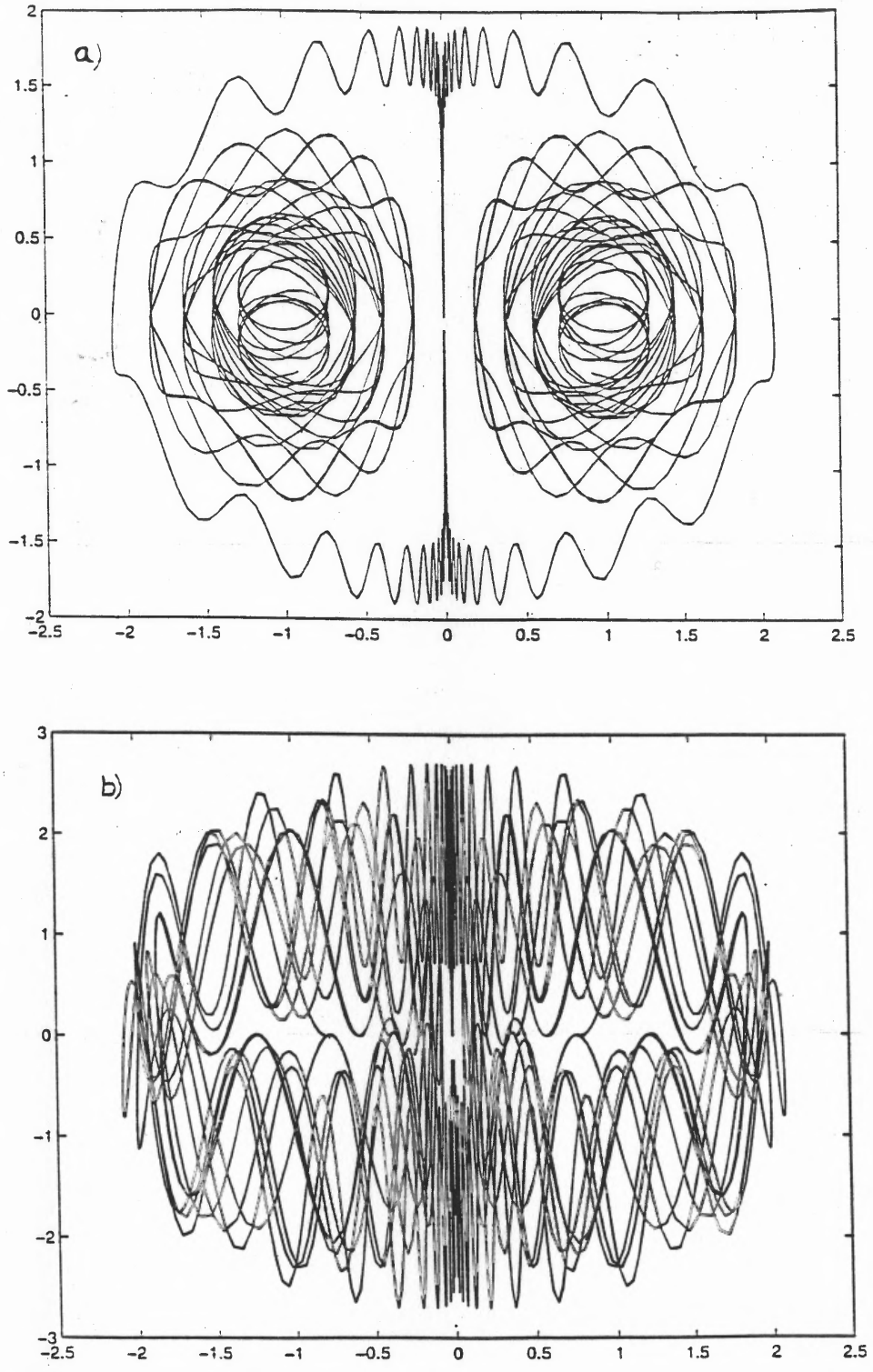

Figure 4.6 Perturbed trajectories of particles: a) periodic trajectories between the invariant tori; b) mixing of particles

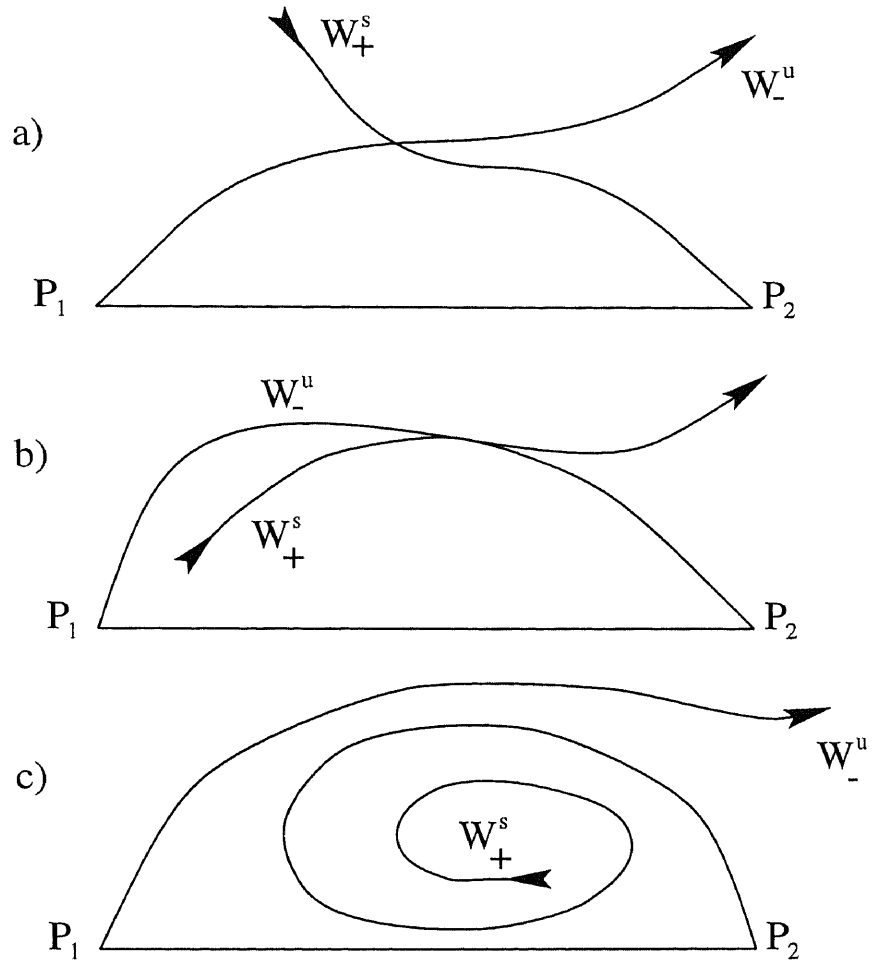

Figure 4.7 Possible positions of the perturbed stable and unstable manifolds

Thus the Melnikov technique requires knowledge of the solution to the unperturbed dynamical system only. The Melnikov theorem [40, 67] states that simple zeros of $M(t_0)$ (i.e., $M(t_0) = 0$, $\partial M/\partial t_0 \neq 0$) imply transverse intersection of the perturbed stable and unstable manifolds $W^s_{+,\varepsilon}$ and $W^u_{-,\varepsilon}$ (see Fig. 4.7a). The case $M(t_0) = 0$, $\partial M/\partial t_0 = 0$ corresponds to tangential intersection of these manifolds (Fig. 4.7b). If $M(t_0) \neq 0$ then the perturbed stable and unstable manifolds do not intersect each other (Fig. 4.7c). The sign of $d(t_0, \varepsilon)$ gives us information concerning the relative orientation of $W^s_{+,\varepsilon}$ and $W^u_{-,\varepsilon}$.

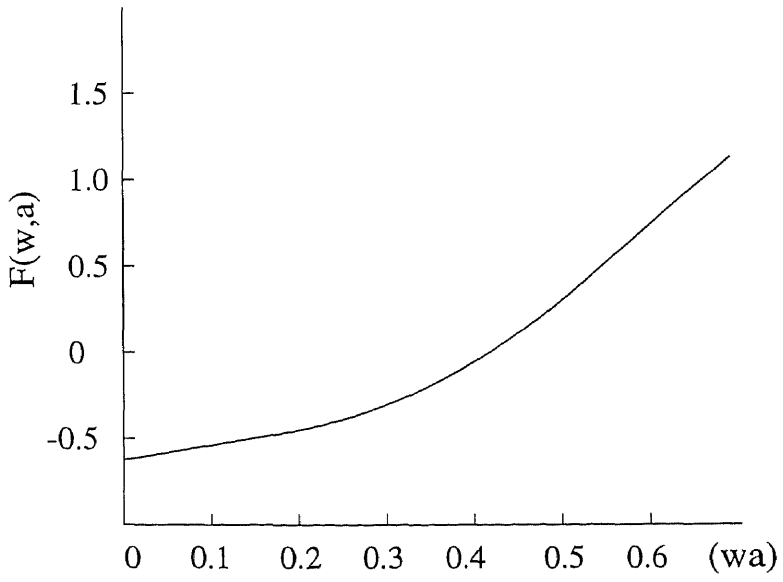

Figure 4.8 Amplitude of the Melnikov function

We calculated the Melnikov function numerically and observed that

$$M(t_0, \omega, a) \sim F\left(\frac{1}{\omega a}\right) sin(\omega t_0). \tag{4.42}$$

The Melnikov function is periodic in t_0 for fixed ω. The function $F(.)$ calculated numerically for the different Poincaré sections is plotted in Fig. 4.8. The numerical calculation indicated the existence of an infinite number of simple zeros of the function $M(t_0, \omega, a)$ (4.42) and, therefore, the existence of an infinite number of intersections of the perturbed stable and unstable manifolds corresponding to the type of dynamics shown in Fig. 4.6b.

CHAPTER 5

GRANULAR FLOWS IN HOPPERS: NUMERICAL SOLUTIONS

Studies of granular flows and processes in conveying particulate materials and, in particular, hopper flows, have been stimulated by industrial needs. In designing plants which involve the handling and processing of particulate solid materials, several problems are encountered which have no counterpart in fluid handling processes; unless this is recognized and appropriate steps are taken, serious and costly problems can be met in operating the plant. Among the most important industrial problems for hoppers is to ensure that when material is required it will discharge, under gravity, at the required rate and that flow will be uninterupted as long as there is material in the hopper. Other problems consist in theoretical prediction of the flooding phenomena that may take place under some conditions in core type hoppers and in estimation of the size-segregation phenomena of a multi-component mix of particles. These and several other problems are still not entirely understood from a mathematical or engineering perspective.

In this chapter we undertake a numerical investigation of a hopper flow model based on the continuum dynamical system (2.25). The chapter is organized as follows: In Section 5.1 we derive the boundary conditions and develop a numerical method for the hopper flow model. The numerical results obtained in this approach are shown in Section 5.2. We compare our solutions with the experimental results and the results of computer simulations of the hopper problem. Intending to capture the behavior of particles in a core type hopper we propose in this section some modifications of our model and present the numerical solutions to the modified equations.

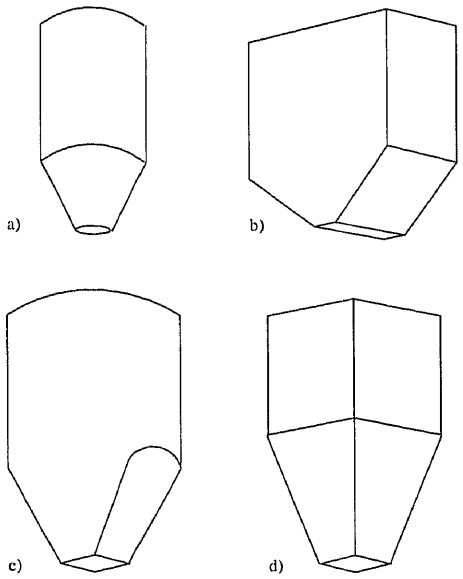

Figure 5.1 Types of industrial hoppers: a) conical or axisymmetric hopper; b) plane-flow wedge hopper; c) plane-flow chisel hopper; d) pyramid hopper.

5.1 Numerical Methods for Hopper Problem

We shall describe granular flows in hoppers using the governing equation (2.25). In addition, in our hopper flow calculations we need to control the conservation of mass by making the integral $\int_D \mathbf{v} \cdot \hat{n}\, ds$ constant for any horizontal slice D of a hopper, were $\hat{n}$ is a unit normal vector.

We assume that the normal component of the velocity field vanishes on the walls:

$$v_n = 0. \tag{5.1}$$

As for the tangential direction, we use the same condition as in the previous section:

$$\frac{\partial v_T}{\partial n} = -k v_T, \tag{5.2}$$

where v_T denotes the tangential component of the particle velocity.

For the boundary conditions at the top of the hopper we assume that the

granular material enters the hopper supply bunker with a small constant vertical speed v_0:

$$v^{(1)} = 0, \quad v^{(2)} = v_0, \tag{5.3}$$

where $v^{(1)}$ and $v^{(2)}$ denote, respectively, the horizontal and vertical components of the velocity field. As for the condition at the outlet of the hopper, particles are assumed to be in free fall directly below the outlet. Namely, we shall assume that the horizontal component of the particle velocity below the outlet is equal to 0 and that

$$\frac{dv^{(2)}}{dy} = Gv^{(2)}, \tag{5.4}$$

where G is the gravity force, and the axis y is directed vertically.

We propose the following method for the numerical solution of the boundary value problem (2.25), (5.1)-(5.4) describing the granular flow in a hopper. Let the funnel walls be nonflat (in the general case) and let their shape be determined by the function $x = \pm g(y)$ (see Fig. 5.2).

The domain occupied by particles is $\{(x, y) \mid x \in [-g(y), g(y)],\ y \in [0, 1]\}$. Let us introduce a system of curvilinear coordinates in the following way:

$$\begin{cases} \tilde{x} = \frac{x}{g(y)}, \\ \tilde{y} = y. \end{cases} \tag{5.5}$$

Then the domain occupied by particles is $\{(\tilde{x}, \tilde{y}) \mid \tilde{x} \in [-1, 1],\ \tilde{y} \in [0, 1]\}$ (see Fig. 5.2). Therefore, the domain of the hopper becomes rectangular in the curvilinear coordinates, which simplifies the use of finite differences for numerical solutions.

The system of coordinates $\tilde{x}, \tilde{y}$ is a natural coordinate system for solving numerically a dynamical system in the complicated space domain. The next step is to find an appropriate function $g(y)$ corresponding to the shape of a hopper.

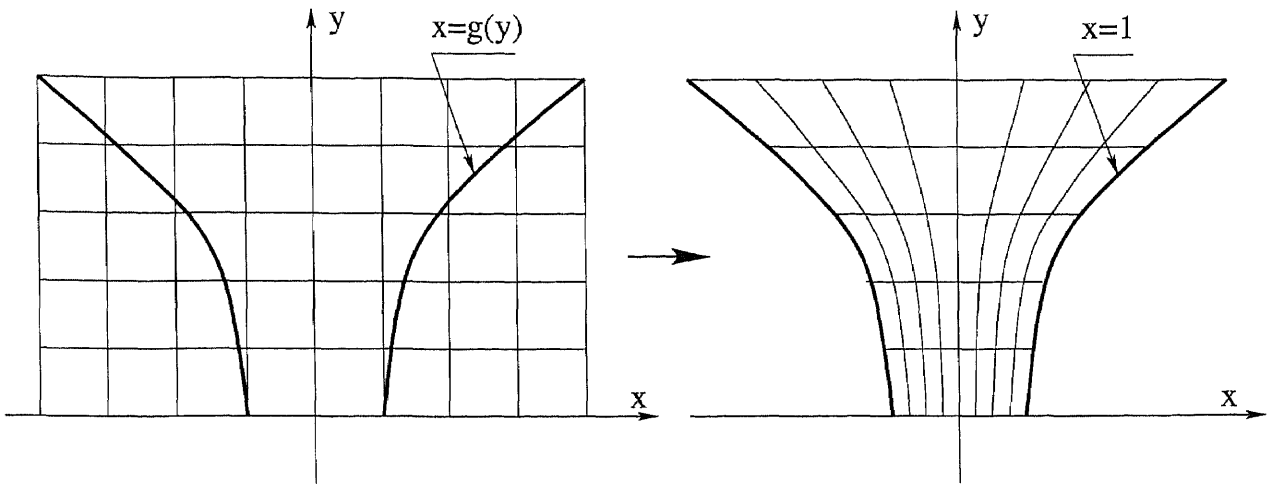

Figure 5.2 Transformation to the "hopper coordinates"

Some typical hoppers used in industry are shown in Fig. 1. They are constructed with cylindrical or rectangular "bins" or "bunkers" and sections with inclined walls. We shall consider an axially-symmetric hopper so that its study can be reduced to the two-dimensional case. The function $g(y)$ in this case is a piece-wise smooth linear function

$$g(y) = ay + b,$$

where a and b are positive constants for the conical domain and $a = 0$ for the upper cylindrical domain. By using the standard rules for the derivative transformation under the transformation of coordinates (5.5), it is easy to show that in the conical domain the governing equations for $v^{(1)}(\tilde{x}, \tilde{y})$ and $v^{(2)}(\tilde{x}, \tilde{y})$ take the form (we have dropped the symbol "$\sim$")

$$\begin{aligned} v_t^{(1)} &= \frac{1}{ay+b}\left[(axv^{(2)} - v^{(1)})v_x^{(1)} - 2\nu a x v_{xy}^{(1)} + \lambda v_{xy}^{(2)}\right] + (\nu v_{yy}^{(1)} - v^{(2)}v_y^{(1)}) + \\ &+ \frac{1}{(ay+b)^2}\left[(\nu(a^2x^2+1)+\lambda)v_{xx}^{(1)} - \lambda a x v_{xx}^{(2)} + \nu a^2 x v_x^{(1)} - \lambda a v_x^{(2)}\right], \qquad (5.6) \\ v_t^{(2)} &= \frac{1}{ay+b}\left[(axv^{(2)} - v^{(1)})v_x^{(2)} - 2(\lambda+\nu)a x v_{xy}^{(2)} + \lambda v_{xy}^{(1)}\right] + ((\lambda+\nu)v_{yy}^{(2)} - v^{(2)}v_y^{(2)}) + \\ &+ \frac{1}{(ay+b)^2}\left[(a^2x^2(\lambda+\nu)+\nu)v_{xx}^{(2)} - \lambda a x v_{xx}^{(1)} + (\lambda+\nu)a^2 x v_x^{(2)} - a\lambda v_x^{(1)}\right] + \mathbf{G}, \end{aligned}$$

while in the cylindrical region the equation (2.25) can be directly written as

$$\begin{aligned} v_t^{(1)} &= \nu(v_{xx}^{(1)} + v_{yy}^{(1)}) - (v^{(1)}v_x^{(1)} + v^{(2)}v_y^{(1)}) + \lambda(v_{xx}^{(1)} + v_{xy}^{(2)}), \\ v_t^{(2)} &= \nu(v_{xx}^{(2)} + v_{yy}^{(2)}) - (v^{(1)}v_x^{(2)} + v^{(2)}v_y^{(2)}) + \lambda(v_{xy}^{(1)} + v_{yy}^{(2)}) + G. \end{aligned} \tag{5.7}$$

Here G is the gravity force and we assume that the external pressure gradient is equal to 0. On the boundary between the cylindrical and conical domains, which we shall denote as (x, y_0), the following matching condition for the velocity field has to be satisfied

$$\mathbf{v}(x, y_0 - 0) = \mathbf{v}(x, y_0 + 0). \tag{5.8}$$

The boundary conditions (5.1)-(5.2) in the cylindrical domain of a hopper take the form

$$v^{(1)} = 0, \quad \frac{dv^{(2)}}{dx} = \mp k v^{(2)} \tag{5.9}$$

with different signs for the left and right walls, respectively. Transformation of the expressions (5.1)-(5.2) to the "hopper coordinates" leads to the following boundary conditions for the conical domain of a hopper:

$$\begin{aligned} &\frac{1 - ax}{ay + b} v_x^{(1)} + v_y^{(1)} = k v^{(1)}, \\ &a v^{(2)} = -v^{(1)} \end{aligned} \tag{5.10}$$

for the left wall, and

$$\begin{aligned} &\frac{1 + ax}{ay + b} v_x^{(1)} - v_y^{(1)} = k v^{(1)}, \\ &a v^{(2)} = v^{(1)} \end{aligned} \tag{5.11}$$

for the right wall. Notice that notations $v^{(1)}(x, y)$ and $v^{(2)}(x, y)$ in the conical region mean that x and y are the "hopper coordinates" but $v^{(1)}(x, y)$ and $v^{(2)}(x, y)$ are still the horizontal and vertical components of the velocity field with respect to the regular Cartesian coordinate system, not "vertical" or "horizontal" with respect

to the hopper coordinate system. In this case we can satisfy easily the matching condition (5.8). Also the boundary conditions (5.4) at the outlet of the hopper remain unchanged.

Equations (5.6)-(5.7), (5.9)-(5.11) can be discretized and solved in the framework of finite-differences. We shall satisfy the matching condition (5.8) in the following manner. Let the points (i, j), $i = 1, \ldots, N$, $j = M$ on the finite-difference grid correspond to the boundary (x, y_0) between the cylindrical and conical domains. Using the initial data, the boundary equations (5.3), (5.9) and the equation (5.7) discretized with the centered-difference formulas for derivatives, we can obtain values of the velocity field at the time $t_0 + \Delta t$ for the domain from the top of the hopper to the level $(i, M+1)$, $i = 1, \ldots, N$. Then using the equation (5.7) discretized with forward-difference formulas we can obtain values of the velocity field on the level (i, M), $i = 1, \ldots, N$. These values can be considered then as the boundary data for the conical domain, and values of the velocity field in the conical domain at later times can be obtained using the discretized version of the equation (5.6) in the centered-differences scheme, the initial data and the boundary data equations for the conical domain.

5.2 Numerical Solutions

Now we shall describe briefly the well known experimentally observable features of granular flows in hoppers (See, for example, [83]). Examination of the flow patterns occurring in storage hoppers during discharge shows that there are two types of hoppers, referred to as core flow (or sometimes funnel flow) and mass flow hoppers.

The flow patterns in a core flow hopper are shown as a sequence of photographs in Fig. 5.3. The diagrams represent a cross-section through a hopper; the horizontal lines are made up of colored particles whose position permits visualization of the

flow pattern. A core flow hopper is therefore characterized by the existence of dead spaces while discharge is taking place.

A mass flow hopper is defined as one in which every particle is in motion when material is being discharged from the hopper; in particular, particles in contact with the walls are sliding downwards. Fig. 5.4 is a set of photographs showing the flow pattern during discharge. A mass flow hopper is therefore characterized by the absence of any dead spaces.

The most important disadvantage of a core flow hopper is that, for a cohesive material, flow from the hopper can stop for no apparent reason. The stoppage may result either from the formation between the hopper walls of an arch, which is strong enough to resist the stress applied to it by the weight of the remaining material, or by piping or rat-holing, in which the material directly above the outlet falls out, leaving an empty cylinder defined by almost vertical powder walls.

An arch may form at some distance above the hopper outlet and then collapse, exerting very large stress on the lower part of the hopper. In an extreme case this can tear away the converging part of the hopper, with disastrous results.

For powders which are easily aretable, which generally means those having a mean particle size (surface-volume mean) in the range $20 - 150\,\mu m$, the collapse of an arch inside the hopper can lead to conditions in which the whole contents of the hopper is fluidized, so that it discharges very rapidly from the hopper. This condition, which is referred to as flooding, can be very dangerous. In addition to this, free flowing particles are very prone to size segregation on handling. If the material is a mixture in which the components have different size distribution, passing it through a core flow hopper may cause a considerable loss of mixing quality.

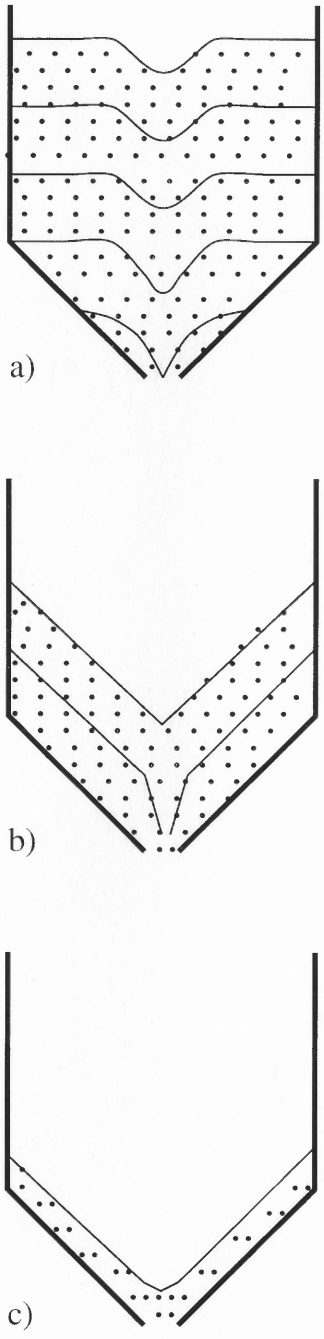

Figure 5.3 Flow patterns in a core type hopper

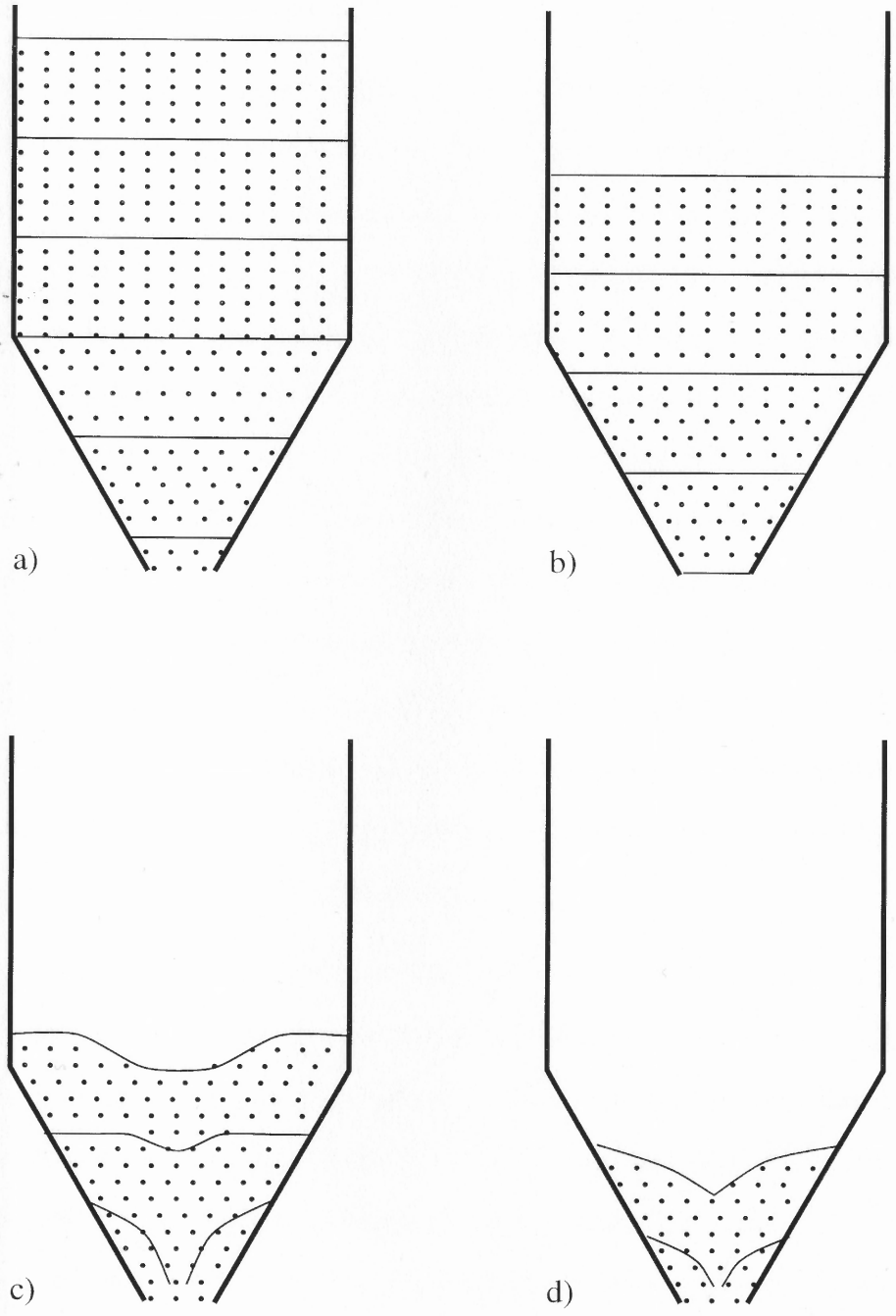

Figure 5.4 Flow patterns in a mass type hopper

Even when flow does not stop, the material coming out of the core flow hopper may be very variable in rate and bulk density. Therefore the mass flow hoppers are more preferable in most industrial applications.

We have shown that some of the typical hopper flows can be modeled by using the model described above. We use an explicit finite difference scheme for solving the system (5.6)-(5.7) with a spatial step $\Delta x = \Delta y = 0.001$ and a time step $\Delta t = 10^{-5}$. Estimates show that such a small time step is needed to satisfy the stability condition for the explicit finite-difference scheme. In view of using explicit forms for the functions $\eta(\cdot)$ and $\Psi(\cdot)$ (2.26) allowing computation of ν and λ, we select different values for these as well as for k in computing solutions. Some typical results are depicted in Fig. 5.5-5.6. These pictures reproduce the experimentally observable results for the mass flow type of hoppers and show how the velocity field at the outlet of the hopper depends on the wall friction coefficient, coefficient of friction between particles and the other parameters in equation (2.25). Comparing numerical solutions with experimental results we can prescribe some particular values of the parameters λ, ν and k corresponding to materials. This makes it possible to model actual granular flows through hoppers.

As for a mathematical description of the flow patterns taking place in a core flow hopper, it seems that all existing continuum mathematical models and, in particular, the hydrodynamic type dynamical system (2.25) can not provide results that are in precise agreement with experimental data. The main reason for this is the nature of friction in solids. The friction coefficient for solids is not a constant but depends on the relative velocity between solids. This dependence is roughly linear for the nonzero velocity and the friction coefficient increases substantially when the relative velocity tends to zero (stationary friction phenomena). This phenomena may be responsible (for ideal noncohesive solid particles) for forming the dead regions and arches near

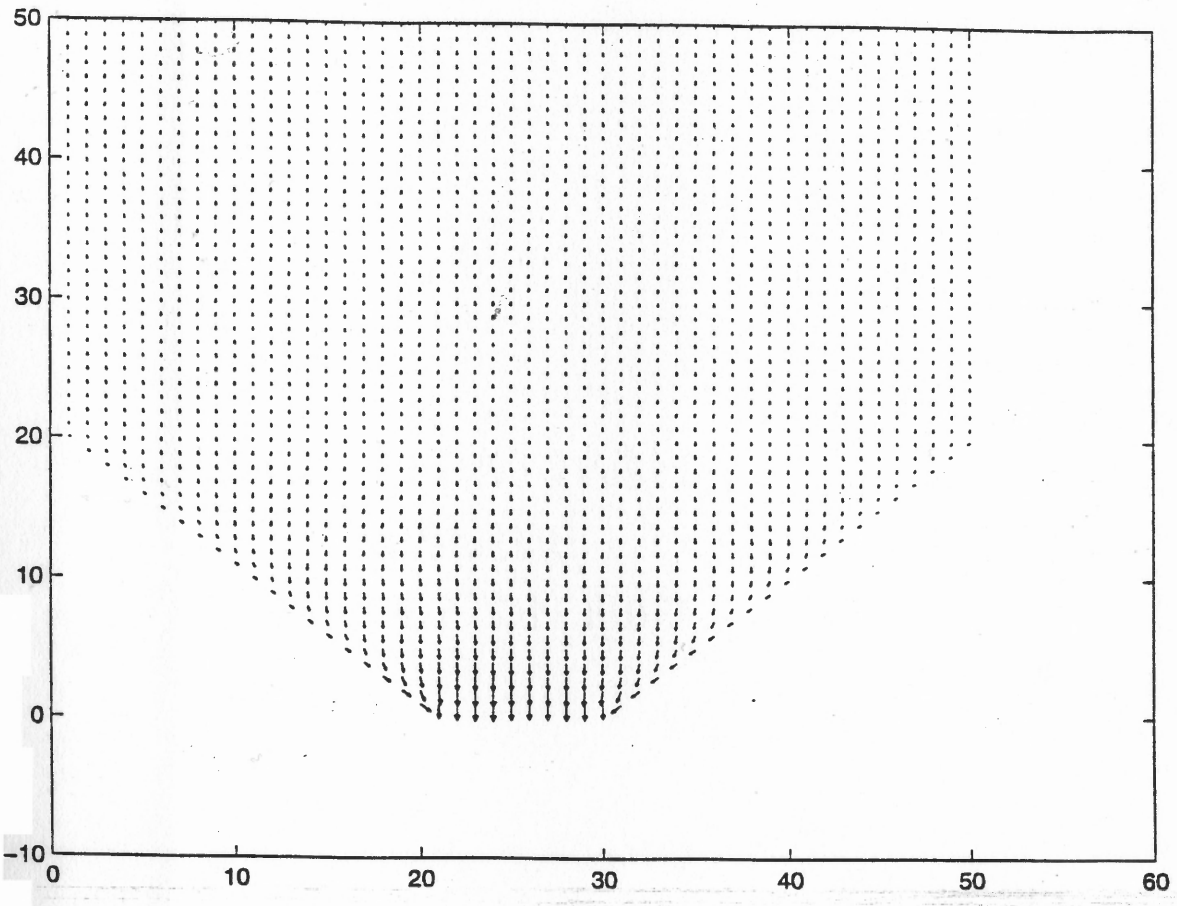

Figure 5.5 Numerical solution to the hopper flow problem; $\lambda = 0.5$, $\nu = 0.7$ (wide outlet)

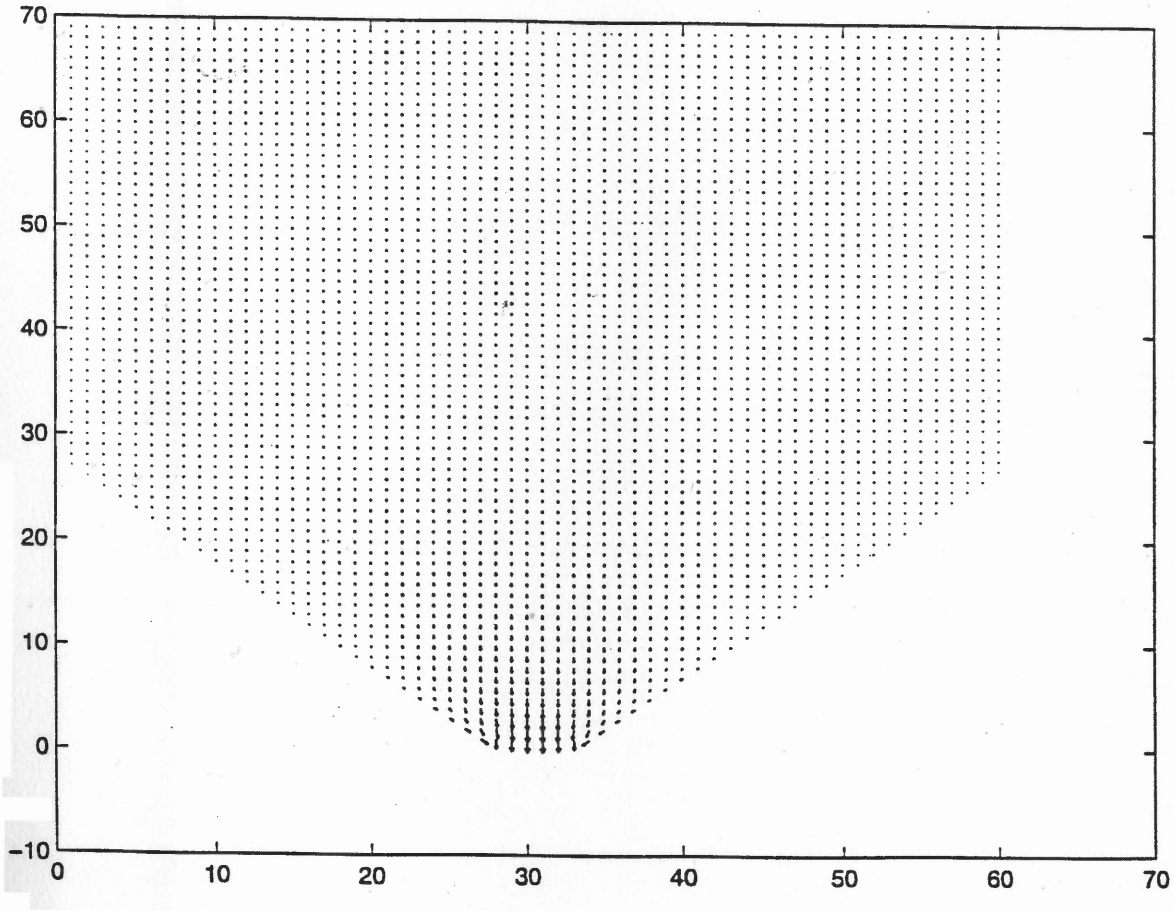

Figure 5.6 Numerical solution to the hopper flow problem; $\lambda = 0.8$, $\nu = 1.0$ (narrow outlet)

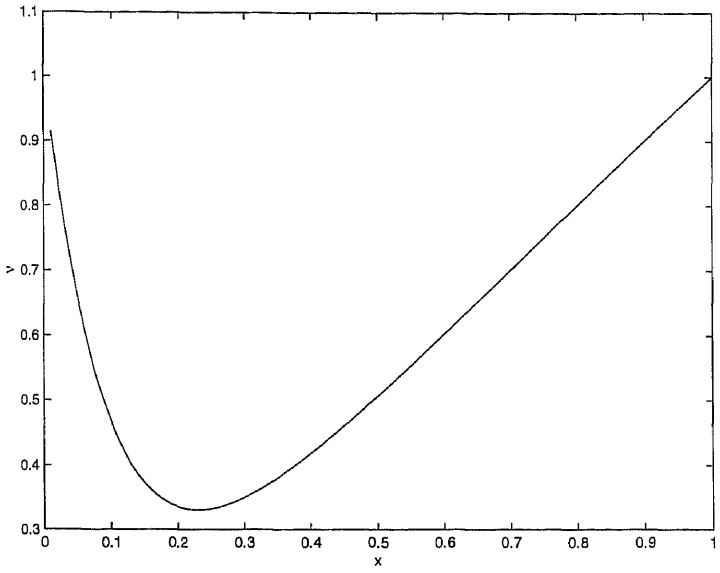

Figure 5.7 Dependence of the coefficient of friction on the relative velocity between particles

the outlet of a core flow hopper. In many practical cases, however, cohesivity plays a more important role in forming these patterns. The continuum mathematical models are usually derived under the assumption of a simple linear dependence of friction, hence their ability to capture the cohesivity in particulate materials is restricted. It seems to us that these phenomena can be best described using a discrete approach such as numerical simulation, but to the best of our knowledge no one has attempted this.

By making the coefficients of friction in the governing equation (2.25) functionally dependent on the relative velocity between particles, as is shown in Fig. 5.7, we were able to model the influence of the stationary friction phenomena and to reproduce roughly in this way experimentally observable behavior. The numerical solution shown in Fig. 5.8 reproduces qualitatively the dead spaces in the core flow type of hoppers and the piping or rat-holing type of discharge in which the material directly above the outlet falls out, leaving an empty cylinder defined by almost vertical powder walls.

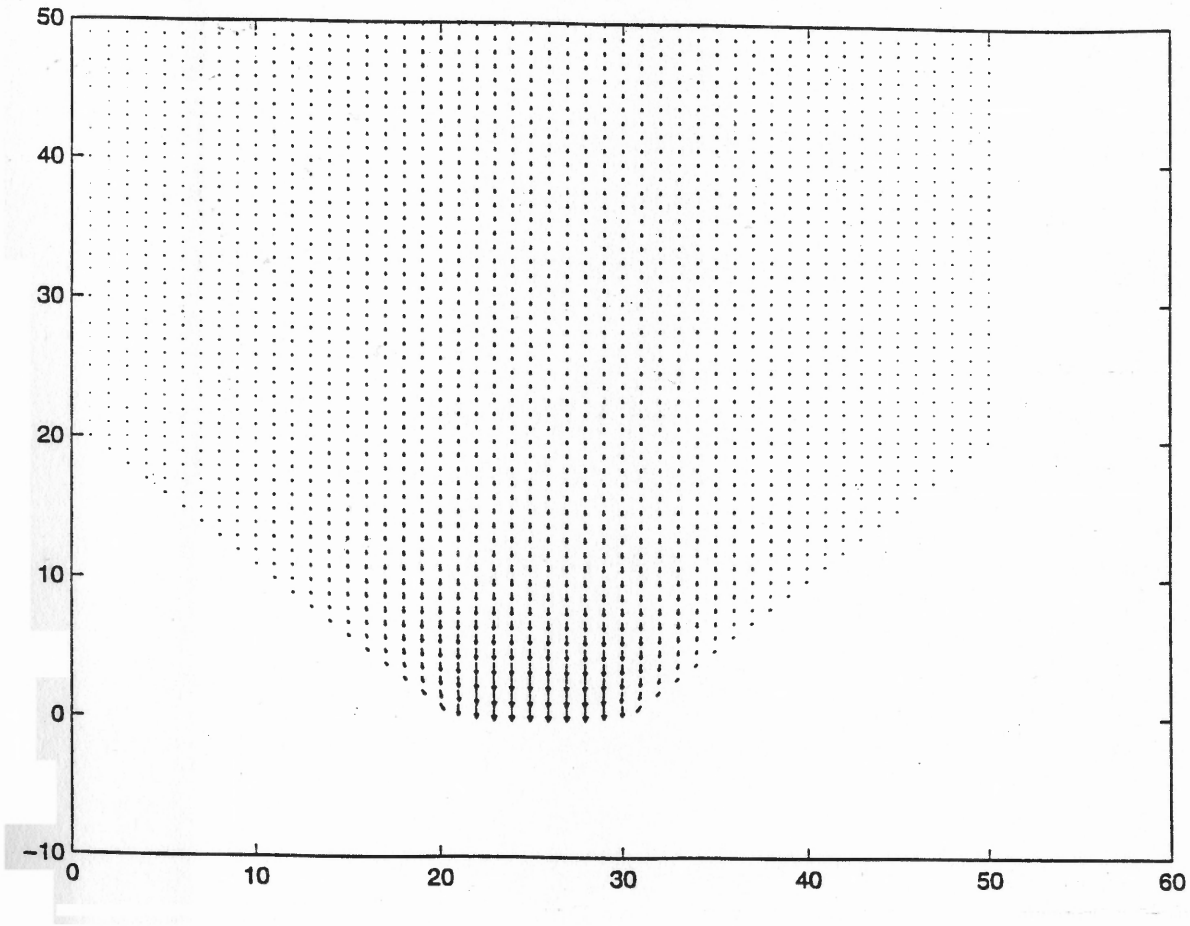

Figure 5.8 Numerical solution to the hopper flow problem with variable friction coefficients

CHAPTER 6

ONE-DIMENSIONAL GRANULAR FLOW DYNAMICAL SYSTEMS AND SOME RELATED PROBLEMS OF FLUID MECHANICS

6.1 Integrability Structures for Burgers Equation

Restriction of the granular flow dynamical system (2.25) to one-dimensional space leads to the well known Burgers equation

$$u_t + uu_x = \beta u_{xx}. \tag{6.1}$$

A one dimensional array of particles between oscillating walls was studied in [12] by using both the set of discrete equations and the equation (6.1). It was shown that the system displays a rich variety of dynamical behavior including period-doubling cascades and chaotic motion.

In this section we shall study the Liouville-Lax integrability structures for the Burgers equation by using the Cartan differential-geometric approach.

Let a Lie group G act transitively on an analytic manifold Y, that is the action $G \times Y \xrightarrow{\rho} Y$ generates some nonlinear exact representation of the Lie group G on the manifold Y. In the frame of the Cartan's differential geometric theory, the representation $G \times Y \xrightarrow{\rho} Y$ can be described by means of a system of differential 1-forms

$$\bar{\beta}^j := dy^j + \sum_{i=1}^{r} \xi_i^j \bar{\omega}^i(a; da) \in \Lambda^1(Y \times G) \tag{6.2}$$

in the Grassmann algebra $\Lambda^1(Y \times G)$ on the product $Y \times G$, where $\bar{\omega}^i(a; da) \in T_a^*(G)$, $1 \leq i \leq r = dim\, G$ is a basis of left invariant Cartan's forms of the Lie group G at a point $a \in G$, $y := \{y^j : 1 \leq j \leq n = dim\, Y\} \in Y$ and $\xi_i^j : Y \times G \to \mathbf{R}$ are some smooth real-valued functions. We shall need the following result of Cartan:

Theorem 3.3(E.Cartan). *The system of differential forms (6.2) is a system of an invariant geometric object if and only if the following conditions are fulfilled:*

i) the coefficients $\xi_i^j \in C^\infty(Y;\mathbf{R})$ *for all* $1 \leq i \leq r$, $1 \leq j \leq n$, *are analytic functions on* Y;

ii) the differential sysetm (6.2) is completely integrable in the Frobenius-Cartan sense.

Theorem 3.3 says that the differential system (6.2) can be written as

$$\bar{\beta}^j := dy^j + \sum_{i=1}^{r} \xi_i^j(y)\bar{\omega}^i(a;da), \tag{6.3}$$

where the one-forms $\{\bar{\omega}^i(a;da) : 1 \leq i \leq r\}$ satisfy the standard Maurer-Cartan equations

$$\bar{\Omega}^j := d\bar{\omega}^j + \frac{1}{2}\sum_{i,k=1}^{r} c_{ik}^j \bar{\omega}^i \wedge \bar{\omega}^k = 0 \tag{6.4}$$

for all $j = 1,\ldots,r$ on G, where the coefficients $c_{ik}^j \in \mathbf{R}$, $1 \leq i,j,k \leq r$, are the corresponding structure constants of the Lie algebra $\mathcal{G}$ of the Lie group G.

Let us consider here a case when the set of canonical Maurer-Cartan one-forms $\{\bar{\omega}^i(a;da) \in T_a^*(G) : i = \overline{1,r}\}$ is defined via the scheme:

$$\begin{array}{ccccc} T^*(M\times Y) & \xrightarrow{s^*} & T^*(\bar{M}) & \xleftarrow{\mu^*} & T^*(G\times Y) \\ M\times Y & \xleftarrow{s} & \bar{M} & \xrightarrow{\mu} & G\times Y \end{array} \tag{6.5}$$

where M is a given smooth finite-dimensional manifold with some submanifold $\bar{M} \subset M$ imbedded in it via $s : \bar{M} \to M \times Y$, and $\mu : \bar{M} \to G \times Y$ is some smooth mapping into $G \times Y$. Under the mappings scheme (6.5) the expression (6.4) takes the following form:

$$s^*\Omega^j\Big|_{\bar{M}} := \mu^*\bar{\Omega}^j\Big|_{\bar{M}} :\Rightarrow 0 \tag{6.6}$$

for all $j = 1,\ldots,r$ upon the integral submanifold $\bar{M} \subset M$, where $\Omega^j \in \Lambda^2(M)$, $j = 1,\ldots,n$, is some *a priori* given system of 2-forms on M.

Assume further that a set $\{\alpha_j \in \Lambda^2(M) : j = 1,\ldots,m_\alpha\}$ is a basis for the space spanned by the two-forms $\{\Omega^j \in \Lambda^2(M) : j = 1,\ldots,r\}$, generating the ideal

$\mathcal{I}(\alpha) \subset \Lambda(M)$. The ideal $\mathcal{I}(\alpha)$ is completely integrable in the Cartan sense. To see this, note that (6.4) implies that $d\Omega^j \in \mathcal{I}(\Omega)$, $j = 1, \ldots, r$, hence $\mathcal{I}(\Omega) \equiv 0$ on $\bar{M}$, and so it follows from the diagram (6.5) that $d\mathcal{I}(\alpha) \subset \mathcal{I}(\alpha)$ since $s^*\mathcal{I}(\alpha) = \mu^*\mathcal{I}(\bar{\Omega})$.

To define now a criterium for a Lie group action $G \times Y \xrightarrow{\rho} Y$ to generate a representation of the Lie group G, we need to construct the ideal $\mathcal{I}(\alpha, \beta) \subset \Lambda(M \times Y)$, corresponding to (6.3) and (6.6), for a some set of forms $\beta^j \in \Lambda^1(M \times Y)$, $j = 1, \ldots, r = n$, where $s^*\beta_j := \mu^*\bar{\beta}_j \in \Lambda(\bar{M} \times Y)$, $j = 1, \ldots, n$, and require that it be closed in $\Lambda(M \times Y)$, that is $d\mathcal{I}(\alpha, \beta) \subset \mathcal{I}(\alpha, \beta)$, or

$$d\beta^j = \sum_{k=1}^{m_\alpha} f_k^j \alpha^k + \sum_{i=1}^{n} g_i^j \wedge \beta^i \tag{6.7}$$

for all $j = 1, \ldots, n$ and some $f_k^j \in \Lambda^0(M \times Y)$, $k = 1, \ldots, m_\alpha$, $g_i^j \in \Lambda^1(M \times Y)$, $i, j = 1, \ldots, n$. The condition (6.7) guarantees the existence of a smooth submanifold $\bar{M}(Y) \subset M \times Y$, on which the nonlinear Lie group G representation acts exactly. Thereby, we establish the validity of the following result.

Theorem 3.4. *The system $\{\beta\}$ of Cartan's one-forms $\beta^j \in \Lambda^1(M \times Y)$, $j = 1, \ldots, n$, generated by the mapping scheme (6.5), describes an exact nonlinear Lie group G representation on a manifold Y if and only if the adjoint ideal $\mathcal{I}(\alpha, \beta)$ generated by the system $\{\beta^j\}$ and a basic system $\{\alpha^j\}$ of "curvature" 2-forms $\Omega^j \in \Lambda^2(M)$, $j = 1, \ldots, r$, of (6.6), is closed together with the corresponding ideal $\mathcal{I}(\alpha) = \mathcal{I}(\alpha, 0)$ in the Grassmann algebras $\Lambda(M \times Y)$ and $\Lambda(M)$ respectively.*

In view of the results stated above, it is natural to consider a special case of Cartan's geometric construction by means of the theory of principal fiber bundles [99]. To begin, let us try to interpret the Cartan differential system $\{\beta^j\}$ on $M \times Y$ as one generating a linear $(r \times r)$ - matrix adjoint representation [23] of the Lie algebra $\mathcal{G}$, defining the functions $\xi_i^j(y) := \sum_{k=1}^r c_{ik}^j y^k$, $i, j = 1, \ldots, r$, when $dim\, Y = n := r$:

$$\beta^j := dy^j + \sum_{i,k=1}^{r} c_{ik}^j y^k b^i(z) \in \Lambda^1(M \times Y), \tag{6.8}$$

where $z \in M$, and the 1-forms $b^i(z)$ on M satisfy the necessary embedding conditions $s^*b^i = \mu^*\bar{\omega}^i$ on $\bar{M} \subset M$ for all $i, j = 1, \ldots, r$ in accordance with the diagram (6.2).

The Lie group G acts on the linear r-dimensional space Y by the usual left shifts as follows: $Y \times G \ni y \times a \xrightarrow{\rho} ay \in Y$ for all $a \in G$. Whence we can easily deduce the following infinitesimal shifts in the Lie group G:

$$da_k^j + \sum_{s=1}^{r} c_{si}^j b^s(z) a_k^i \in \Lambda^1(M \times G).$$

These expressions ultimately generate the following $\mathcal{G}$-valued Ad-invariant 1-form ω on $M \times G$ via the isomorphic mapping $\rho^* : \Lambda^1(M \times Y) \to \Lambda^1(M \times G) \otimes \mathcal{G}$:

$$\{\beta\} :\xrightarrow{\rho^*} \omega := a^{-1}da + Ad_{a^{-1}}\Gamma(z), \tag{6.9}$$

where the one-forms matrix $\Gamma(z) := \left(\Gamma_k^j(z)\right)$, $j, k = 1, \ldots, r$, belongs to the $(r \times r)$-matrix representation of the Lie algebra $\mathcal{G}$ via the construction: $\left(\Gamma_k^j(z)\right) := \left(\sum_{i=1}^r c_{ik}^j b^i(z)\right) \in T^*(M) \otimes \mathcal{G}$. The results above can be naturally interpreted as a way of defining [99] a $\mathcal{G}$-valued connection Γ on a principal fibered space $P(M; G)$, carrying the $\mathcal{G}$-valued connection 1-form (6.9). The corresponding Cartan 1-forms determine the horizontal subspace of the parallel transport vectors of the fiber bundle $P(M; G, Y)$ associated with $P(M; G)$ according to the general theory [99] of fibered spaces with connections.

Thus, we have defined the $\mathcal{G}$-valued connection 1-form (6.9) at a point $(z, a) \in P(M; G)$ as $\omega := \bar{\omega}(a) + Ad_{a^{-1}}\Gamma(z)$, where $\bar{\omega}(a) \in T^*(G) \otimes \mathcal{G}$ is the standard Maurer-Cartan left- invariant $\mathcal{G}$- valued 1-form on the Lie group G. The connection 1-form (6.9) vanishes on the horizontal subspace, consisting of vector fields on $P(M; G)$, which generate a Lie group G representation on the space Y . This means, that this horizontal subspace necessarily defines a completely integrable differential system on $P(M; G)$, or equivalently, the corresponding curvature $\Omega \in \Lambda^2(M) \otimes \mathcal{G}$ of the

connection Γ vanishes on the integral submanifold $\bar{M} \subset M$:

$$\Omega := d\omega + \omega \wedge \omega = Ad_{a^{-1}}(d\Gamma(z) + \Gamma(z) \wedge \Gamma(z)) = \frac{1}{2} Ad_{a^{-1}} \sum_{j=1}^{m} \Omega_{jk} dz^j \wedge dz^k = 0 \text{ on } \bar{M}. \tag{6.10}$$

Whence, we obtain

$$\Omega_{ij}(z) := \frac{\partial \Gamma_j(z)}{\partial z_i} - \frac{\partial \Gamma_i(z)}{\partial z_j} + [\Gamma_i(z), \Gamma_j(z)], \tag{6.11}$$

$$\Gamma(z) := \sum_{j=1}^{m} \Gamma_j(z) dz^j := \sum_{j=1}^{m} \sum_{k=1}^{r} \Gamma_j^k(z) dz^j A_k.$$

The vanishing of the curvature Ω (6.10) on the submanifold $\bar{M} \subset M$ is easily explained by means of the following commuting diagram:

$$\begin{array}{ccccc} T^*(G) & \xrightarrow{\mu^*} & T^*(P(\bar{M};G)) & \xleftarrow{s^*} & T^*(P(M;G)) \quad \xleftarrow{\rho^*} \quad T^*(P(M;G,Y)) \\ G & \xleftarrow{\mu} & P(\bar{M};G) & \xrightarrow{s} & P(M;G) \quad \xrightarrow{\rho} \quad P(M;G,Y) \end{array} \tag{6.12}$$

We can now see from (6.12), that owing to (6.9),

$$\rho^*\{\beta\} = \omega, \quad s^*\Gamma_k^j = \sum_{i=1}^{r} c_{ik}^j \mu^* \bar{\omega}^i \;\Rightarrow\; s^*\Omega = \mu^*\bar{\Omega} = 0, \tag{6.13}$$

from which (6.10) follows.

Thus, if some integrable ideal $\mathcal{I}(\alpha) \subset \Lambda(M)$ is *a priori* given on the manifold M, the equation (6.10) on $\Lambda(M)$,

$$\sum_{j,k=1}^{m} \Omega_{jk} dz^j \wedge dz^k \subset \mathcal{I}(\alpha)$$

both determines the $\mathcal{G}$-valued 1-forms $\Gamma_j(z) \in T^*(M) \otimes \mathcal{G}$, $j = 1, \ldots, m$, and the Lie algebra structure of $\mathcal{G}$, owing to the holonomy Lie group reduction theorem of Ambrose, Singer and Loos [4, 56]. In particular, the holonomy Lie algebra $\mathcal{G}(h) \subset \mathcal{G}$ is generated by composition of covariant derivatives of the $\mathcal{G}$-valued curvature form $\Omega \in T^*(M) \otimes \mathcal{G}$:

$$\mathcal{G}(h) := span_{\mathbf{R}}\{\nabla_1^{j_1} \nabla_2^{j_2} \ldots \nabla_n^{j_n} \Omega_{si} \in \mathcal{G} : \; j_k \in \mathbf{Z}_+, \; s, i, k = 1, \ldots, n\} \tag{6.14}$$

where, by definition, the covariant derivative $\nabla_j := \Lambda(M) \to \Lambda(M)$, $j = 1, \ldots, n$, is defined as

$$\nabla_j := \partial/\partial z^j + \Gamma_j(z). \tag{6.15}$$

If $\mathcal{G}(h) = span_{\mathbf{R}}\{\Omega_{st} \in \mathcal{G} : \ s, l = 1, \ldots, n\}$, that is the inclusion $[\mathcal{G}(h), \mathcal{G}(h)] \subset \mathcal{G}(h)$ obtains, the holonomy Lie algebra $\mathcal{G}(h)$ is called perfect. Thus, we can formulate the following equivalence theorem.

Theorem 3.5 *Given a closed ideal $\mathcal{I}(\alpha)$ on a manifold M, $d\mathcal{I}(\alpha) \subset \mathcal{I}(\alpha)$, its 1-forms augmentation $\mathcal{I}(\alpha, \beta)$ on $M \times Y$ by means of a special set $\{\beta\}$ of 1-forms*

$$\{\beta\} := \{\beta^j = dy^j + \sum_{k=1}^{n} \xi_k^j(y) b^k(z) : \ b^j(z) \in T^*(M), \ j = 1, \ldots, n\}, \tag{6.16}$$

compatible with the scheme (6.12), is Frobenius-Cartan integrable criterium if and only if there exists a Lie group G action on Y, such that the adjoint connection (6.9) on a fibered space $P(M; G)$ with the structure group G vanishes on the integral submanifold $\bar{M} \subset M$ of the ideal $\mathcal{I}(\alpha) \subset \Lambda(M)$. The latter can serve as the alhorithm of determining the structure of the Lie group G in conjunction with the holonomy Lie algebra reduction theorem of Ambrose-Singer-Loos [4, 56].

If the conditions of Theorem 3.5 are fulfilled, the set of 1-forms $\{\beta\}$ (6.16) generates a representation of the Lie group G on the analytic manifold Y according to the Cartan theorem 3.3. The Lie algebra $\mathcal{G}$ of the Lie group G can be reduced to the holonomy Lie algebra $\mathcal{G}(h)$, generated via (6.14) by the curvature 2-form Ω of the connection Γ on the principal fiber bundle $P(M; G)$ constructed above.

Let us consider some set $\{\beta^j\}$ defining a Cartan Lie group G invariant object on a manifold $M \times Y$:

$$\beta^j := dy^j + \sum_{k=1}^{r} \xi_k^j(y) b^k(z), \tag{6.17}$$

where $i = 1, \ldots, n = dim\, Y$, $r = dim\, G$, satisfies the mapping scheme (6.5) for a chosen integral submanifold $\bar{M} \subset M$. Then the set (6.17) defines on the manifold

Y a set $\{\xi_s\}$ of vector fields comprising a representation $\rho : \mathcal{G} \to \{\xi_s\}$ of the Lie algebra $\mathcal{G}$; that is, the vector fields $\xi_s := \sum_{j=1}^{n} \xi_s^j(y)\frac{\partial}{\partial y^j} \in \{\xi_s\}$, $s = 1, \ldots, r$, satisfy the following Lie algebra $\mathcal{G}$ relationships

$$[\xi_s, \xi_l] = \sum_{k=1}^{r} c_{sl}^k \xi_k \tag{6.18}$$

for all $s, l, k = 1, \ldots, n$. We can now compute the differentials $d\beta^j \in \Lambda^2(M \times Y)$, $j = 1, \ldots, n$, using (6.17) and (6.18) as follows:

$$d\beta^j = \sum_{l=1}^{n}\sum_{k=1}^{r} \frac{\partial \xi_k^j(y)}{\partial y^l}\left(\beta^l - \sum_{s=1}^{r} \xi_s^l(y) b^s(z)\right) \wedge b^k(z) + \tag{6.19}$$

$$+ \sum_{l=1}^{n}\sum_{k=1}^{r} \xi_k^j(y) db^k(z) = \sum_{l=1}^{n}\sum_{k=1}^{r} \frac{\partial \xi_k^j(y)}{\partial y^l}\beta^l \wedge b^k(z) -$$

$$- \sum_{l=1}^{n}\sum_{k,s=1}^{r} \frac{\partial \xi_k^j(y)}{\partial y^l}\xi_s^l(y) b^s(z) \wedge b^k(z) + \sum_{k=1}^{r} \xi_k^j(y) db^k(z) =$$

$$= \sum_{l=1}^{n}\sum_{k=1}^{r} \frac{\partial \xi_k^j(y)}{\partial y^l}\beta^l \wedge b_k(z) + \frac{1}{2}\sum_{l=1}^{n}\sum_{k,s=1}^{r}\left[\frac{\partial \xi_k^j(y)}{\partial y^l}\xi_s^l(y) - \frac{\partial \xi_s^j(y)}{\partial y^l}\xi_k^l(y)\right] \times$$

$$\times db^k(z) \wedge db^s(z) + \sum_{k=1}^{r} \xi_k^j(y) db^k(z) =$$

$$= \sum_{l=1}^{n}\sum_{k=1}^{r} \frac{\partial \xi_k^j(y)}{\partial y^l}\beta^l \wedge b_k(z) + \frac{1}{2}\sum_{k,s=1}^{r} [\xi_s, \xi_k]^j db^k(z) \wedge db^s(z) +$$

$$+ \sum_{k=1}^{r} \xi_k^j(y) db^k(z) = \sum_{l=1}^{n}\sum_{k=1}^{r} \frac{\partial \xi_k^j(y)}{\partial y^l}\beta^l \wedge b_k(z) +$$

$$+ \frac{1}{2}\sum_{l=1}^{n}\sum_{k,s=1}^{r} c_{ks}^l \xi_l^j db^k(z) \wedge db^s(z) + \sum_{k=1}^{r} \xi_k^j(y) db^k(z) \Rightarrow \sum_{l=1}^{n}\sum_{k=1}^{r} \frac{\partial \xi_k^j(y)}{\partial y^l}\beta^l \wedge b_k(z) +$$

$$+ \sum_{l=1}^{r} \xi_l^j \left(db^l(z) + \frac{1}{2}\sum_{k,s=1}^{r} c_{ks}^l db^k(z) \wedge db^s(z)\right) : \in \mathcal{I}(\alpha, \beta) \subset \Lambda(M \times Y),$$

where $\{\alpha^j\} \subset \Lambda^2(M)$ is given integrable system of 2-forms on M, vanishing on the integral submanifold $\bar{M} \subset M$. It is obvious that inclusions (6.19) hold if and only if the following conditions obtain: for all $j = 1, \ldots, r$,

$$db^j(z) + \frac{1}{2}\sum_{k,s=1}^{r} c_{ks}^j db^k(z) \wedge db^s(z) \in \mathcal{I}(\alpha). \tag{6.20}$$

In particular, the inclusions (6.20) imply that on the integral submanifold $\bar{M} \subset M$ of the ideal $\mathcal{I}(\alpha) \subset \Lambda(M)$, the equalities

$$\mu^* \bar{\omega}^j \equiv s^* b^j, \tag{6.21}$$

hold, where $\bar{\omega}^j \in T_e^*(G)$, $j = 1, \ldots, r$, are the left invariant Maurer-Cartan forms on the invariance Lie group G. Thus, due to the inclusions (6.20) all conditions of Cartan's Theorem 3.3 are satisfied, making it possible to obtain the set of forms $b^j(z) \in \Lambda^1(M)$ explicitly. To do this, let us define a $\mathcal{G}$-valued curvature 1-form $\omega \in \Lambda^1(P(M;G)) \otimes \mathcal{G}$ as follows

$$\omega := Ad_{a^{-1}} \left(\sum_{j=1}^{r} A_j b^j \right) + \bar{\omega} \tag{6.22}$$

where $\bar{\omega} \in \mathcal{G}$ is the standard Maurer-Cartan 1-form on G, constructed in Chapter 2. This 1-form satisfies the canonical structure inclusion (6.10) for $\Gamma := \sum_{j=1}^{r} A_j b^j \in \Lambda^1(M) \otimes \mathcal{G}$:

$$d\Gamma + \Gamma \wedge \Gamma \in \mathcal{I}(\alpha) \otimes \mathcal{G}, \tag{6.23}$$

which along with (6.20) provides the means for determining the form (6.22). To proceed further we need to describe the set $\{\alpha^j\} \subset \Lambda^2(M)$ in explicit form.

Applications to the Burgers dynamical system.

Let the following Burgers dynamical system be given on a functional manifold $M \subset C^\infty(\mathbf{R};\mathbf{R})$:

$$u_t = uu_x + u_{xx}, \tag{6.24}$$

where $u \in M$, and $t \in \mathbf{R}$ is an evolution parameter. The flow (6.24) on M can be recast in terms of a set of 2-forms $\{\alpha^j\} \subset \Lambda^2(J(\mathbf{R}^2;\mathbf{R}))$ on the adjoint jet-manifold $J(\mathbf{R}^2;\mathbf{R})$ as follows:

$$\{\alpha^j\} = \Big\{ du^{(0)} \wedge dt - u^{(1)} dx \wedge dt = \alpha^1,\ du^{(0)} \wedge dx + u^{(0)} du^{(0)} \wedge dt + \tag{6.25}$$

$$+du^{(1)} \wedge dt = \alpha^2 : \ \left(x, t; u^{(0)}, u^{(1)}\right)^T \in M^4 \subset J^1(\mathbf{R}^2; \mathbf{R})\Big\},$$

where M^4 is some finite-dimensional submanifold in $J^1(\mathbf{R}^2; \mathbf{R})$) with coordinates $\left(x, t, u^{(0)} = u, u^{(1)} = u_x\right)$. The set of 2-forms (6.25) generates a closed ideal $\mathcal{I}(\alpha)$, since

$$d\alpha^1 = dx \wedge \alpha^2 - u^{(0)} dx \wedge \alpha^1, \quad d\alpha^2 = 0. \tag{6.26}$$

Define the integral submanifold $\bar{M} = \{x, t \in \mathbf{R}\} \subset M^4$ by the condition $\mathcal{I}(\alpha) = 0$. We now look for a reduced "curvature" 1-form $\Gamma \in \Lambda^1(M^4) \otimes \mathcal{G}$, belonging to some as yet undetermined Lie algebra $\mathcal{G}$. This 1-form can be represented using (6.25) as follows:

$$\Gamma := b^{(x)}(u^{(0)}, u^{(1)})dx + b^{(t)}(u^{(0)}, u^{(1)})dt, \tag{6.27}$$

where elements $b^{(x)}, b^{(t)} \in \mathcal{G}$ satisfy a defining equations denerated by (6.23):

$$\frac{\partial b^{(x)}}{\partial u^{(0)}} du^{(0)} \wedge dx + \frac{\partial b^{(x)}}{\partial u^{(1)}} du^{(1)} \wedge dx + \frac{\partial b^{(t)}}{\partial u^{(0)}} du^{(0)} \wedge dt + \tag{6.28}$$

$$\frac{\partial b^{(t)}}{\partial u^{(1)}} du^{(1)} \wedge dt + [b^{(x)}, b^{(t)}] dx \wedge dt \equiv \Omega \Rightarrow$$

$$\Rightarrow g_1(du^{(0)} \wedge dt - u^{(1)} dx \wedge dt) + g_2(du^{(0)} \wedge dx +$$

$$+ u^{(0)} du^{(0)} \wedge dt + du^{(1)} \wedge dt) \in \mathcal{I}(\alpha) \otimes \mathcal{G}$$

for some $\mathcal{G}$-valued functions g_1, g_2 on M. From (6.28) it follows that

$$\frac{\partial b^{(x)}}{\partial u^{(0)}} = g_2, \quad \frac{\partial b^{(x)}}{\partial u^{(1)}} = 0, \quad \frac{\partial b^{(t)}}{\partial u^{(0)}} = g_1 + g_2 u^{(0)}, \tag{6.29}$$

$$\frac{\partial b^{(t)}}{\partial u^{(1)}} = g_2, \quad [b^{(x)}, b^{(t)}] = -u^{(1)} g_1.$$

The equations (6.29) have the following unique solution

$$b^{(x)} = A_0 + A_1 u^{(0)}. \tag{6.30}$$

$$b^{(t)} = u^{(1)} A_1 + \frac{u^{(0)^2}}{2} A_1 + [A_1, A_0] u^{(0)} + A_2,$$

where $A_j \in \mathcal{G}$, $j = 0, 1, 2$, are constant elements on M of the Lie algebra $\mathcal{G}$ that we seak and satisfy the following Lie structure equations:

$$[A_0, A_2] = 0,$$

$$[A_0, [A_1, A_0]] + [A_1, A_2] = 0, \tag{6.31}$$

$$[A_1, [A_1, A_0]] + \frac{1}{2}[A_0, A_1] = 0.$$

From (6.29) one can see that the curvature 2-form $\Omega \in span_{\mathbf{R}}\{A_1, [A_0, A_1] : A_j \in \mathcal{G}, j = 0, 1\}$. Therefore, using the Ambrose-Singer theorem to reduce the associated principal fibered frame space $P(M; G = GL(n))$ to the principal fiber bundle $P(M; G(h))$, where $G(h) \subset G$ is the corresponding holonomy Lie group of the connection Γ on P, we see that the following conditions are necessary for $\mathcal{G}(h) \subset \mathcal{G}$ to be a Lie subalgebra in $\mathcal{G}$: $\nabla_x^m \nabla_t^n \Omega \in \mathcal{G}(h)$ for all $m, n \in \mathbf{Z}_+$.

Let us try now to complete the above transfinite procedure by requiring that

$$\mathcal{G}(h) = \mathcal{G}(h)_0 := span_{\mathbf{R}}\{\nabla_x^m \nabla_x^n \Omega \in \mathcal{G} : m + n = 0\} \tag{6.32}$$

This means that

$$\mathcal{G}(h)_0 = span_{\mathbf{R}}\{A_1, A_3 = [A_0, A_1]\}. \tag{6.33}$$

To satisfy the equations (6.31), we need to use expansions over the basis (6.33) of the external elements $A_0, A_2 \in \mathcal{G}(h)$:

$$\begin{aligned} A_0 &= q_{01} A_1 + q_{13} A_3, \\ A_2 &= q_{21} A_1 + q_{23} A_3. \end{aligned} \tag{6.34}$$

Substituting expansions (6.34) into (6.31), we find that $q_{01} = q_{23} = \lambda$, $q_{21} = -\lambda^2/2$ and $q_{03} = -2$ for some arbitrary real parameter $\lambda \in \mathbf{R}$, that is $\mathcal{G}(h) = span_{\mathbf{R}}\{A_1, A_3\}$, where

$$[A_1, A_3] = A_3/2; \quad A_0 = \lambda A_1 - 2A_3, \tag{6.35}$$

$$A_2 = -\lambda^2 A_1/2 + \lambda A_3.$$

It follows from (6.35) that the holonomy Lie algebra $\mathcal{G}(h)$ is a real two-dimensional one, assuming the following (2×2)-matrix representation:

$$A_1 = \begin{pmatrix} 1/4 & 0 \\ 0 & -1/4 \end{pmatrix}, \quad A_3 = \begin{pmatrix} 0 & 1 \\ 0 & 0 \end{pmatrix}, \tag{6.36}$$

$$A_0 = \begin{pmatrix} \lambda/4 & -2 \\ 0 & -\lambda/4 \end{pmatrix}, \quad A_2 = \begin{pmatrix} -\lambda^2/8 & \lambda \\ 0 & \lambda^2/8 \end{pmatrix}.$$

Thereby, from (6.27), (6.30) and (6.36) we obtain the following reduced curvature 1-form $\Gamma \in \Lambda^1(M) \otimes \mathcal{G}$

$$\Gamma = (A_0 + uA_1)dx + ((u_x + u^2/2)A_1 - uA_3 + A_2)dt, \tag{6.37}$$

generating the parallel transport of vectors from the representation space Y of the holonomy Lie algebra $\mathcal{G}(h)$:

$$dy + \Gamma y = 0 \tag{6.38}$$

upon the integral submanifold $\bar{M} \subset M^4$ of the ideal $\mathcal{I}(\alpha)$, generated by the set of 2-forms (6.25). The result (6.38) means also that the dynamical system (6.24) is endowed with the standard Lax type representation, having the spectral parameter $\lambda \in \mathbf{R}$ necessary for its integrability in quadratures.

In the case when the condition

$$\mathcal{G}(h) = \mathcal{G}(h)_1 := span_{\mathbf{R}}\{\nabla_x^m \nabla_t^n \Omega \in \mathcal{G} : m + n = 0, 1\}$$

is satisfied, one can compute that

$$\mathcal{G}(h)_1 := span_{\mathbf{R}}\{\nabla_x^m \nabla_t^n g_j \in \mathcal{G} : j = \overline{1,2}, m + n = 0, 1\} =$$

$$= span_{\mathbf{R}}\{g_j \in \mathcal{G};\ \partial g_j/\partial x + [g_j, A_0 + A_1 u^{(0)}],$$

$$\partial g_j/\partial t + [g_j, u^{(1)}A_1 + u^{(0)}A_1/2 + [A_1, A_0]u^{(0)} + A_2] \in \mathcal{G} : j = 1, 2\} = \tag{6.39}$$

$$= span_{\mathbf{R}}\{A_1, [A_1, A_0], [[A_1, A_0], A_0], [[A_1, A_0], A_1],$$

$$[A_1, A_2], [[A_1, A_0], A_2] \in \mathcal{G}\} = span_{\mathbf{R}}\{A_{j\neq 2} \in \mathcal{G} : \ j = \overline{1,7}\},$$

where, by definition,

$$[A_1, A_0] = A_3, \quad [A_3, A_0] = A_4, \quad [A_3, A_2] = A_7, \tag{6.40}$$

$$[A_3, A_1] = A_5, \quad [A_1, A_2] = A_6.$$

As a result, we have the following expansions for the unknown elements $A_0, A_2 \in \mathcal{G}$

$$A_0 := \sum_{j=1, j\neq 2}^{7} q_{0j} A_j, \quad A_2 := \sum_{j=1, j\neq 2}^{7} q_{2j} A_j, \tag{6.41}$$

where $q_{0j}, q_{2j} \in \mathbf{R}$ are some real numbers and can be found from conditions (6.39) and (6.40) together with the standard Jacobi identities. Having found a finite-dimensional representation of the Lie algebra $\mathcal{G}(h) = \mathcal{G}(h)_1$ (6.39) and substituted it into (6.37), we will be in a position to write down the parallel transport equation (6.38) in a new Lax type form useful for the study of exact solutions to the Burgers dynamical system (6.24). Analogous calculations can be performed for any other nonlinear dynamical systems [77] that are Lax integrable on some infinite-dimensional functional spaces.

6.2 Dynamical Systems for the Description of Granular and Fluid Layers

In this section we discuss continuum mathematical models for the description of vibrating granular layers. They lead, under some simplifying assumptions, to completely integrable (in the sense of Liouville-Lax) dynamical systems.

Central to the model derived in [26] is the experimental observation that the position of the bottom of the layer of granular material is closely modeled by the motion of a single, totally inelastic particle . This is because all the energy is lost upon impact in the inelastic collision between the grains. The force driving the

patterns is thus proportional to the acceleration of the inelastic particle, minus the acceleration of gravity g. At each impact, this relative acceleration $\gamma(t)$ is strongly peaked and its strength is related to the velocity of impact.

Eggers and Riecke in [26] considered very thin layers and assumed that they can be characterized by their thickness and mean horizontal velocity alone. For simpicity, they considered only one-dimensional motion and did not address the nonlinear pattern-selection problem that arises in two-dimensional patterns (e.g. stripes *vs.* squares). From mass and momentum conservation considerations they arrived at equations quite similar to those of a fluid layer in the lubrication approximation, exept for some crucial differences to be elaborated below. The equations are

$$v_t + vv_x = -\gamma(t)\frac{h_x}{\sqrt{1+h_x^2}} - Bv + (D_1 v_x)_x, \tag{6.42}$$

$$h_t + (vh)_x = (D_2 h_x)_x. \tag{6.43}$$

Equation (6.43) comes from mass conservation, with an Edwards-Wilkinson diffusion term on the right, which describes the tumbling of grains atop one another [25]. Equation (6.42) expresses the momentum balance where v is the horizontal velocity integrated over the layer height h. It contains a driving term proportional to both the acceleration $\gamma(t)$ relative to a freely falling reference frame as well as the slope h_x, since particle motion gets started only if the surface is inclined. The denominator reflects the assumption that upon impact the grains are isotropically dispersed but only those scattered out of the layer contribute to the horizontal flux. Note that this ensures finite driving in the limit $h_x \to \infty$. The wave solutions, which were found numerically without the denominator, became progressively higher and more peaked, leading to an unphysical finite-time singularity. The second and third term on the right describe the internal friction due to vertical gradients in the velocity field and the viscous-like friction due to horizontal gradients, respectively. Since the

vertical gradients are not resolved in this thin-layer approach they lead to a bulk damping term.

The model (6.42)-(6.43) differs from the fluid problem in a number of ways. Through the assumption of random scattering of the grains upon impact, the driving is nonlinear in h_x. In contrast to liquids, the granular layer lifts off the plate when the acceleration of the plate exceeds g. Thus, the aceleration term $\gamma(t)$ vanishes over large parts of the cycle and is largest when the granular layer hits the plate. It is assumed in [26] that it consists mainly of a series of δ-functions. There is no surface tension in the granular material. Instead an additional diffusion term appears in the equation for h.

Under certain simplifying assumptions ($D_1 = -D_2 = const$, $B = 0$, $\gamma(t)/\sqrt{1+h_x^2} = 1$) the model (6.42)-(6.43) reduces to the exactly integrable (in the sense of Liouville-Lax) dynamical system of Benney-Kaup type [77]:

$$\left.\begin{aligned} u_t + uu_x &= h_x + \alpha u_{xx} \\ h_t + (uh)_x &= -\alpha h_{xx} \end{aligned}\right\}. \tag{6.44}$$

We shall study various generalizations of the Benney-Kaup dynamical system that can be used for the description of granular flow layers as well as for the study of some surface phenomena in fluids. The integrability structures for the Benney-Kaup dynamical system can be found in [77] and will be presented later.

Model for potential flow in a thin fluid sheet

Let us consider the irrotational flow of an incompressible fluid between two free surfaces and bounded on either side by a passive medium. The equation of motion

in dimensional coordinates is given by

$$\nabla^2\hat{\phi}(x,y) = 0, \tag{6.45}$$

with the kinematic boundary condition, and the Bernoulli equation at each interface $y = s(x,t)$,

$$\hat{\phi}_y = \hat{s}_t + \hat{\phi}_x\hat{s}_x, \tag{6.46}$$

$$\hat{\phi}_t + \frac{1}{2}|\nabla\hat{\phi}|^2 = \frac{\sigma}{\rho}\frac{\hat{s}_{xx}}{(1+\hat{s}_x^2)^{3/2}}. \tag{6.47}$$

where σ is the surface tension between the two phases and ρ is the density of the fluid sheet.

We wish to consider disturbances where the characteristic aspect ratio ϵ is small. We thus define the dimensionless variables $\xi = x/X$, $\eta = y/Y$, $\tau = t/T$, $\phi = \hat{\phi}/\Phi$, $s = \hat{s}/Y$, with the assumption that $Y/X \ll 1$. Equations (6.45)-(6.47) become

$$\phi_{\eta\eta} + \frac{Y^2}{X^2}\phi_{\xi\xi} = 0, \tag{6.48}$$

$$\phi_\eta = \frac{Y^2}{\Phi T}s_\tau + \frac{Y^2}{X^2}\phi_\xi s_\xi, \tag{6.49}$$

$$\frac{1}{2}\phi_\eta^2 + \frac{Y^2}{\Phi T}\phi_\tau + \frac{1}{2}\frac{Y^2}{X^2}\phi_\xi^2 = \frac{\sigma Y^3}{\rho X^2\Phi^2}s_{\xi\xi}\left[1+\left(\frac{Y}{X}s_\xi\right)^2\right]^{-3/2}. \tag{6.50}$$

Balancing the right-hand side of (6.49) yields the relation $X^2 = \Phi T$, and to balance the right-hand side of (6.50) with the unsteady and ϕ_ξ^2 term requires that $\sigma Y = \rho\Phi^2$. If we let $Y/X = \epsilon \ll 1$ and $T = 1$, then we derive the scaling used in [49]

$$X = \left(\frac{\epsilon\sigma}{\rho}\right)^{1/3}, \quad Y = \left(\frac{\sigma\epsilon^4}{\rho}\right)^{1/3}, \quad \Phi = \left(\frac{\sigma\epsilon}{\rho}\right)^{2/3}. \tag{6.51}$$

Note that the choice of $T = 1$ is arbitrary, and a wide choice of scalings is possible which will lead to the following dimensionless system

$$\phi_{\eta\eta} + \epsilon^2\phi_{\xi\xi} = 0, \tag{6.52}$$

$$\phi_\eta - \epsilon^2[s_\tau + \phi_\xi s_\xi] = 0 \text{ at } \eta = s(\xi,\tau), \tag{6.53}$$

$$\phi_\eta^2 + \epsilon^2 \left\{ \phi_\tau + \frac{1}{2}\phi_\xi^3 - s_{\xi\xi}[1 + (\epsilon s_\xi)^2]^{-3/2} \right\} = 0 \text{ at } \eta = s(\xi, \tau). \tag{6.54}$$

We also include the centerline condition $\phi_\eta = 0$ at $\eta = 0$, and consider solutions symmetric about the centerline, or varicose solutions.

We expand the dependent variables in a power series in ϵ^2,

$$\phi = \phi_0(\xi, \eta, \tau) + \epsilon^2 \phi_1(\xi, \eta, \tau) + \ldots, \tag{6.55}$$

$$s = s_0(\xi, \tau) + \epsilon^2 s_1(\xi, \tau) + \ldots. \tag{6.56}$$

The leading order solution $\phi_0 = \phi_0(\xi, \tau)$ solves the equation (6.52) and satisfies both boundary conditions (6.53), (6.54). At next order, we find that $\phi_1 = B_1(\xi, \tau) - \eta^2 \phi_{0\xi\xi}/2$, and the kinematic and Bernoulli boundary conditions yield the following coupled system of partial differential equations for ϕ_0, s_0:

$$s_{0\tau} + (\phi_{0\xi} s)_\xi = 0, \tag{6.57}$$

$$\phi_{0\tau} + \frac{1}{2}\phi_{0\xi}^2 = s_{0\xi\xi}. \tag{6.58}$$

Letting $v = \phi_{0\xi}$, dropping the subscript on s_0 and differentiating the Bernoulli relation by ξ, we find

$$s_\tau + (vs)_\xi = 0, \tag{6.59}$$

$$v_\tau + v v_\xi = s_{\xi\xi\xi}. \tag{6.60}$$

The dynamical system (6.59)-(6.60) was used in [81] for the description of axisymmetric fluid jets. It was shown that solutions to the system loose smoothness in finite time for all initial condition in the space of functions of a compact support. In the following, we derive a proof that the dynamical system (6.59)-(6.60) on a periodic manifold admits a class of exact finite-dimensional reductions and that quasi-periodic in time, spatially periodic solutions to this system must exist.

For spatially periodic solutions, let $x = 2\pi\xi/L$, $t = (2\pi/L)^2\tau$, and $u = (2\pi/L)v$; then we have s, u 2π-periodic in x, and

$$\begin{pmatrix} u_t \\ s_t \end{pmatrix} = K\left[\begin{pmatrix} u \\ s \end{pmatrix}\right] = \begin{pmatrix} \alpha s_{xxx} - uu_x \\ -(su)_x \end{pmatrix}. \tag{6.61}$$

Let the dynamical system (6.61) be given on the manifold $M \simeq C^{(\infty)}_{2\pi}(\mathbf{R};\mathbf{R}^2)$ of pairs of smooth 2π periodic functions. We denote by $K \in TM$ the Fréchet smooth tangent vector field on the manifold M representing the dynamical system (6.61). Let $\mathcal{D}(M)$ be the space of Fréchet smooth functionals on M. We shall define the operator grad : $\mathcal{D}(M) \to T^*M$ by

$$\operatorname{grad} F = \begin{pmatrix} \frac{\delta F}{\delta u} \\ \frac{\delta F}{\delta s} \end{pmatrix}, \quad \forall F \in \mathcal{D}(M), \tag{6.62}$$

where $\frac{\delta}{\delta w_i}$ is the Euler variational derivative

$$\frac{\delta}{\delta w_i} = \sum_{|k|=0}^{\infty} (-1)^{|k|} \prod_{j=1}^{m} \left(\frac{d}{dx_j}\right)^{k_j} \frac{\partial}{\partial w_i^{(k)}}. \tag{6.63}$$

The Poisson bracket of any pair of functionals F, $G \in \mathcal{D}(M)$ is a functional $\{F,G\}_\theta$ defined by

$$\{F,G\}_\theta = (\operatorname{grad} F, \theta \operatorname{grad} G), \tag{6.64}$$

where θ is a skew-symmetric operator $\theta : T^*M \to TM$ choosen in such a way, that the Poisson bracket (6.64) satisfies the Jacobi identity

$$\{\{F,G\}_\theta, P\}_\theta + \{\{G,P\}_\theta, F\}_\theta + \{\{P,F\}_\theta, G\}_\theta = 0$$

for all $F, G, P \in \mathcal{D}(M)$. Therefore, the operator θ determines a symplectic structure on the manifold M. It is known [36, 77] that the symplectic structure determined by the operator θ is invariant with respect to the phase flow of a dynamical system

$$w_t = K[w], \quad w \in M, \tag{6.65}$$

if and only if

$$L_K \theta = 0, \tag{6.66}$$

where L_K is the Lie derivative along the tangent vector field K. An operator possessing this property is called a Noetherian operator; the explicit form of the expression (6.66) is

$$\frac{\partial \theta}{\partial t} - \theta K'^{*} - K'\theta = 0, \tag{6.67}$$

where K' is the Fréchet derivative of the vector field K and K'^{*} is the adjoint operator to K'. In this case the Jacobi identity for the Poisson bracket (6.64) is satisfied automatically [36] and the dynamical system (6.65) can be represented in the Hamiltonian form. Namely, there exists a functional $H \in \mathcal{D}(M)$, called the Hamiltonian function, that is a conservation law for the dynamical system (6.65) and the following equation holds

$$w_t = K = -\theta \operatorname{grad} H. \tag{6.68}$$

Similarly to (6.65), a functional $F \in \mathcal{D}(M)$ is a conservation law of a dynamical system determined by the vector field $K \in TM$ if and only if

$$L_K \operatorname{grad} F = 0, \tag{6.69}$$

or, in explicit form,

$$\frac{\partial}{\partial t}\operatorname{grad} F + K'^{*}\operatorname{grad} F = 0. \tag{6.70}$$

The equations (6.67) and (6.70) can be solved by using some special asymptotic methods developed in [69, 77]. In particular, it can be shown that the solutions to the equation (6.70) are the following functionals

$$\begin{aligned} &H_1 = \textstyle\int_{x_0}^{x_0+2\pi} u\,dx, \quad \tilde{H}_1 = \int_{x_0}^{x_0+2\pi} s\,dx, \\ &H_2 = \textstyle\int_{x_0}^{x_0+2\pi} us\,dx, \\ &H_3 = \textstyle\int_{x_0}^{x_0+2\pi} (\alpha s_x^2 + u^2 s)\,dx, \end{aligned} \tag{6.71}$$

which are the conservation laws for the dynamical system (6.61).

The symplest solution to the equation (6.67) is

$$\theta = \begin{pmatrix} 0 & \partial \\ \partial & 0 \end{pmatrix}. \tag{6.72}$$

The operator θ defines by the formula (6.64) the canonical symplectic structure on T^*M. The dynamical system (6.61) can be written in the Hamiltonian form

$$\frac{\partial}{\partial t}\begin{pmatrix} u \\ s \end{pmatrix} = -\frac{1}{2}\theta \operatorname{grad} H_3. \tag{6.73}$$

It can be shown that the conservation laws (6.71) are in involution with respect to the canonical symplectic structure (6.64), (6.72):

$$\{H_i, H_j\}_\theta = 0, \quad 1 \le i, j \le 3. \tag{6.74}$$

It is known [69] that a set of N conservation laws in involution for a dynamical system given in the form (6.65) defines the mutually commuting tangent vector fields (dynamical systems) on the manifold M:

$$K_j = -\theta \operatorname{grad} H_j, \quad 1 \le j \le N.$$

The set of fixed points of one vector field is a finite-dimensional submanifold M_N invariant with respect to the dynamics of the other vector fields. The invariant submanifold M_N can be represented as follows:

$$M_N = \{w \in M : \frac{\delta \mathcal{L}_N}{\delta w} = 0\}, \tag{6.75}$$

where $\mathcal{L}_N$ is a Lagrangian function

$$\mathcal{L}_N = \sum_{j=0}^{N} c_j H_j, \tag{6.76}$$

and c_j are arbitrary complex numbers. There is a natural set of the canonical (Hamiltonian) variables on the manifold M_N. The system

$$\frac{\delta \mathcal{L}_N}{\delta w} = 0 \tag{6.77}$$

is a Lagrangian dynamical system but it can be represented also in the form of the canonical Hamiltonian equations defining the Liouville integrable dynamical system (vector field) d/dx. The corresponding Hamiltonian function $h^{(x)}$ is a solution to the following equation

$$\frac{d}{dx}h^{(x)} = -\left\langle \frac{\delta \mathcal{L}_N}{\delta w}, \frac{\partial w}{\partial x} \right\rangle. \tag{6.78}$$

Any solution to the Hamiltonian system which belongs to M_N can be used as an initial condition for the given infinite-dimensional dynamical system (6.65). The dynamics of these integral curves of the vector field d/dx is defined by the finite-dimensional vector field d/dt on M_N that is an exact reduction of the dynamical system (6.65). It can be shown (see [69]) that d/dt is also a Liouville integrable Hamiltonian vector field with the canonical Poisson structure and the Hamiltonian function $h^{(t)}$ determined by the equation

$$\frac{d}{dx}h^{(t)} = -\left\langle \frac{\delta \mathcal{L}_N}{\delta w}, K[w] \right\rangle. \tag{6.79}$$

The Liouville integrability of the vector field d/dt implies [7] the existence of the quasiperiodic dynamics of the solutions starting from the integral curves of the vector field d/dx.

We shall demonstrate these ideas on the example of the dymanical system (6.61). Let us consider the finite-dimensional reductions of the dynamical system (6.61) on the submanifold M_3 of critical points of the following Lagrangian function

$$\mathcal{L}_3 \equiv \int_{x_0}^{x_0+2\pi} Q\,dx = c_1(H_1 + \tilde{H}_1) + c_2 H_2 + c_3 H_3. \tag{6.80}$$

The equation (6.77) defines the Lagrangian dynamical system and the constraint $2c_3u + c_1/s + c_2 = 0$. The canonical Hamiltonian variables q and p on the submanifold M_3 are

$$q = s, \qquad p = \frac{\partial Q}{\partial s_x} = 2\alpha c_3 s_x. \tag{6.81}$$

By using the equations (6.78)-(6.79) we can obtain the Hamiltonian functions $h^{(x)}$ and $h^{(t)}$ determining the Hamiltonian vector fields d/dx and d/dt on M_3:

$$\begin{aligned} h^{(x)} &= \frac{1}{4\alpha c_3} p^2 + \left(\frac{c_2^2}{4c_3} - c_1\right) q + \frac{c_1^2}{4c_3}\frac{1}{q}, \\ h^{(t)} &= \frac{c_2}{8\alpha c_3^2} p^2 - \left(\frac{c_1 c_2}{2c_3} - \frac{c_2^3}{8c_3^2}\right) q + \frac{c_1^2 c_2}{8c_3^2}\frac{1}{q} \end{aligned} \tag{6.82}$$

We integrated the corresponding Hamiltonian equations numerically by using the Runge-Cutta method for the following numerical values of the parameters: $c_1 = 1$, $c_2 = \sqrt{4 + 1/\pi^2}$, $c_3 = 1$. The phase portrait of the dynamical system d/dx is plotted in the Figure 6.1. There two fixed points in the phase space of the system d/dx: the hyperbolic point with coordinates $(-\pi, 0)$ and the elliptic one located at $(\pi, 0)$. The physically realistic solutions corresponding to the subdomain of positive values of q are periodic in x. Some typical solutions defining the initial conditions for the infinite-dimensional dynamical system (6.61) are shown in Figure 6.2. Notice that the independent and dependent variables can be rescaled to obtain $2\pi-$periodicity of any curve. We studied the dynamics due to the vector field d/dt and found the time evolution of the initial data. Figure 6.3 shows the snapshots at different moments of time of the solution corresponding to the initial condition given in Figure 6.2.1. The solution has the form of a small amplitude travelling wave.

Integrability structures for the Benney-Kaup dynamical system

We showed in this section that the Riecke-Eggers model of the dynamics of a thin granular layer (6.42)-(6.43) can be reduced to the nonlinear Benney-Kaup dynamical system (6.44). This system has been widely studied from the Liouville-Lax integrability point of view (see [77] and references cited there). By using methods described above, one can show that the Benney-Kaup dynamical system (6.44) on a manifold of smooth periodic functions $M \simeq C^{(\infty)}_{2\pi}(\mathbf{R}; \mathbf{R}^2)$ possesses the pair of Noetherian

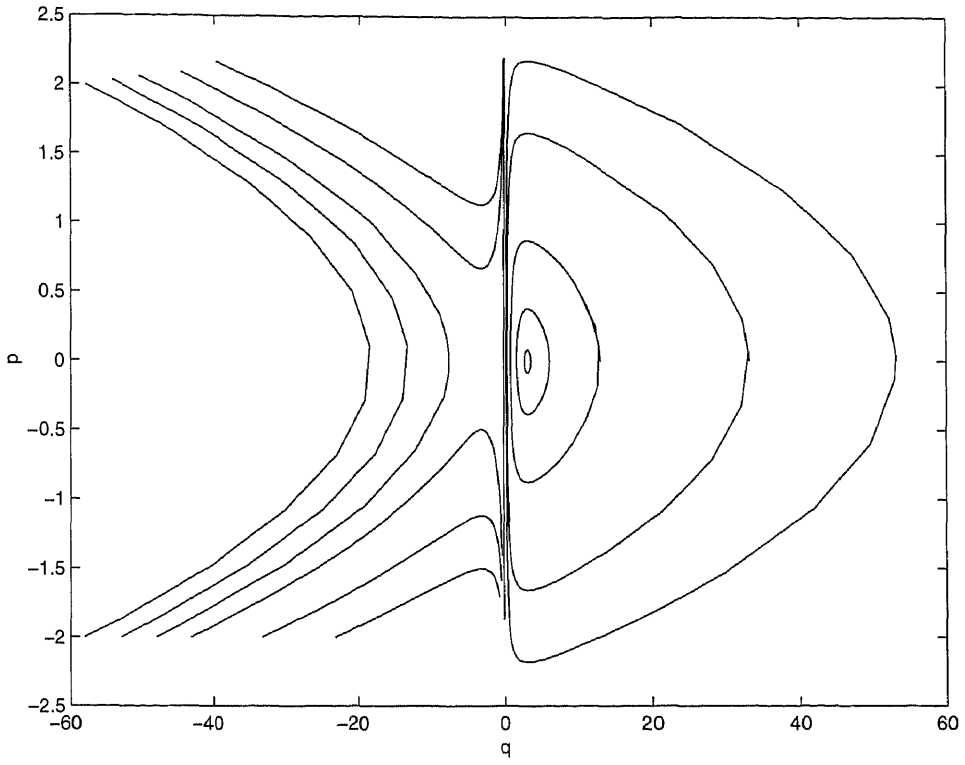

Figure 6.1 Phase portrait of the dynamical system $\frac{d}{dx}$

operators

$$\theta = \begin{pmatrix} 0 & \partial \\ \partial & 0 \end{pmatrix}, \quad \tilde{\theta} = \begin{pmatrix} 2\partial & \partial u - h^2 \\ u\partial + \partial^2 & h\partial + \partial h \end{pmatrix}, \tag{6.83}$$

determining the Poisson brackets on M via (6.64), the infinite hierarchy of conservation laws in involution, the bi-Hamiltonian representation and the Lax representation

$$[L, M] = 0, \tag{6.84}$$

where

$$L = \frac{\partial}{\partial x} - \begin{pmatrix} \frac{1}{2}(u - \lambda) & -h \\ 1 & \frac{1}{2}(\lambda - u) \end{pmatrix}, \tag{6.85}$$

and

$$M = \frac{\partial}{\partial t} - \begin{pmatrix} -\frac{1}{4}(u^2 - \lambda^2 - u_x) & -\frac{h}{2}(u + \lambda) - \frac{1}{2}h_x \\ \frac{1}{2}(u + \lambda) & \frac{1}{4}(u^2 - \lambda^2 - u_x) \end{pmatrix}. \tag{6.86}$$

Therefore the system (6.44) is an exactly Liouville-Lax integrable Hamiltonian flow.

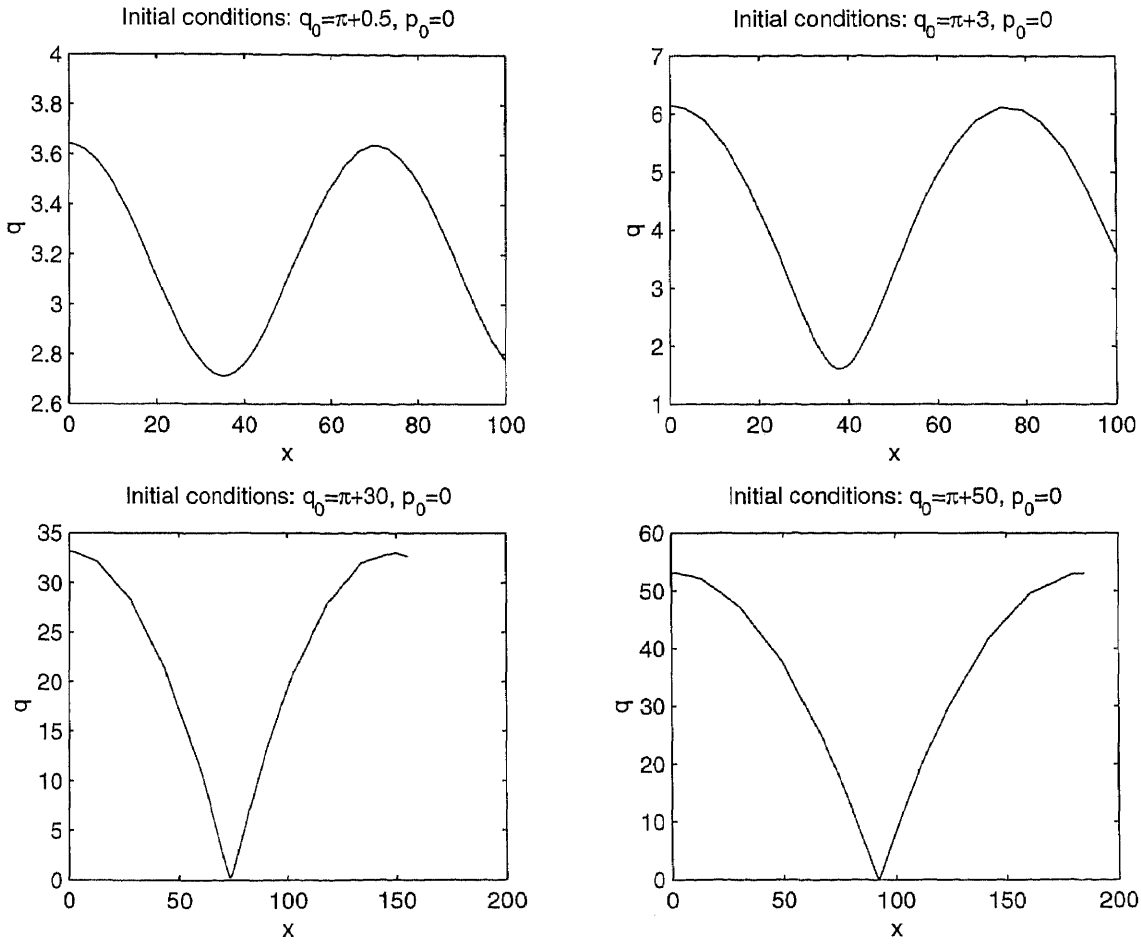

Figure 6.2 Solutions $s = s(x)$ of the dynamical system $\frac{d}{dx}$ starting at different initial conditions

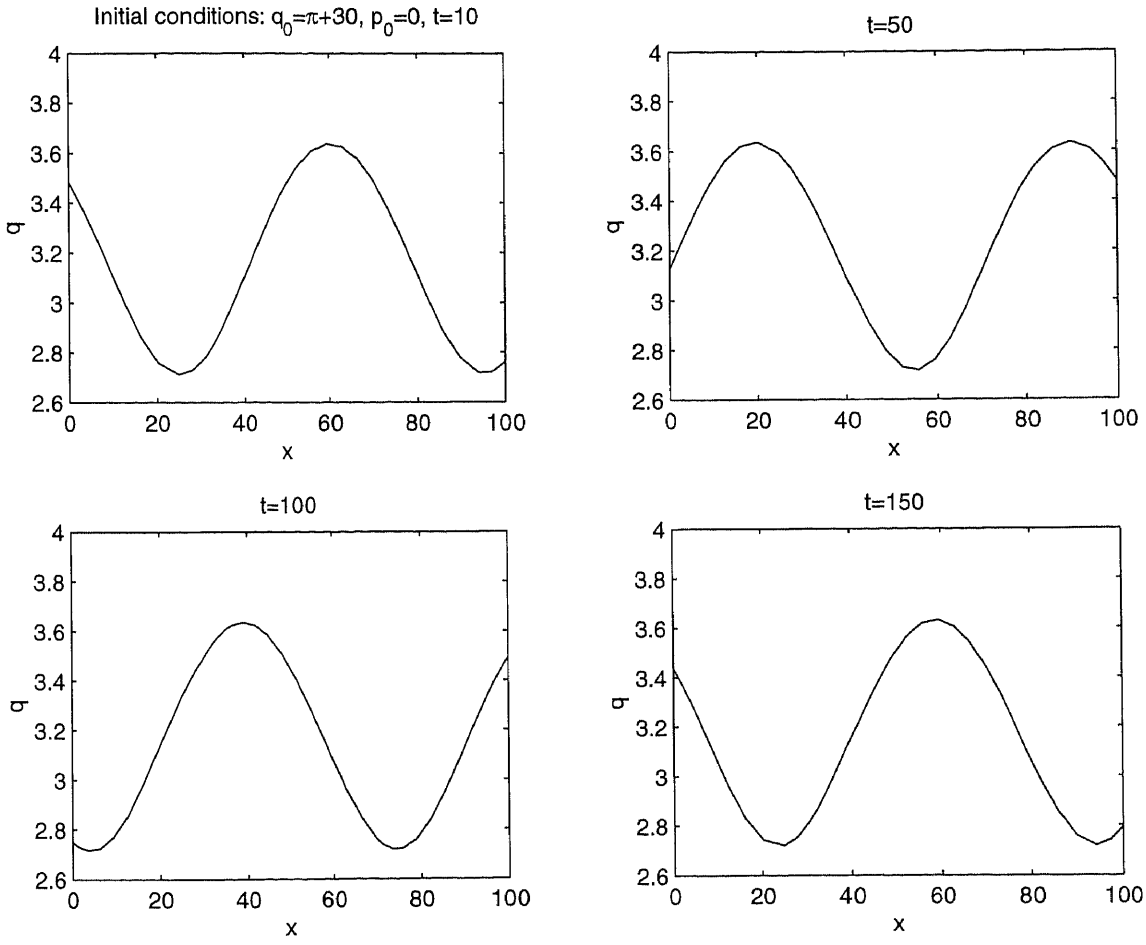

Figure 6.3 Small amplitude travelling wave solutions

The generalized Benney type dynamical system

In the sequel we shall describe some interesting features of generalized Benney-Kaup dynamical systems. Consider the following nonlinear Schrödinger type dynamical system

$$\begin{pmatrix} \psi_t \\ \psi_t^* \end{pmatrix} = K\left[\begin{pmatrix} \psi \\ \psi^* \end{pmatrix}\right] = \begin{pmatrix} \frac{i}{2}\psi_{xx} - i\beta\psi^*\psi\psi + 2\alpha\psi^*\psi\psi_x \\ -\frac{i}{2}\psi_{xx}^* + i\beta\psi^*\psi^*\psi + 2\alpha\psi_x^*\psi^*\psi \end{pmatrix} \tag{6.87}$$

on some functional manifold $M_{(\psi,\psi^*)} \ni (\psi,\psi^*)^\tau$. It is well known [69, 27, 77] that the dynamical system (6.87) is completely Lax type integrable both in the quantum and classical cases. The last property is very important on account of the following circumstance: as we shall show later, the quasi-classical approximation of the dynamical system (6.87) via the scheme of Zakharov [111] gives rise to the generalized nonlinear Benney type hydrodynamical system of equations. Thus we can assert that the Benney type dynamical system possesses on the manifold $M_{(u,\rho)}$ an infinite hierarchy of involutive polynomial conservation laws with respect to a pair of compatible implectic structures.

Let us change the variables in (6.87) as follows

$$\begin{aligned} \psi(x) &= \sqrt{\rho(x)}\exp(-\tfrac{i}{2}\textstyle\int_{x_0}^{x} u(y)dy + \tfrac{i}{2}\int_{x}^{x_0+2\pi} u(y)dy), \\ \psi^*(x) &= \sqrt{\rho(x)}\exp(\tfrac{i}{2}\textstyle\int_{x_0}^{x} u(y)dy - \tfrac{i}{2}\int_{x}^{x_0+2\pi} u(y)dy), \end{aligned} \tag{6.88}$$

where $\rho \in C^\infty(\mathbf{R}/2\pi\mathbf{Z};\mathbf{R}_+)$ is the quasi-classical particle density of fields (6.92), $u \in C^\infty(\mathbf{R}/2\pi\mathbf{Z};\mathbf{R})$ is the phase velocity of particles at $x \in \mathbf{R}$, and $x_0 \in \mathbf{R}$ is an arbitrary fixed point.

By substituting (6.88) into (6.87), using the quasi-classical approximations $d/dt \to \epsilon d/dt$ and $d/dx \to \epsilon d/dx$ and passing to the limit as $\epsilon \to 0$, we obtain the generalized Benney dynamical system

$$\begin{pmatrix} u_t \\ \rho_t \end{pmatrix} = K\left[\begin{pmatrix} u \\ \rho \end{pmatrix}\right] = \begin{pmatrix} -uu_x - (\beta\rho + 2\alpha u\rho)_x \\ -(u\rho)_x - 2\alpha\rho\rho_x \end{pmatrix}, \tag{6.89}$$

defined on the functional manifold $M_{(u,\rho)}$. In accordance with the assertion of the complete integrability of the dynamical system (6.87) on the manifold $M_{(\psi,\psi^*)}$, there exists a hierarchy of involutive conservation laws, among which are

$$\begin{aligned} H_0 &= \int_0^{2\pi} dx\psi^*\psi, \quad H_1 = i\int_0^{2\pi} dx(\psi^*\psi - \psi_x^*\psi), \\ H_2 &= \tfrac{1}{2}\int_0^{2\pi} dx(\psi^*\psi + \beta\psi^*\psi^*\psi\psi + 2i\psi^*\psi^*\psi_x\psi), \ldots \end{aligned} \tag{6.90}$$

The Poisson bracket on the manifold $M_{(\psi,\psi^*)}$ corresponding to (6.87), satisfies in accordance with the Dirac principle, the following expressions:

$$\begin{aligned} &\{\psi(x), \psi^*(y)\} = -i\delta(x-y), \\ &\{\psi(x), \psi(y)\} = 0 = \{\psi^*(x), \psi^*(y)\}. \end{aligned} \tag{6.91}$$

Substituting now the expression (6.88) into (6.90), one finds an infinite hierarchy of the hydrodynamic conservation laws of the Benney type dynamical system (6.94):

$$\begin{aligned} H_0 &= \int_0^{2\pi} dx\rho, \quad H_1 = \int_0^{2\pi} dxu\rho, \\ H_2 &= \tfrac{1}{2}\int_0^{2\pi} dx(u^2\rho + \beta\rho^2 + 2\alpha\rho^2 u), \ldots \end{aligned} \tag{6.92}$$

In the analogous way one can recalculate the symplectic structure on the manifold $M_{(\psi,\psi^*)}$ as a symplectic structure on the manifold $M_{(u,\rho)}$: for any $x, y \in \mathbf{R}$

$$\begin{aligned} \{u(x), u(y)\}_\theta &= 0 = \{\rho(x), \rho(y)\}_\theta, \\ \{u(x), \rho(y)\}_\theta &= \delta'(x-y). \end{aligned} \tag{6.93}$$

Thus the hydrodynamical system (6.89) on the manifold $M_{(u,\rho)}$ is a Hamiltonian flow represented as follows:

$$(u_t, \rho_t)^\tau = -\theta \mathrm{grad} H = K[u, \rho], \tag{6.94}$$

where the above implectic operator $\theta : T^*(M_{(u,\rho)}) \to T(M_{(u,\rho)})$ is defined by the explicit expression:

$$\theta = \begin{pmatrix} 0 & \partial \\ \partial & 0 \end{pmatrix} \tag{6.95}$$

and the functional $H = H_2 \in \mathcal{D}(M_{(u,\rho)})$ is the Hamiltonian function for the vector field (6.89). This result follows from the natural fact that after passing to the limit in the quasi-classical transformation (6.88) of Bäcklund type, the Schrödinger dynamical system (6.87) together with its infinite hierarchy of compatible implectic structures on $M_{(\psi,\psi^*)}$ for any $\alpha, \beta \in \mathbf{R}$ transforms into the Hamiltonian system (6.89) with another hierarchy of compatible implectic structures on the manifold $M_{(u,\rho)}$ [22]. Therefore, the Benney type system (6.89) is a bi-Hamiltonian flow with a compatible implectic pair of noetherian operators. The second implectic operator $\eta : T^*(M_{(u,\rho)}) \to T(M_{(u,\rho)})$ is defined as follows:

$$\eta = \begin{pmatrix} \beta\partial + \alpha(\partial u + u\partial) & \partial u/2 + \alpha\rho\partial \\ \alpha\partial\rho + u\partial/2 & (\rho\partial + \partial\rho)/2 \end{pmatrix}. \tag{6.96}$$

By using the operator (6.96), one can rewrite (6.94) as

$$(u_t\rho_t)^\tau = -\eta \mathrm{grad}\tilde{H} = K[u,\rho], \tag{6.97}$$

where $\tilde{H} := H_1 \in \mathcal{D}(M_{(u,\rho)})$. In virtue of the compatibility of the symplectic structures (6.95) and (6.96), the dynamical system (6.89) possesses an infinite hierarchy of involutive conservation laws $\gamma_j \in \mathcal{D}(M_{(u,\rho)})$, $j \in \mathbf{Z}$, which are calculated using the formula:

$$\mathrm{grad}\gamma_j = (\theta^{-1}\eta)^j \mathrm{grad}\gamma_0, \tag{6.98}$$

where $\gamma_0 = H_0 \in \mathcal{D}(M_{(u,\rho)})$, $j \in \mathbf{Z}$. In particular,

$$\begin{aligned} &\gamma_0 = \textstyle\int_0^{2\pi} dx\, \rho, \quad \tilde{\gamma}_0 = \frac{1}{2}\int_0^{2\pi} dx\, u, \quad \gamma_1 = \int_0^{2\pi} dx\, u\rho, \\ &\gamma_2 = \tfrac{1}{2}\textstyle\int_0^{2\pi} dx\, (u^2\rho + \beta\rho^2 + 2\alpha\rho^2 u), \\ &\gamma_3 = \tfrac{1}{4}\textstyle\int_0^{2\pi} dx\, (u^3\rho + 6\alpha u^2\rho^2 + 4\alpha^2\rho^3 u + 3\beta\rho^2 u + 2\alpha\beta\rho^3), \ldots \text{etc.}, \end{aligned} \tag{6.99}$$

where the trivial conservation laws γ_0 and $\tilde{\gamma}_0$ follow from the original form of equation (6.89).

Remark. The dynamical system (6.89) admits the following multi-component generalization :

$$\frac{d}{dt}\begin{pmatrix} u \\ \rho \end{pmatrix} = K_{(N)}\left[\begin{pmatrix} u \\ \rho \end{pmatrix}\right] = \begin{pmatrix} -u_n u_{n,x} - \left[\sum_{k=1}^{N} \rho_k(\beta + 2\alpha u_n)\right]_x \\ -(\rho_n u_n)_x - 2\alpha \sum_{k=1}^{N} \rho_k \rho_{n,x} \end{pmatrix} \tag{6.100}$$

where $n = 1, \ldots, N$, $N \in \mathbf{Z}_+$. It is easy to see that the dynamical system (6.100) is Hamiltonian on the corresponding functional manifold $M_{U,\rho}$,

$$(u_t, \rho_t)^\tau = -\theta \mathrm{grad} H_{(N)} = K_N[u, \rho], \tag{6.101}$$

where the Hamiltonian functional $H_{(N)} \in \mathcal{D}(M_{(u,\rho)})$ has the form:

$$H_{(N)} = \frac{1}{2}\int_0^{2\pi} dx \left[\sum_{n=1}^{N} \rho_n u_n^2 + \sum_{m,n=1}^{N} (\beta \rho_m \rho_n) + 2\alpha \rho_m \rho_n u_n)\right], \tag{6.102}$$

The system (6.100) can be deduced in an analogous way from the quasi-classical limit of the following many-component generalization of the Schrödinger dynamical system:

$$\begin{aligned} \psi_{n,t} &= \tfrac{i}{2}\psi_{n,xx} - i\beta \textstyle\sum_{k=1}^{N} \psi_k^* \psi_k \psi_n + 2\alpha \sum_{k=1}^{N} \psi_k^* \psi_n \psi_{m,x}, \\ \psi_{n,t}^* &= -\tfrac{i}{2}\psi_{n,xx}^* + i\beta \textstyle\sum_{k=1}^{N} \psi_k^* \psi_k \psi_n^* + 2\alpha \sum_{k=1}^{N} \psi_k^* \psi_n \psi_{m,x}, \end{aligned} \tag{6.103}$$

where $n = 1, \ldots, N$, $x \in \mathbf{R}$. Namely, substituting into (6.103) the expressions

$$\begin{aligned} \psi_n(x) &= \sqrt{\rho_n(x)} \exp\left(-\tfrac{i}{2}\textstyle\int_{x_0}^{x} dy\, u_n(y) + \tfrac{i}{2}\int_x^{x_0+2\pi} dy\, u_n(y)\right), \\ \psi_n^*(x) &= \sqrt{\rho_n(x)} \exp\left(\tfrac{i}{2}\textstyle\int_{x_0}^{x} dy\, u_n(y) - \tfrac{i}{2}\int_x^{x_0+2\pi} dy\, u_n(y)\right) \end{aligned} \tag{6.104}$$

and passing to the quasi-classical limit, one finds explicitly the many-component hydrodynamical system (6.100). Taking into account that the dynamical system (6.103) on the manifold $M_{(\psi,\psi^*)}$ is a bi-Hamiltonian completely integrable flow, we arrive at the conclusion that the Benney type hydrodynamical system (6.100) is also a bi-Hamiltonian system possessing an infinite hierarchy of polynomial conservation laws.

CHAPTER 7

CONCLUSIONS

Starting with well-established representations for particle-particle normal and tangential frictional forces (based on sound theoretical principles and a large body of experimental observations), we derived a new class of integro-partial differential equations to describe the velocity field in the granular flow of rough, inelastic particles. These granular flow models were obtained by taking a dynamical limit as $N \to \infty$ of the Newtonian system of differential equations of motion of an $N-$particle array using integral averages of an assumed uniform distribution of particles comprising the flow field. Then by employing Taylor series expansions of key variables of the flow field, we were able to obtain an infinite collection of approximations of the model equations in the form of a system of nonlinear partial differential equations for the velocity components of the granular flow. The simplest of these approximate models, obtained by retaining only the first two terms in the Taylor expansions, is a system of equations that is significantly less complicated than most of the continuum models currently being used to investigate particle flow dynamics.

Our models, and especially the simplest of the approximations, certainly do not incorporate as much of the physics involved in granular flows as do the more comprehensive partial differential equation models, yet they appear to be quite promising instrumentalities for the prediction of particle flow behavior. A good indication of this are the results of our application of the simplest model to granular flow through a vertical tube and fully developed flow down an inclined plane which produced extremely simple solutions that compared remarkably well, in a qualitative sense, with experimental observations and the predictions of more complete models. This suggests that, in spite of the simplifying assumptions we used in the derivation,

these models may be capable of accurately predicting dynamical properties of a wider range of granular flow configurations than one might imagine. And that they certainly warrant further investigation and testing. Moreover, the new models are far more amenable to analysis (particularly from the viewpoint of infinite-dimensional dynamical systems theory) than the majority of governing equations in the literature. Therefore it is quite possible that one may be able to apprehend important new insights into several elusive granular flow phenomena from a more penetrating mathematical investigation of the properties of the new equations.

In Chapter 3 we investigated the mathematical structure of the granular flow equations from the dynamical systems theory viewpoint. To make our theoretical analysis more complete we included into consideration the well-posedness of a boundary-value problem involving the granular flow dynamical system. Namely, we considered steady-state flows in an axisymmetric tube with curvilinear walls. This problem generalizes various cases of granular flows in tubes and hoppers. By using the Faedo-Galerkin method we proved the existence of a solution to the boundary value problem. The corresponding theorem on the uniqueness of a solution holds for some particular range of constant parameters and norms of the velocity fields. These results are similar to those obtained for the Navier-Stokes equations.

We did not study in detail in this manuscript the problem of existence of an approximate inertial manifolds for the granular flow dynamical system although we developed a method for its inertial form calculation; rather, we studied the AIM existence problem for one form of our model equations. Many efforts have been made to prove the existence of an exact inertial manifolds for the Navier-Stokes equations, but no one succeded in this, due to some tricky technical difficulties. The only exact result was formulated recently by Kwak [50] for the Navier-Stokes equations restricted to a sphere, but it was later shown that his proof is incorrect.

Therefore the problem still remains an open question despite "empirical evidence". These difficulties finally lead to the development of the approximate inertial manifold theory. The existence of an approximate inertial manifold for the Navier-Stokes equations has been widely studied in the literature [105]. Because of the same type of dissipativity and nonlinearity in (2.25) and in the Navier-Stokes equation, it can be shown that an AIM exists for the granular flow dynamical system. A proof of this fact requires only minor changes to the proof presented in [105].

Using ideas from the theory of approximate inertial manifolds, we developed a numerical method for the inertial form calculation in the finite-difference framework and applied it to a granular flow dynamical system. This approach leads to the increase of accuracy over the standard finite-difference schemes. The main advantage of the method is its applicability to different types of boundary conditions, while the spectral AIM-methods based on the eigenfunction expansion of a solution deal only with periodic boundary conditions. The Neumann type of boundary conditions or mixed ones, for example, do not require any changes in the main formulas for the AIM. The computational cost of the inertial form calculation is slightly bigger than the cost of the standard finite-difference method, but derivation of the inertial manifold formulas for a particular dynamical system is much more difficult with respect to the spectral AIM-method. The last problem can effectively be solved by using computer systems for analytical calculations (Maple, Mathematica, etc.).

Our studies of the vibrating bed model were stimulated by an interesting and important phenomena of size-segregation in vibrating mixes of particles. We presented in Chapter 4 some numerical solutions to the vibrating bed model involving the granular flow dynamical system (2.25). We found that even in the simplest case, where we neglect the arching phenomena and surface waves, these solutions exhibit some of the typical features that have been observed in simulation and exper-

imental studies of vibrating beds. In an effort to study the dynamics analytically, we employed asymptotic expansions and made a few simplifying assumptions. The ansatz for solutions of the resulting simplified governing equations only approximate the granular flow fields for the vibrating bed. Nevertheless, these approximate solutions were found to share several important features with actual granular flows. Using this approach we showed the existence KAM-tori for the perturbed motion and bifurcation to chaotic motion by employing Melnikov theory to analytically estimate the bifurcation parameter values. The vortex solutions we obtained for the perturbed motion and the solutions corresponding to the vortex disintegration agree qualitatively with the dynamics obtained numerically. We believe that this and similar simplified analytical approaches might be useful for the investigation of such phenomena as the creation and destruction of various types of structures in granular flow and for the study of chaotic transport, and could lead to a better understanding of granular flow dynamics.

In Chapter 5 we developed methods for solving the hopper problem numerically and compared our results with experimental data. Our numerical solutions reproduce experimentally observable results in mass type hoppers. Intending to capture the behavior of particles in a core type hopper, we proposed some modifications of our model and presented the numerical solutions to the modified equations. These modifications refer to the coefficients of the model. Continuum mathematical models for granular flows are usually derived under the assumption of a simple linear dependence of friction between particles on the relative velocity, and the ability of such models to capture the cohesivity of particulate materials and stationary friction phenomena is restricted. By making coefficients in the governing equations functionally dependent on the gradient of the velocity field, we were able to model the influence of the stationary friction phenomena in solids and in this way reproduce results typical for core type hoppers.

In the last chapter we discussed mathematical models for the continuum description of thin granular layers (including vibrating ones) as well as some related fluid dynamics models. It was proved that some of these models are, under some simplifying assumptions, (Liouville-Lax) complete intergable dynamical systems. By using the Cartan calculus of differential forms, Grassman algebras over jet-manifolds associated with the granular flow dynamical systems, the gradient-holonomic algorithm and generalized Hamiltonian methods we were able to construct the integrability structures for one-dimensional models. We also constructed a class of exact finite-dimensional reduction of the dynamical system describing a thin fluid sheet. The reduced system is a pair of two-dimensional systems of ODE's defining the vector fields d/dx and d/dt on the finite- dimensional submanifold M_N which is invariant with respect to the dynamics of the initial infinite-dimensional dynamical system. The vector fields d/dx and d/dt are Liouville integrable Hamiltonian flows on M_N. We found a class of quasi-periodic solutions for these equation which gives exact solutions for the infinite-dimensional model equations. This explains the regularity and quasi-periodicity of solutions obtained numerically for the infinite-dimensional dynamical system.

REFERENCES

1. Abraham, R. and Marsden, J., *Foundations of Mechanics*, MA: Addison, Wesley, 1978.

2. Adams, M.R., Harnard, J. and Previato, E., Isospectral Hamiltonian flows in finite and infinite dimensions, *Comm. Math. Phys.*, **117** (1988), 451–500.

3. Adams, M.R., Harnard, J. and Hurtubise, J., Dual moment maps into loop algebras, *Lett. Math. Phys.*, **20** (1990), 299–308.

4. Ambrose, N. and Singer, J.M., A theorem on holonomy, *Trans. AMS*, **75** (1953), 428-443.

5. An, L. and Pierce, A., A weakly nonlinear analysis of elasto-plastic microstructure, *SIAM J. Appl. Math.*, **55** (1995), 136-155.

6. Anderson, K. and Jackson, R., A comparison of some proposed equations of motions of granular materials for fully developed flow down inclined planes, *J. Fluid Mech.*, **241** (1992), 145-168.

7. Arnold V.I., *Mathematical Methods of Classical Mechanics*, Springer Graduate Texts in Math. N.60, Springer-Verlag, N.Y., 1940.

8. Babin, A.V. and Vishnik, M.I., Attractors of partial differential equations and estimate of their dimension, *Uspekhi Mat. Nauk*, **38** (1983), 133-187 (in Russian), *Russian Math. Surveys*, **38** (1883), 151-213 (in English).

9. Bagrets, A.A. and Bagrets, D.A., Nonintegrability of two problems in vortex dynamics, *Chaos*, **7** (1997), 368-375.

10. Baxter G.W. and Behringer R.P., Cellular automata models of granular flow, *Phys. Rev. A*, **42** (1990), 1017-1020.

11. Blackmore, D., Rosato, A. and Samulyak, R., New mathematical models for particle flow dynamics, *J. Nonlin. Math. Phys*, **6** (1999), No. 3.

12. Blackmore, D. and Dave, R., "Chaos in one-dimensional granular flow with oscillating boundaries", *Powders and Grains 97*, Behringer and Jenkins (eds), Balkema, Rotterdam, 1997, 409-412.

13. Blackmore, D. and Knio, O., KAM theory analysis of the dynamics of three coaxial vortex rings, Preprint, New Jersey Institute of Technology, 1998.

14. Blackmore, D., Simple dynamical model for vortex breakdown of the B-type, *Acta Mech.*, **102** (1994), 91-101.

15. Blackmore, D., The mathematical theory of chaos, *Comp. and Math. Appl. B*, **12** (1986), 1039-1045.

16. Bogoliubov, N.N.(Jr.), Prykarpatsky, A.K. and Samoilenko, V.G., On Neumann type dynamical systems and its completely integrability, *Doklady Akad. Nauk USSR*, **285** (1985), 1095–1101. (in Russian)

17. Bogoliubov, N.N.(Jr.), Prykarpatsky, A.K. and Samoilenko, V.H., Hamiltonian structure of hydrodynamic equation of Benney type and associated with them Boltzmann-Vlasov equations on axis, Kiev: NAS Inst. Math., Preprint N 91-25, 1991.

18. Bogoyavlensky, O.I. and Novikov, S.P., On connection of Hamiltonian formalisms of stationary and non-stationary problems, *Func. Anal. Appl.*, **10** (1976), 9–13.

19. Bogoyavlensky O.I., Integrable cases of solid dynamics and integrable systems on spheres $\mathbf{S}^N$, *Izvestiya Akad. Nauk USSR*, Ser. Matem., **49** (1985), 889–915. (in Russian)

20. Bourzutschky, M. and Miller, J., "Granular" convection in a vibrated fluid, *Phys. Rev. Lett.*, 1995, V.74, 2216-2219.

21. Caram H. and Hong D.C., Random-walk approach to granular flows, *Phys. Rev. Lett.*, 1991, V.67, 828-831.

22. Cavalcante, J. and Mc Kean, H.P., The classical shallow water equations: symplectic geometry, *Physica 4D*, **2** (1982), 253-260.

23. Chevalley, C., *Theorie des Groupes de Lie*, V. 1-3, Paris, Hermann D.C., 1955.

24. Dirac, P.A.M., Generalized Hamiltonian dynamics, *Canad. J. of Math.*, **2** (1950), 129-148.

25. Edwards, S. and Wilkinson, D., The surface statistics of a granular aggregate, *Proc. Royal Soc. Lond.*, A**381** (1982), 17-31.

26. Eggers, J. and Riecke, H., A continuum description of vibrated sand, LANL Archives, patt-sol/9801004v3.

27. Faddeev, L.D. and Takhtadjan, L.A., *Hamiltonian Approach in the Soliton Theory*, Springer, N.Y., 1986.

28. Fan, L. and Zhu, C., Principles of Gas-Solid Flows, Preprint, Cambridge University, 1992.

29. Farrel, M., Lun, C. and Savage, S., A simple kinetic theory for granular flow of binary mixtures of smooth, inelastic spherical particles, *Acta Mech.*, **63** (1986), 45-60.

30. Foias, C. and Jolly, M.S., On the numerical algebraic approximation of global attractors, *Nonlinearity*, **8** (1995), 295-319.

31. Foias, C. and Titi, E.S., Determining nodes, finite differences and inertial manifolds, *Nonlinearity*, **4** (1991), 135-153.

32. Foias, C. and Temam, R., Approximation algebrique des attracteurs, I. Le cas de la dimension finie, *C.R. Acad. Sci., Paris*, **307** (1988), pp. Serie I. 5-8.

33. Foias, C., Manley, O. and Temam, R., Modeling of the interaction of small and large eddies in two dimensional turbulent flows, *Math. Mod. Numer. Anal.*, **22** (1988), 93-114.

34. Foias, C., Sell, G.R. and Titi, E.S., Exponential tracking and approximation of inertial manifolds for dissipative equations, *J. Dynamics and Differential Equations*, **1** (1989), 199-224.

35. Foias, C. and Temam, R., The algebraic approximation of attractors: The finite dimensional case, *Physica D*, **32** (1988), 163-182.

36. Fuchssteiner, B. and Fokas, A.S., Symplectic structures, their Bäcklund transformations and hereditary symmetries, *Physica D.*, **4** (1981), 47-66.

37. Gardiner, C. and Schaeffer, D., Numerical simulation of uniaxial compression of granular material with wall friction, *SIAM J. Appl. Math.*, **54** (1994), 1676-1692.

38. Goldhirsch I., Tan M.-L. and Zanetti G., A molecular dynamical study of granular fluids I: the unforces granular gas in two dimensions, *J. Sci. Comp.*, 1993, V.8, 1-40.

39. Goldshtein, A. and Shapiro, M., Mechanics of collisional motion of granular materials, Part 1. General hydrodynamic equations, *J. Fluid Mech.*, **282** (1995), 75-114.

40. Guckenheimer, J. and Holmes, P., *Nonlinear Oscillations, Dynamical Systems and Bifurcations of Vector Fields*, Springer-Verlag: New York, 1997.

41. Hayakawa, H. and Hong, D., Two hydrodynamical models of granular convection, *Powders and Grains 97*, Behringer and Jenkins (eds), Balkema, Rotterdam, 1997, 417-420.

42. Holm, D.D. and Kupershmidt, B.A., Poisson brackets and Klebsch representations for magnetohydrodynamics, multifluid plasmas, and elasticity, *Physca D.*, **6** (1983), 347-363.

43. Holm, D.D., Marsden, J.E. and Ratiu, T.S., The Hamiltonian structure of continuum mechanics in material, spatial and convective representation, *Sem. Math. Sup. (Les Presses de L'Univ. de Montreal)*, **100** (1986), 11-122.

44. Jauberteau, F., Rosier, C. and Temam, R., The nonlinear Galerkin method in computational fluid dynamics, *Appl. Numer. Math.*, **6** (1990), 361-370.

45. Jenike, A. and Shield, R., On the plastic flow of Coulomb solids beyond original failure, *J. Appl. Mech.*, **26** (1959), 599-602.

46. Jenkins, J. and Richman, M., Grad's 13-moment system for a dense gas of inelastic spheres, *Arch. Rat. Mech. Anal.*, **87** (1985), 355-377.

47. Jenkins, J., Savage, S., A theory for rapid flow of identical smooth, nearly elastic particles, *J. Fluid Mech.*, **130**, (1983), 187-202.

48. Johnson, P., Nott, P. and Jackson, R., Frictional-collisional equations of motion for particulate flows and their application to chutes, *J. Fluid Mech.*, **210** (1990), 501-535.

49. Keller, J. and Miksis, M., Surface tension driven flows, *SIAM J. Appl. Math.*, **43** (1983), 268-277.

50. Kwak, M., Finite dimensional inertial form for the 2D-Navier-Stokes equations, *Indiana Univ. Math. J.*, **41** (1993), 927-981.

51. Lamb, H., *Hydrodynamics*, Dover: New York, 1940.

52. Lan, Y. and Rosato, A., Convection related phenomena in vibrating granular beds, *Phys. Fluids*, **9** (12) (1997), 3615-3624.

53. Lan, Y. and Rosato, A., Macroscopic behavior of a vibrating bed of smooth inelastic particles, *Phys. Fluids*, **7** (1995), 1818-1831.

54. Langston, P. and Tüzün, U., *Powder Technology*, **85**, 153 (1995).

55. Lions, J.L. and Magenes, E., *Nonhomogeneous Boundary Value Problems and Applications*, Springer-Verlag, Berlin, 1972.

56. Loos H.G., Internal holonomy groups of Yang-Mills fields, *J. Math. Phys.*, **8** (1967), 2114-2124.

57. Lun, C., Savage, S., Jeffrey, D. and Chepurniy, A., Kinetic theories for granular flow: Inelastic particles in Couette flow and slightly inelastic particles in a general flow field, *J. Fluid. Mech.*, **140** (1984), 223.

58. Lun, C. and Savage, S., A simple kinetic theory for granular flow of rough, inelastic spherical particles, *J. Appl. Mech.*, **54** (1987), 47-53.

59. Lun, C., A kinetic theory for granular flow of dense, slightly inelastic, slightly rough spheres, *J. Fluid Mech.*, **233** (1991), 539-559.

60. Margolin, L.G. and Jones, D.A., An approximate inertial manifold for computing Burgers' equation, *Physica D*, **60** (1992), 175-184.

61. Marion, M. and Temam, R., Nonlinear Galerkin methods, *SIAM J. Numer. Anal.*, **26** (1989), 1139-1157.

62. Marsden, J. and Weinstein, A., Reduction of symplectic manifolds with symmetry, *Rep. Math. Phys.*, **5** (1974), 121-130.

63. Marsden, J., Ratiu, T. and Weinstein, A., Semidirect products and reduction in mechanics, *Trans. Amer. Math. Soc.*, **281** (1984), 147-177.

64. Marsden, J., Ratiu, T. and Weinstein, A., Reduction and Hamiltonian structures on duals of semidirect product Lie algebras, *Contemp. Math.*, **25** (1984), 55-100.

65. Marsden, J. and Ratiu, T., *Introduction to Mechanics and Symmetry*, Texts in Appl. Math., Vol. 17, Springer-Verlag, Berlin – New-York, 1994.

66. McNamara S. and Luding S, Energy flows in vibrated bed granular media, *Phys. Rev E*, 1998, V.58, 813.

67. Melnikov, V.K., On the stability of the center for the periodic perturbations, *Trans. Moscow Math.*, **12** (1963), 1-57.

68. Mitropolsky, Yu.A., Bogoliubov, N.N. (Jr.), Prykarpatsky, A.K. and Samoilenko, V.H., *Integrable Dynamical Systems*, Naukova Dumka, Kiev, 1987. (in Russian)

69. Novikov, S.P. (ed.), *Theory of Solitons*, Consultants Bureau, New York - London, 1984.

70. Numan, K. and Keller, J., Effective viscosity of a periodic suspension, *J. Fluid Mech.*, **142** (1984), 269-287.

71. Olver, P., *Applications of Lie Groups to Differential Equations*, New-York-Berlin-Heidelberg-Tokyo: Springer-Verlag, 1986.

72. Pasquarell, G., Granular flows: boundary conditions for slightly bumpy walls, *ASCE J. Eng. Mech.*, **117** (1991), 312-318.

73. Peyret, R. and Taylor, T., *Computational Methods for Fluid Flow*, Springer-Verlag, New York, 1983.

74. Pitman, E. B., Gudonov method for localization in elastoplastic granular flow, *Int. J. Num. Anal. Methods*, **17** (1993), 385-400.

75. Pöschel, T. and Herrmann, H.J., Size segregation and convection, *Europhys. Lett.*, **29** (1995), 123-128.

76. Potapov, A. and Campbell, C., Computer simulation of particle fracture and hopper flows, Third Year Progress Report to the International Fine Particle Research Institute, USC Report IFPRI.4, Department of Mechanical Engineering, University of Southern California, Los Angeles, 1995.

77. Prykarpatsky, A.K. and Mykytiuk, I.V., *Algebraic Aspects of Integrability of Dynamical Systems on Manifolds*, Kiev: Nauk.dumka, 1991. (in Russian)

78. Prykarpatsky, A.K., Hentosh, O., Kopych, M. and Samulyak, R., Neumann-Bogoliubov-Rosochatius Oscillatory Dynamical Systems and their Integrability via Dual moment maps. I, *J. Nonl. Math. Phys.*, **2** (1995), 98–113.

79. Prykarpatsky, A.K., Blackmore, D.L., Strampp, W., Sydorenko, Yu. and Samulyak, R., Some remarks on Lagrangian and Hamiltonian formalisms related to infinite dimensional dynamical systems with symmetries, *Condensed Matter Phys.*, **6** (1995), 79–104.

80. Prykarpatsky, A.K. and Samulyak, R.V., The Higgs model as an integrable bi-Hamiltonian dynamical system of the classical field theory. *Proceedings of the Nat. Acad. of Sci. of Ukraine*, **1** (1995), 34–37.

81. Pugh, M. and Shelly, M., Singularity formation in thin jets with surfacetension, *Comm. Pure Appl. Math.*, **51** (1998), 733-795.

82. Rajagopal, K., Existence of solutions to the equations governing the flow of granular material, *Euro. J. Mech. B/Fluids*, **11** (1992), 265-276.

83. Rhodes, M. (Editor), *Principles of Powder Technology*, John Wiley and Sons Ltd, 1990.

84. Richman, M., "Boundary conditions for granular flows at randomly fluctuating bumpy boundaries", *Advances in Micromechanics of Granular Materials*, Shen, H. et al. eds., Elsevier, Amsterdam, 1992, 111-122.

85. Richtmyer, R.D., *Principles of Advanced Mathematical Physics. V.1*, New-York-Heidelberg-Berlin: Springer-Verlag, 1978.

86. Rom-Kedar, V., Leonard, A. and Wiggins, S., An analytical study of transport, mixing and chaos in an unsteady vortical flow, *J. Fluid Mech.*, **214** (1990), 347-394.

87. Rosato, A., Dave, R., LaRosa, A. and Mosch, E., Experimental study of vibrational size segregation, *Proc. First Int. Particle Tech. Forum, AIChE* (1994), 325-330.

88. Rosato, A. and Kim, H., Particle dynamics calculation of wall stresses and slip velocities for granular Couette flow of smooth inelastic spheres, *Cont. Mech. & Thermo.*, **6** (1994), 1-21.

89. Rosato, A., Lan, Y., Macroscopic behavior of vibrating beds of smooth inelastic spheres, *Phys. Fluids*, **7** (8) (1995), 1818-1831.

90. Rosato, A. and Lan, Y., Granular dynamics modeling of vibration-induced convection of rough inelastic spheres, *Proc. First Int. Particle Tech. Forum, AIChE* (1994), 446-453.

91. Samulyak, R., Blackmore, D. and Dave, R., Approximate inertial manifold in finite differencies for granular flow dynamical system, *SIAM J. Numer. Anal.* (under review).

92. Savage, S., The mechanics of rapid granular flows, *Adv. in Appl. Mech.*, **24** (1984), 289-366.

93. Savage, S., Studies of granular shear flow. Wall slip velocities, "layering" and self-diffusions, *Mech. Gran. Mater.*, **16** (1993), 225-238.

94. Savage, S. and Jeffrey, D., The stress tensor in a granular flow at high shear rates, *J. Fluid Mech.*, **110** (1981), 225-272.

95. Schaeffer, D., Instability in the evolution equations describing incompressible granular flow, *J. Diff. Eq.*, **66**, 19-50.

96. Schaeffer, D., Shearer, M. and Pitman, B., Instability in critical state theories of granular flow, *SIAM J. Appl. Math.*, **50** (1990), 33-47.

97. Shen, H. and Ackermann, N., Constitutive equations for a simple shear flow of a disk shaped granular mixture, *Int. J. Eng. Sci.*, **7** (1984), 829-840.

98. Shilling, R.J., Neumann systems for the algebraic AKNS problem. *Memoires of the AMS*, **97** (1992), 1–59.

99. Sulanke, R. and Wintgen, P., *Differential geometry und faser-bundel*, bound 75, Veb. Deutscher Verlag der Wissenschaften, Berlin, 1972.

100. Swinney H., Umbanhowar P. and Melo F., "Stripes, squares, hexagons and localized structures in vertically vibrated granular layers", *Powders and Grains 97*, Behringer and Jenkins (eds), 369-372, 1997 Balkema, Rotterdam, ISBN 90 5410 8843.

101. Tabor, M., *Chaos and Integrability in Nonlinear Dynamics*, Wiley, New York, 1989.

102. Temam, R., *Infinite Dimensional Dynamical Systems in Mechanics and Physics*. Springer-Verlag, New York, 1988.

103. Temam, R., *Navier-Stokes Equations: Theory and Numerical Analysis*, Elsevier, Amsterdam, 1984.

104. Temam, R., *Navier-Stokes Equations and Nonlinear Functional Analysis*, Springer-Verlag: New York, Heidelberg, Berlin, 1995.

105. Titi, E.S., On approximate inertial manifolds to the Navier-Stokes equations, *J. Math. Anal. Appl.*, **149** (1990), 540-557.

106. Tsimring L. and Aranson I., Localized and cellular patterns in a vibrated granular layer, *Phys. Rev. Lett.*, 1997, V.79, 213-216.

107. Walton, O., "Numerical simulation of inelastic, frictional particle-particle interactions", *Particulate Two-phase Flow*, edited by M.C.Roco (Butterworth-Heinemann, Boston, 1992), 884-911.

108. Walton, O., "Numerical simulation of inclined chute flows of monodisperse, inelastic frictional spheres", *Advanced Micromechanics of Granular Materials*, edited by H.Shen, M.Satake, M.Mehrabadi, C.Chang, and C.Campbell (Elsevier, Amsterdam, 1992), p.453.

109. Wassgren, C., Brennen, C. and Hunt, M., Vertical vibration of a bed of granular material in a container, *J. Appl. Mech.*, **63** (3) (1996).

110. Wiggins, S., *Global Bifurcations and Chaos - Analytical Methods.* Springer-Verlag: New York, Heidelberg, Berlin, 1988.

111. Zakharov, V.E., The Benney equation and quasi-classical approximations in the inverse scattering problem, *Functional Anal. Appl.*, **14** (1980), 15-24.

112. Zaslavsky, G.M., *Chaos in Dynamical Systems.* Harwood Academic, New York, 1985.